ON-LINE OPTIMIZATION OF A WATER-GAS SHIFT REACTOR IN THE PRESENCE OF NOISE

by

Howard Edward Wise, B.Sc.

A thesis submitted for
the Degree of Doctor of Philosophy
in the Faculty of Engineering
of the University of London

Department of Chemical Engineering
and Chemical Technology,
Imperial College of Science and Technology,
London S.W.7.

July 1968.

ABSTRACT

Extremum seeking controllers have been widely studied in recent years, but mainly with regard to systems having stationary optima, and when moving extrema have been considered the investigations have frequently been purely theoretical. The present study investigates both experimentally and theoretically the possibility of improving the simple on-line optimizer which uses a sinusoidal perturbation signal to deal more adequately with a system which is being disturbed. The system used was a small experimental water gas shift reacter and the disturbances ranged from random to second order integrated.

The method was based on Box and Jenkins' technique which combines a stochastic model of the disturbances and a dynamic model of the system to formulate a predictor controller. Difficulties encountered in applying this method to optimization arise mainly from non-linearities in the dynamics which are introduced by the optimizer, and to a lesser extent by the non-quadratic nature of the objective function.

Two parameters, the amplitude and the frequency of the perturbation signal, were studied by means of a two by two factorial design, while the other parameters were maintained at best values found by Price and Kisiel. Because of difficulties in operating the experimental apparatus the

practical results were not entirely satisfactory, although they did show the recessity of operating with the lower frequency perturbation signals.

The simulation studies confirmed that better following was obtained with a slower perturbation signal, and in addition they showed that the ability of the predictor optimizer improved considerably over that of the simple optimizer as the frequency of the disturbances decreased.

ACKNOWLEDGEMENTS

I would like to express by sincerest gratitude to Dr. D.W.T. Rippin for the constant help, advice and encouragement that he has given me throughout this work. I am also grateful to Professor G.M. Jenkins for the interest he has shown during frequent consultations and to Professor R.W.H. Sargent for taking me under his wing after Dr. Rippin's departure to Lancaster.

I am indebted to Mr. L. Tyley and members of the departmental electronics workshop for building some of the electronic equipment and helping in the general maintenance of the whole system. The Chemical Engineering workshop has also assisted in the construction of the apparatus; of its members I would particularly like to thank Messrs. R. Barnes and B. Lucas.

The Science Research Council originally sponsored this project and provided me with a studentship for which I am grateful. I am also indebted to I.B.M. for their fellowship which enabled me to complete this research programme.

Finally, I would like to thank my parents and my wife for their patience and generosity.

To my parents.

LIST OF CONTENTS

LIST OF FIGURES

LIST OF TABLES

LIST OF SYMBOLS

Because of the large number of symbols required, it has been impossible to ensure that every symbol has only one meaning; however on all occasions the symbols are defined in the context in which they are used, so difficulties should not arise. However, in order to reduce still further the possibility of confusion arising, the symbols are listed separately for each chapter.

Chapter 2

A	vector of random elements entering stochastic process
A_c	amplitude of correlating signal
A_s	amplitude of perturbation signal
a	vector defining amplitude of perturbation sinusoid
a	parameter defining parabola
a_p	random element entering stochastic process at instant p
B	backward shift operator
b	vector defining step change entering system
b	coefficient of cubic term in non-quadratic objective function
C_1, C_2	parameters in objective function
c_j	j^{th} element of autocovariance matrix
e_p	deviation from set point at instant p
$\hat{e}_p$	prediction of e_p
g, g_1, g_2	steady-state gains of system

k, k_1, k_2	parameters defining first order transfer function
L_ϕ	function describing autoregressive process
L_ψ	function describing moving average process
m_p	element of output at instant p due to measurement noise
n_p	element of output at instant p due to combined noise
$\hat{n}_p$	prediction of n_p
P_x	probability of operating between $x - \frac{dx}{2}$ and $x + \frac{dx}{2}$
r_j	j^{th} element of autocorrelation matrix
S	summing operator
S_0, S_t	values of objective function
S_r, S_ϕ	statistics of auto- and partial auto-correlations
T	sampling interval or operating temperature
v	transient used to define weighting coefficients
X	matrix of present and passed sampled values of stochastic process
x	defining initial mean operating position
$\underline{x}$	vector defining position of optimum
x_t	output from dynamic system at instant t
x_t^*	controlable variable input to dynamic system
y	current value of profit function
$\underline{y}$	maximum value of profit function
y_t	intermediate value in dynamic system
Z	column vector of elements of the stochastic series
z_p	value of stochastic series at instant p

α_p	error at instant p through modelling mixed process with a pure AR series
β	parameter defining parabola
γ_{-1}, γ_0, γ_1	parameters of simple stochastic model
Δ	difference operator
ε_p	random term at instant p
η_p	output at instant p due to disturbances entering system
θ_i	i^{th} coefficient of polynomial modelling dynamics
λ	dead time of system
μ	mean of Gaussian distributed disturbances
$\mu_{\omega F}$	attenuation due to high pass filter for angular velocity ω
$\mu_{\omega p}$	attenuation due to plant dynamics for angular velocity ω
σ^2	variance of Gaussian distributed disturbances
σ_r^2, σ_ϕ^2	variance of auto- and partial autocorrelations
$\sigma_{\omega F}$	phase shift due to high pass filter for angular velocity ω
$\sigma_{\omega p}$	phase shift due to plant dynamics for angular velocity ω
τ	time constant
Φ	vector of parameters defining autoregressive process
ϕ_i	i^{th} coefficient of autoregressive process
ϕ_{kk}	k^{th} partial autocorrelation
ψ_i	i^{th} coefficient of moving average process
ω_i	i^{th} weighting term

Chapter 3

x	orifice reading
y	total flow rate

Chapter 4

A	parameter in kinetic constant
A_K	parameter in equilibrium constant
a	cross-sectional area of reactor
a_k	parameter in kinetic constant
b_j	j^{th} parameter being fitted
D	delaying operator
E_K	energy term in equilibrium constant
E_k	activation energy
$F_{\alpha}(\ )$	F statistic at α level
ΔH^+	enthalpy
h	Plank's constant
h	integration step length
$h(t)$	impulse response function at time t
K	Boltzmann's constant
K_e	equilibrium constant of the reaction
k	kinetic constant
k	number of parameters in model
n	total number of data points
R	Universal gas constant
r	moles of carbon monoxide produced per unit time and unit of volume of reactor

$\Delta S^{\dagger}$	entropy
S_0	standard error of the estimate of the minimum sum of squares
$S_0^2\ c_{jj}$	j^{th} diagonal element of the variance-covariance matrix
T	absolute temperature
T_{HP}	time constant of high pass filter
T_{IR1}, T_{IR2}	time constants of infra-red analyser
T_{TR}	time constant on temperature side of reactor
$t_{1-a'(n-k)}$	two tailed $(1 - a')$ point of Student's t-distribution
u	velocity of gases in reactor
x	length along reactor
x_0	total length of catalyst packed bed
x_t	input to system
y_n	value of integral at n^{th} stage
y_t	output from system
Z_{in}, Z_{out}	signals to and from linear sequential filter
z	$\frac{d}{dt}$ (IRA reading)
$\theta(D)$	characteristic polynomial of linear sequential filter
ν	time
τ	time
$\Phi_{critical}$	sum of squared errors at the edge of the confidence region
$\Phi_{optimal}$	sum of squared errors at the point of optimal fit
$\phi_{xx}(\tau)$	autocorrelation at delay τ

$\phi_{xy}(\tau)$	cross-correlation at delay τ
(A)	concentration of component A
$\oplus$	modulo two adder

Chapter 5

a_p	random element of stochastic disturbance at instant p
N	number of points used
$\hat{s}$	unbiased standard deviation
$\hat{s}_\Delta$	unbiased standard deviation of difference
$\bar{x}$	mean difference in results between Controllers I and II
z_p	p^{th} sample of stochastic disturbance

CHAPTER 1

INTRODUCTION AND LITERATURE SURVEY

1.1. Introduction

With the advent of cheap and reliable computing facilities, the chemical industry is beginning to view on-line optimization of processes in a more favourable light. The need for such facilities frequently arises in situations where the optimum is moving, since otherwise off-line, steady-state optimization would be sufficient. However, before final decisions can be made regarding the economic feasibility of installing a form of direct computer optimizing control on a plant, an estimate of the expected increase in overall profits is essential. Such information can only be obtained with the use of realistic objective functions, which could depend on more than one variable. Should preliminary studies show that installation of on-line optimization is indeed economically sound, it is then necessary to decide upon the type of system to be used. Sometimes, an accurate dynamic model of the process being investigated is available, and, as a result, it may be possible to employ sophisticated techniques such as optimal control or dynamic programming. Frequently, however, it is found that knowledge of the system is limited, and so reliance is placed on more empirical methods. One such class, generally known as "extremum seeking", has received considerable attention recently.

Several methods have been developed for use in extremum seeking control, perhaps the most primitive being that of a straight-forward search on each parameter in turn. In this, a slow ramp function or a series of steps is initiated in the chosen parameter, and maintained until the optimum has just been passed; at this stage the process is reversed or another variable is examined. To improve the performance of this optimizer in the region of the optimum, limits, based on the last best value of the objective function, are specified, below (or, in the case of a minimum, above) which the output must go before a change of direction occurs. This is to prevent a change of direction due to some noisy disturbance in the system. The main limitations of this first method are that the movement towards the optimum should be slow enough for the resulting system output to be unaffected by its dynamics, and that optimization may only be carried out with respect to one variable at a time. Successful attempts have been made to deal with both these problems by obtaining an estimate of the gradient at the current operating point, and then taking a step towards the optimum proportional to the gradient; the same procedure is then repeated. Although time has to be allowed for settling, both when testing for the gradient and when moving towards the optimum, it is nevertheless faster than the straight forward search technique. In the multivariate case, the partial derivatives with respect to each parameter are found; they are then used to calculate the total gradient which may in turn

be acted upon in two possible ways. In the first, known as the "steepest ascent" (descent) method, movement is initiated along the gradient until the optimal point in this direction is reached, whereupon the gradient is recalculated and the procedure repeated. The other, referred to as the "gradient" method, allows a step of a given size to be made along the gradient, before repeating the procedure. The latter technique is extremely successful a long way from the optimum, but whenever hunting in the optimum's vicinity is taking place, it is best to use the former. An improvement on the gradient method is to make the stepwise movement in the direction of the optimum proportional to the magnitude of the gradient.

The above methods do however still suffer from the disadvantage of being slow in their movement towards the optimum. This may be partially attributed to the way the gradients are measured; it is necessary both to measure the partial derivatives separately and also to have the system free from transients during their measurement. The simplest method so far used to measure gradients involves disturbing the parameter of interest a small distance to each side of its normal operating point; measurement of the steady-state output at these two levels then yields sufficient information for the gradient to be calculated. Another method which has been used is to superimpose a perturbing signal, such as a square-wave or a sinusoid on the parameter control signal; after

multiplying the original perturbing signal with the A.C. part of the output from the system, a signal is obtained which indicates the direction of the optimum. Moreover, integration of this same signal over a complete perturbing cycle gives a value proportional to the gradient. A great advantage of such a system is that, if perturbing signals of sufficiently differing frequencies are used, it is possible to measure partial derivatives of serveral parameters with a minimum of aliasing. When the latter method was first introduced, care still had to be taken to ensure that the transients caused by intiating the perturbing signal were allowed to die before starting optimization, and the frequency of perturbation had to be low enough for the phase shift, caused by the system dynamics, to be insignificant. Although the former limitation still holds, the frequency of perturbation, and therefore the rate at which information about the gradient is obtained, can be increased by introducing a compensating phase shift into the correlating signal by-passing the system.

Apart from initially stating that extremum seeking controllers were useful for climbing optima which move slowly, it has been implicitly assumed that the systems being dealt with were free from noise. Unfortunately, this is not usually the case, so for a more realistic approach the influence of noisy disturbances should be considered. The types of noise that might be encountered are classifiable in four categories:

(1) very low frequency noise, which is best treated by steady-state optimization at regular intervals;

(2) low frequency noise in the presence of which extremum seeking controllers do show an improvement;

(3) higher frequency disturbances which can be measured at their entry points and therefore their effects corrected with some form of feedforward control system;

(4) noise which is of such high frequency that because of the dynamics it would die out in its passage through the system, or would be generated within the system as measurement noise.

The categories of greatest interest, when dealing with extremum seeking controllers, are the second and fourth. The latter, generally being encountered whenever the extremum seeking controllers are used, requires that care be taken in measurement of the gradients to ensure that reasonable values are obtained for these. Therefore, it is necessary to have a perturbation signal of a high enough amplitude to drown any effects of the noise; also, because of the attenuating effect of the dynamics, a limitation, dependent on the time constants of the system, should be placed on the maximum possible frequency of perturbation. Originally, continuous gradient measuring and optimizing systems were used, but in the presence of measurement noise there is the possibility of movement taking place away from the optimum. If, instead, a sample data scheme from the optimizer to the system is used, it is

possible for the error to average itself out over the intervening period, thus reducing the likelihood of movement taking place away from the optimum.

The main point of interest in this study is concerned with the second category, which defines more specifically the circumstances in which extremum seeking controllers may be used to counteract the effects of noisy disturbances. Although the type and power of noise that can be dealt with, using different conventional controllers has been studied, little attention has been paid to the development of a new control philosophy for use in conjunction with the same basic optimizer. In this study, techniques developed for the modelling and prediction of discrete time series have been used to formulate a type of feedback predictor controller. The advantages of the method, together with its shortcomings, have been enumerated, and in addition to carrying out tests to a limited extent on a water gas shift pilot plant, further work has been done on an IBM 7090 computer with the use of a digital simulation model of the system.

1.2. Literature Survey

1.2.1. Gradient measurement by means of sampling steps.

(a) Stability in the presence of disturbances.

Perhaps the earliest study of the effects of noise on an extremum seeking controller was carried out experimentally by Stakhorskii (S1). This was in fact part of a programme to

assess the capabilities of a two variable optimizer that had been built. A small sampling step made to either side of the operating point was used in measuring the partial derivative with respect to a given parameter, combination of this with the other partial derivatives then yielding the gradient of the surface. Initially, both parameters were perturbed by sinusoidal signals of a given amplitude, the ability of the controller to follow the optimum which moved in a horizontal plane was then studied. Stakhorskii found that if the amplitudes of the disturbing signals were maintained, constant, but the frequencies increased, then there was a point, dependent on the size of the gradient sampling step δx, at which the controller became completely disorganized, and that this critical frequency could be raised by increasing the size of δx. He also discovered that there was an optimal value for movement towards the extremum when operating with a given sampling size and noise frequency. This study was further extended by feeding in white noise of up to a few cycles per second; here again it was found that for a given δx there was a maximum velocity of movement, the direction of which was dependent upon the direction of the last δx. Finally a study of stability in the presence of interference showed that, when systems which are continuous in time are involved, the optimizer coped quite successfully; however, when dealing with discrete systems, it needed to repeat and average the measurement of the gradient several times.

(b) Expected losses due to disturbances

Initial, if somewhat unrealistic theoretical analysis was made by Fel'dbaum (F1) when he put forward a method for calculating the expected losses incurred when a system is subject to slowly drifting input noise and fairly high frequency output noise. Because he chose a system having a modular characteristic

i.e. $y = |x|$

and no dynamics, it was possible to specify that at any instant the probability of making a false step was a constant p. In assessing the magnitude of p, a value for the test step signal δx first had to be chosen. This was done, bearing in mind two criteria:

(i) too high a value of δx would cause large hunting losses,

(ii) too low a value would cause δx to be drowned by the noise.

Having obtained a value for p, Fel'dbaum specified that the system could only adopt certain discrete states, which were also states in a Markov process. From this, it was then possible to evaluate the expected losses incurred by the extremal controller when operating under noisy conditions.

The above work was slightly extended by Tovstukha (T1), who introduced a parabolic objective function. However, in this case, only measurement noise was considered. Thus it was reasonable for her to show that, over long periods of time, it

was best for the sampling step to be very close to zero, as this virtually eliminates errors due to factors other than the disturbances.

Fel'dbaum (F2) improved his own method when he considered a multichannel system with a quadratic characteristic. The analysis was performed for a case in which there was low frequency noise entering through each input channel, as well as high frequency noise being added at the output. When operating under steady-state conditions, it was found that the expected error was dependent solely upon the variance of the measurement noise, and not, as would also have been expected, on its statistical distribution.

Paulauskas (P1) continued work on a multi-dimensional system with high frequency noise at the inputs and outputs, as well as drifts occurring in the input channels. He was able to show that the error got larger with either increasing variance of input and output noise or increasing drift. The minimum error was found for constant noise parameters and increasing number of channels and vice-versa. Further minimization of this error was carried out by varying the operating and test steps. Finally, Paulauskas found that in the case of a system with a small number of channels and little drift, the output measurement noise had the greater influence on the magnitude of the error; however, this influence reverted to the input noise after the system had grown beyond a certain number of channels.

Use was again made of the Markov process technique by Perel'man (P2), to obtain the statistical characteristic of simple extremal control systems under steady-state condition, in the presence of measurement noise and horizontal drift. After deciding that the overall operating error was a more important criterion of performance than speed of response, he developed a grapho-analytical method for calculating its expected value. Gorelick (G1) also developed a method for calculating the mathematical expectation of the deviations from the optimum for a system being disturbed by stationary random noise at its input and output, and by a slow drift at its input. Although he only developed the method for application to a one channel system, it does have the advantage of being applicable to any case in which autocorrelation function of the input noise is known.

(c) Effect of controller's structure

So far reference has only been made to methods developed for assessing the performance of step-testing extremal controllers, with no mention of how the structure of the controller could be changed to improve this. Perel'man (P3) suggested using an extrapolating method of control, in which the shape of the system's characteristic would have to be known, and therefore the parameters describing this would have to be free from change. However, he did define the areas of input and measurement noise in which the method was applicable and found

that in them the system yielded a faster search and greater accuracy. Kutuzov and Tarasenko (K1) also made a contribution towards examining ways in which the controller structure could be changed. They stated that if measurement noise was the main disturbance, then it was better to average the estimates of the gradient over several time cycles, before carrying out a control step. However, if the hill itself were moving, then it would be better to reduce the number of storage states before taking control action. Similarly, if the operating point was at a large distance from the optimum, it would be better to use a longer control step, than if it were only a short distance away. Thus they proposed three alternative control structures:

(i) fixed operating step and variable number of storage units,

(ii) variable operating step and fixed number of storage units,

(iii) variable operating step and variable number of storage units.

The changes to the controllers being made on either the basis of trials being performed before each operating step or on the outcome of the analysis of results of several preceding steps. They analysed, for two different criteria, the relative performance of all three systems when started from the same point and subject to disturbances having the same signal-to-noise ratio. The performance criteria specified were namely: mean

scanning time and steady-state error, the latter reducing to the determination of the steady-state probabilities.

Van Nice (V1) was probably one of the first occidentals to make a contribution towards the study of extremal controllers under the influence of disturbances other than the measurement noise. He considered a one-variable plant having a quadratic hill and no constraint on the controlled variable. The system was subject firstly to rapid drifts at the input which varied in a step-wise manner at random intervals and with random amplitude, and secondly to high frequency measurement noise at the output. Again the method of step-wise sensing was used to find the gradient, and with knowledge of the parameter describing the parabola, it was possible to move directly to the optimum by means of an extrapolating method. After each controlled movement, time was allowed for transients to die out, hence the system was effectively simplified to one free from dynamics. Based on the premise that Van Nice could evaluate the probability of there being no change due to the bias in a given sampling interval, he was able, using the method of 'z' transforms, to calculate the expected losses with and without adaptive control. Thus, for given system parameters, it was possible to specify bias-to-noise ratios beyond which adaptive control could show no improvement. Besides measuring the gradient by taking a sample step to either side of the operating point and thus necessitating two time intervals between making control changes, Van Nice

also tried what he called the "alternate biasing" method, in which the sample step was taken in one direction, the gradient calculated and control action carried out, then the operation was repeated with the sample step being made in the opposite direction. This increased the rate of control, thus allowing faster drifts to be followed; unfortunately, it also meant that there was a greater likelihood of incorrect control action taking place in the presence of the same measurement noise.

1.2.2. Gradient measurement by means of perturbing signals.

(a) Benefit of sampling control.

So far, a description has been made of the work carried out in studying systems which use a test step to measure the gradient, with no reference to other more continuous types of adaptive controllers. Draper and Li (D1) first put forward the idea of using a continuous perturbation signal as a means of measuring the gradient. In their system the process was excited with a slowly moving sinusoid, as a result of which, since the system would be considered linear over the region of perturbation, a sinusoidal signal, attenuated by the slope of the objective function, was obtained at the output. After removing the D.C. level from the output signal by passing it through a high pass filter, it was correlated with the input sinusoid, by multiplying the two and integrating the result over a complete cycle. They studied the effects

of measurement noise and disturbances arising from the control action itself in a very empirical manner, and came to the conclusion that it was better to take control action at fixed intervals in a perturbation cycle rather than continuously throughout. This finding has since been confirmed by several other workers (D2, H1) and is explained by the fact that if more time is allowed for measurement, then the effects of the noise are able to average themselves out to zero and the previous control action can settle down.

(b) Influence of measurement noise

Recently Aris et al (S4) described some simulations that had been performed to investigate adaptive optimization systems of the type suggested by Draper and Li. The study was carried out on a reaction system of two stirred tanks in series in which an exothermic reaction was taking place. It was desired to adjust the temperatures of the reactors so that the total conversion would be maximised. In order to do this, the controllable variables were specified to be the input temperature of the reactants and the flow rate through the cooling coil placed in each reactor. The search for the maximum was carried out by perturbing the flow rate into each cooling coil by approximately 60% of its mean operating value, these perturbations being injected slowly enough for the dynamics of the system to have no influence on the results. A separate performance integral for each reactor, dependent

upon the gradient, was evaluated at the end of each cycle and after considering how they compared with their values at the end of the previous probing cycle, control action was taken, either on the reactants inlet temperature in the case of the first tank or on the coolant flow rate in the case of the second. The problem of starting the hill-climbing was overcome by taking a standard step in the direction indicated for the first cycle, and excessive control action was curtailed by placing an upper limit on the change that could take place in one cycle. Finally, the optimizer was operated so that after each change, transients were allowed to die out before further action took place.

Besides carrying out simulation runs in the absence of noise to test the ability of the extremum controller to seek out the optimum, Aris et al fed random noise signals of mean zero and variance σ^2 on to their performance integrals. They found the optimizer dealt adequately with errors of variance 0.4, where the amplitude variation of the performance integral (PI) at the start of the hill-climb was 0.38, hence the errors covered a range twice the size of this. The performance of the system was also studied at higher noise levels and with different control policies such as taking two adjacent values of PI or doubling the number of sample points examined per cycle. Another more radical change was to place confidence limits around the performance integral and only to update when departure was made from this region.

In two further papers (S5, S6) Aris et al extended their simulation studies to cover truly two variable optimization systems in which they considered simultaneous and alternate questing together with the problems of aliasing which arise in the first case, and also to cover more realistic economic systems. Again disturbances were introduced on to the performance integral to consider the possible effects of measurement noise. The main shortcomings of their work is that the systems are only perturbed slowly to eliminate the effects of the dynamics and for the same reason time is allowed between each cycle used in calculating the performance integral. Finally, the disturbances fed in were not of a type to make the optimum move about directly.

(c) Experimental study of the effect of disturbances

A certain amount of theoretical work has appeared in the Russian literature dealing with perturbed extremum seeking systems. Again, because of the extreme mathematical difficulties involved in analysing such systems most of the publications have dealt with systems having either quadratic or modular inertialess characteristics with no associated time delays.

Grishko (G2) described an experimental system in which a square wave was used as the perturbing signal. When the level changed in this, the objective function signal was switched from one integrator to another; thus by calculating

the difference between their outputs at the end of each cycle an estimate of the gradient was obtained. Comparison was made of two forms of control which were tested both in the steady-state and under the influence of outside disturbances; they were basically: the use of either a step or ramp function to move to the new indicated position of the optimum. The noise injected was a slow sequence of triangular waves, used to shift the position of the hill in a horizontal direction, and random disturbances at the output which simulated measurement noise. Under these conditions Grishko found that when using the ramp control function, the optimizer was more able to follow the extremum.

Subsequently, this work was extended theoretically (G3). The equations of motion for the extremal system were derived taking into account any external disturbances entering this; knowledge was required, however, of the statistics describing this noise. As a result of these, it was now possible to derive an expression capable of calculating the expected steady-state loss, which was found to depend not so much on the amplitude of the disturbances as on their rate of change.

(d) Theoretical study of the effect of disturbances

The solution to a more realistic problem was tried by Pervozvanskii (P4) who considered an inertialess characteristic embedded between two generalized linear transfer functions, and wished to account for two types of change: slow drifts and

high frequency disturbances. The former was treated as a useful signal, while the latter was mere interference which had to be filtered out. However, it was assumed that between the band spread of these there would be a free band width which could be used for the testing signal. The question was: how far should the square wave or sinusoidal signal be limited to this free band width? The testing signal and therefore the control action were taken to pass through the whole plant, whereas the noise only entered at two points: immediately before and after the inertialess characteristic. Using a Taylor series expansion, Pervozvanskii derived an implicit expression for the steady-state deviation of the system from its optimum. This expression was found to be difficult to solve, but after making the assumption that only low frequency noise entered before the characteristic, and high frequency after, it was possible to approximate terms in the expression which resulted in what was termed statistical linearization of this. Thus, in the end, he was able to define the variance of error if given the spectral density of the disturbances entering the system.

More recently Roberts (R1) published some work in which he considered a fairly generalized system, very similar to Pervozvanskii's. Again there was noise being fed in immediately before and after the characteristic, which in this case was quadratic. However, measurement noise was also entering at the system output. In each instance, the

disturbances were taken to be white noise of specified power spectral density, operated on by a general linear transfer function, although for noise entering before the characteristic this function was specified. Thus Roberts was faced with a rather complicated system containing four general and one specific transfer function. Before proceeding further he found it necessary to reduce the system to one having a general transfer function which came after the characteristic. In order to accomplish this simplication, however, he had to ensure that certain limitations were placed on the transfer function $E(p)$ situated in front of the inertialess module; namely that $(1/p)\, E(p)^{-1}$ was realisable. Subsequently, with the help of an approximation, he replaces the problem dealing with a quadratic non-linearity having a randomly moving apex, to one involving a randomly fluctuating linear element: as a result of this, it became essentially a problem of "non-stationary" linear filtering. With knowledge of the system's transition matrix, and using the method put forward by Kalman and Bucy (K2), it was possible to express the mean and covariance matrix for the "a posteriori" probability distribution of the state variables. There still remained at this stage the problem of solving for the estimates of the state variables of interest, which was difficult because of the interdependence of the equations and in some cases the time dependency of the system matrix; nevertheless, Roberts specifies and illustrates with examples, situations where

this is reasonably easy to do. Criteria indicating when, and in that case how much improvement is to be expected from introducing a perturbation signal into a system are also given. The main disadvantages of the method are firstly that it is only relevant to systems having quadratic characteristics, although correction can be made in certain other cases, and secondly the need for a limitation on the transfer function coming before the hill.

1.2.3. Stochastic prediction techniques.

(a) Predictor-control systems

So far, most of the literature has covered studies of how given plant and extremum seeking regulators operate together, and therefore has dealt with finding expected losses in the presence of noise. Although indications have been given regarding the design of conventional adaptive optimizers as put forward by Draper and Li, no suggestions have been seen concerning a logical approach to the derivation and design of regulator structures to deal with given types of system drift. As a logical sequel to their work on the design of feedback predictor controllers, Box and Jenkins (B2) put forward such a method at a meeting of the Royal Statistical Society.

In the control problem, the object is to maintain a given parameter at, or close to a specified set point, the deviations from this, known as errors, are then used to decide the control action. In the event of there being disturbances entering the system that affect the error, it may be found

necessary to redesign the controller. Box and Jenkins have shown how this can be done with a knowledge of the past history of the errors and control actions, together with a model of the system's dynamics. Firstly, a correction is made to the time series of the errors for the effects of the control action's past history, then analysis is carried out on the adjusted sequence to fit a stochastic model. This model defines how the adjusted sequence is obtained from a white noise source and hence can be used as a predictor of future values of the error, the discrepancies of prediction turning out to be the unpredictable output of the random generator. By using their stochastic predictor and compensating for the system's dynamics, Box and Jenkins were able to show that the effects of the disturbances could be reduced to a random series of errors between the operating and set points; they also show that this is equivalent to minimizing the mean squared error deviation.

(b) Predictor-optimizing systems

When dealing with an extremum seeking system, the objective may be to maintain the operating point as close as possible to the optimum; in this instance, therefore, the error is the distance between these two points. Again, account was taken of the system's dynamics in formulating a stochastic predictor for the error, which in turn can be shown to be equivalent to predicting the movement of the

extremum. In a similar manner to the control problem, the stochastic and dynamic model of the system was then used to reformulate the extremum seeking regulator, the action of which was to reduce the deviations from the optimum to a random series. In their original publication, Box and Jenkins required that the dynamics of the system be known with reasonable accuracy; this is something that is not always available, nor is it necessarily possible to ascertain independently. However, they did suggest a method whereby parameters could be fitted to a combined dynamic stochastic model of known structure (B3), but because of the increased dimensionality of the problem, this fitting is difficult and hence only fairly simple models can be developed. Nevertheless, they put forward the view, based on their experience, that a simplified model of each was generally sufficient to describe most systems.

(c) Practical application of predictor-optimization

For some years now, twin projects studying the practical application of sinusoidal adaptive optimization techniques have been going on at the University of Wisconsin, USA (A1, A2, B4, D3) where a pilot scale natural gas conversion system has been used, and at Imperial College, London (K3, K4, P5, P6) on a pilot scale water gas shift pilot plant. Kotnour (B4) was the first to try the practical application of the Box and Jenkins method to this type of system; the fundamental

difference being that in Box and Jenkins' work an estimate of the deviation from the optimum set point was used, whereas Kotnour only had an estimate of the gradient; nevertheless, when dealing with plants having quadratic response surfaces, it may be shown that the two are proportional. Kotnour disturbed his system with two types of noise, both of which were non-stationary in nature, and in each case studied the effect of the frequency of sampling. In order to show the benefit of using predictor control, each block was made up of five runs, one of which was considered to be optimal, three sub-optimal, and the last merely the sampled estimate of gradient fed back to the process input. Kotnour found, however, that in two out of four of the cases studied, when using optimal controller settings, worse performance was obtained than with some of the sub-optimal settings. The possibility of this being due to a poorly defined performance criterion or experimental error was discounted, and therefore the only conclusion that could be drawn was that the estimates were in fact non-optimal. It was suggested that this non-optimality was probably due to the non-quadratic nature of the response curve. Thus the main failing of the Box and Jenkins method was shown up, since it is only fully applicable to systems having linear dynamics and a quadratic objective function.

1.2.4. Conclusions

In the preceding passages, a survey has been given of

the literature dealing with the influence of noise on adaptive optimizers. Although mention has been made of the work done in studying the effects of high frequency measurement noise, greater emphasis has been placed on investigations concerning noise which would cause the extremum of a system to move. Techniques used to analyse somewhat idealised systems have been reported, and in conclusion a method of designing an extremum seeking regulator for minimizing the effects of noise has been described, together with the account of a case where it has been applied experimentally.

CHAPTER 2

Theoretical Background

2.1. Introduction

A short description of the method of optimization used in this project is followed by a brief outline of the techniques of modelling stochastic processes in the time domain. Methods are indicated for expressing the dynamic models of systems in a form compatible with the derived stochastic model of the disturbances and it is shown how these should be combined to form an efficient predictor regulator. For cases where the dynamics of the system are unknown, a way of formulating and fitting a simplified stochastic-dynamic model is reported. The limitations of transforming the methods available to ones useful for developing adaptive-predictor optimizers are outlined and illustrated with a computer simulation study. Finally, as the theory stands, it is shown to be applicable mainly to systems having symmetrical parabolic objective functions; however, a method is put forward for improving the performance of non-quadratic systems.

2.2. Basic Optimization Method

The objective function used in optimizing the system with respect to temperature depends solely on the percentage of carbon monoxide in the dry output gases, and is given by:

$$S_0 = C_1 - C_2(CO\%) \qquad (2.2.1)$$

where

S = value of objective function

C_1, C_2 = cost parameters

Perturbation of the mean reactor temperature with a sinusoidal signal results in a time dependent variation in the value of the objective function which can be approximated by the first two terms of the Taylor series expansion, namely

$$S_t = S_0 - A_s \mu_{\omega p} \sin(\omega t - \sigma_{\omega p}) \frac{d(CO\%)}{dT} \qquad (2.2.2)$$

where

A_s = amplitude of perturbing signal

$\mu_{\omega p}$ = attenuation due to plant dynamics for angular velocity ω

$\sigma_{\omega p}$ = phase shift due to plant dynamics for angular velocity ω

In the vicinity of the optimum, however, it is found necessary to use further terms of the Taylor series which naturally introduces higher frequency harmonics. Fortunately these are later eliminated in the correlating process.

Before proceeding with the correlation, in order to minimize the magnitude of the signal being dealt with, the D.C. portion of the objective function output is removed by passing it through a high pass filter.

HP filter output = $- A_s \mu_{\omega p} \mu_{\omega F} \sin(\omega t - \sigma_{\omega p} - \sigma_{\omega F}) \frac{d(CO\%)}{dT}$ (2.2.3)

where

$\mu_{\omega F}$ = attenuation due to high pass filter for angular velocity ω

$\sigma_{\omega F}$ = phase shift due to plant dynamics for angular velocity ω

Integrating the product of the filter output and $\sin(\omega t - \sigma_{\omega p} - \sigma_{\omega F})$ over a complete cycle yields:

$$\text{correlator output} = - A_s \; A_c \; \mu_{\omega p} \; \mu_{\omega F} \; \frac{\pi}{\omega} \frac{d(CO\%)}{dT} \qquad (2.2.4)$$

where A_c = amplitude of correlating signal.

Should the phases shift of the correlating signal be wrong by an angle θ (2.2.4) becomes

$$= - A_s \; A_c \; \mu_{\omega p} \; \mu_{\omega F} \; \frac{\pi}{\omega} \cos\theta \; \frac{d(CO\%)}{dT} \qquad (2.2.4a)$$

Once parameters have been set for the perturbing and correlating signals (2.2.4) shows that the correlation output depends entirely on the derivative of the objective function.

Further discussion of the one and two variable adaptive optimization techniques is given by Price (P6).

2.3. Modelling Time Series

The methods available for modelling time series fall into two general categories, namely analysis based on either the frequency or the time domain. Although the results obtained in one domain are interchangeable with the other, each gives a different insight into the stochastic process being studied. However, because in this work action is only taken at discrete intervals of time, only methods belonging to the second category are described; furthermore, the analysis of processes in

which there are hidden periodicities, such as arise in seasonal time series, is not considered.

2.3.1. Time domain approach

A stationary time series may be described by an auto-regressive process of the type:

$$z_p = \sum_{i=1}^{\infty} \phi_i \, z_{p-i} + a_p \qquad (2.3.1)$$

in which ϕ's are weighting terms for the process and a's are random variables having mean zero and variance σ_a^2. On the other hand the given series may be described as a moving average process like

$$z_p = \sum_{i=1}^{\infty} \psi_i \, a_{p-i} + a_p \qquad (2.3.2)$$

Using the backward shift operator B (2.3.1) becomes

$$\left(1 - \sum_{i=1}^{\infty} \phi_i \, B^i\right) z_p = L_\phi(z_p) = a_p \qquad (2.3.3)$$

and (2.3.2) becomes:

$$z_p = \left(1 + \sum_{i=1}^{\infty} \psi_i \, B^i\right) a_p = L_\psi(a_p) \qquad (2.3.4)$$

$$\therefore L_\phi = L_\psi^{-1} \qquad (2.3.5)$$

Thus it has been shown that the two processes as defined above are interchangeable. The apparent shortcoming of having to evaluate an infinite number of weighting functions does not generally arise, because most series met can be described by either a finite moving average (henceforth MA) process, a finite autoregressive (AR) process or a mixture of the two.

The above suggests that two stages must be undergone in modelling time series: firstly analysis has to be carried out to decide on a structure for the model, and secondly, parameters must be fitted to the chosen structure. A third stage also exists in which the fitted model is tested and improved if necessary.

2.3.2. Analysis of moving average processes

Consider the stationary series:

$$z_p = \sum_{i=1}^{l} \psi_i \, a_{p-i} + a_p \qquad (2.3.6)$$

of which n terms are available. The mean of the series, because of the stationarity assumptions, is zero and the autocovariance is given by:

$$(cov) = \begin{bmatrix} c_0 & c_1 & \cdots & c_k \\ c_1 & c_0 & \ddots & \vdots \\ \vdots & \ddots & \ddots & c_1 \\ c_k & \cdots & c_1 & c_0 \end{bmatrix} = c_0 \times \begin{bmatrix} 1 & r_1 & \cdots & r_k \\ r_1 & 1 & \ddots & \vdots \\ \vdots & \ddots & \ddots & r_1 \\ r_k & \cdots & r_1 & 1 \end{bmatrix} \qquad (2.3.7)$$

the second matrix, which is the dimensionless form, being called the autocorrelation matrix. Individual autocovariances are calculated by considering products of the type

$$\text{Average}(z_p z_{p-j}) = \text{Average}\big((a_p + \psi_1 a_{p-1} \ldots + \psi_l a_{p-l}) \times (a_{p-j} + \psi_1 a_{p-j-1} \ldots + \psi_l a_{p-j-l})\big) \qquad (2.3.8)$$

which because there is no correlation in the a's reduces to

$$c_j = \sigma_a^2 \left(\psi_j + \psi_1 \psi_{j+1} \ldots + \psi_{l-j} \psi_l\right) \qquad (2.3.9)$$

As the lag j in the autocovariance increases it is seen that its magnitude will decrease and finally cut-off at the lag $j > l$. Study of the autocorrelations therefore gives the order of the MA process that describes the series. Should the stochastic process be AR in nature then inverting to an MA process produces an infinite series which clearly gives no cut-off point in the autocorrelations.

Having decided on the order of the finite MA process required to model a series, the weighting terms are fitted by means of a non-linear hill-climbing technique.

2.3.3. Analysis of autoregressive processes

In the process described by

$$z_p = \sum_{i=1}^{l} \phi_i z_{p-i} + a_p \qquad (2.3.10)$$

the autocorrelations are calculated from elements of the form

$$z_p z_{p-j} = \phi_1 z_{p-1} z_{p-j} \ldots + \phi_l z_{p-l} z_{p-j} + a_p z_{p-j} \qquad (2.3.11)$$

Since the last term z_{p-j} is measured before the random variable a_p is produced, there can be no correlation between then, hence the last term in (2.3.11) goes to zero on averaging, and it follows that the autocorrelations are given by

$$r_j = \phi_1 r_{j-1} \ldots + \phi_l r_{j-l} \qquad (2.3.12)$$

Should attempts be made to describe a time series by an AR process of order k, then the last weighting function ϕ_k is also

known as the k^{th} partial autocorrelation $\phi_{k,k}$. It is seen therefore that if a process of order k is modelled by one of order $k + 1$ then $\phi_{k+1,k+1}$ will prove to be zero. Thus the order of an AR process is defined by evaluating successively the partial autocorrelations of the series and ascertaining the point where the cut-off occurs. On the other hand, if the process is MA then inversion to the AR scheme yields an infinite series which cannot give a cut-off in the partial autocorrelations. A straightforward method of evaluating the partial autocorrelations is by making use of the linear relationship

$$\begin{bmatrix} r_k \\ \vdots \\ r_{k-j} \end{bmatrix} = \begin{bmatrix} r_{k-1} & \cdots & r_{k-j} \\ \vdots & & \vdots \\ r_{k-j-1} & \cdots & r_{k-2j-1} \end{bmatrix} \times \begin{bmatrix} \phi_1 \\ \vdots \\ \phi_j \end{bmatrix} \qquad (2.3.13)$$

Once the order of the AR process has been decided, the second stage of the modelling may be carried out by fitting the weighting terms

$$\begin{bmatrix} z_n \\ \vdots \\ z_j \end{bmatrix} = \begin{bmatrix} z_{n-1} & \cdots & z_{n-j} \\ \vdots & & \vdots \\ z_{j-1} & \cdots & z_0 \end{bmatrix} \times \begin{bmatrix} \phi_1 \\ \vdots \\ \phi_j \end{bmatrix} + \begin{bmatrix} a_n \\ \vdots \\ a_j \end{bmatrix} \qquad (2.3.14)$$

Rewriting this as

$$Z = X\Phi + A \qquad (2.3.15)$$

The vector of weighting terms is obtained by means of a linear least squares fit.

$$\Phi = \left(X^T X\right)^{-1} XZ \qquad (2.3.16)$$

2.3.4. Mixed autoregressive, moving average processes

Frequently it is found that neither the auto- or partial autocorrelations display any cut-off, in which case, assuming stationarity, the process may possibly be described by a mixture of the two. In this eventuality, Box and Jenkins (B1) propose using an iterative technique in which an MA process is fitted to the original data and an AR process to the residuals.

2.3.5. Testing for cut-off

Because of measurement and estimating errors it is frequently found difficult to see at what stage cut-off occurs in either the auto- or partial autocorrelation series, thus it is necessary to have a method available with which to test for these. Assuming a normal distribution of the errors it is possible to specify whether or not the estimated function lies within the 95% confidence region of the zero value. This is accomplished using the variance estimate of the given function and the statistics

$$S_{\phi} = \frac{\phi}{\sqrt{\sigma_{\phi}^2}} \qquad \text{and} \qquad S_r = \frac{r}{\sqrt{\sigma_r^2}}$$

Should either function be significantly non-zero the statistic S will prove to be greater than 1.96.

The variance of the partial autocorrelation ϕ_{kk} is calculated on the assumption that the series of n terms is AR of order $k - 1$, and is approximated (B1) by

$$\text{var}\left(\phi_{kk}/AR(k-1)\right) \approx \frac{1}{n - k} = \sigma_{\phi}^2 \qquad (2.3.17)$$

Whereas for the autocorrelations the variance is

$$\mathrm{var}(r_k) \approx \frac{1}{n}\left(1 + 2\sum_{i=1}^{k-1} r_i^2\right) = \sigma_r^2 \qquad (2.3.18)$$

2.3.6. Constraints on coefficients

Consider the autoregressive part of a mixed ARMA process

$$z_p = \sum_{i=1}^{l} \phi_i \, z_{p-i} + \alpha_p \qquad (2.3.19)$$

using the backward shift operator this converts to

$$\left(1 - \sum_{i=1}^{l} \phi_i \, B^i\right) z_p = \alpha_p \qquad (2.3.20)$$

The roots of the polynomial $\left(1 - \sum_{i=1}^{l} \phi_i \, B^i\right)$ have to lie outside the unit circle; should this not be the case it is found that on inversion to a MA scheme, greater weighting is given to values of the error α in the distant past, a fact which causes instability.

In the case of the MA process, if the characteristic equation

$$\alpha_p = \left(1 + \sum_{i=1}^{l} \psi_i \, B^i\right) \alpha_p \qquad (2.3.21)$$

has roots which do not lie outside the unit circle, then on inversion it is found that the weightings increase with the age of the α's, which is again not reasonable and means that the series is not invertible.

2.3.7. Non-stationary series

In the previous section it was stated that should the characteristic polynomial of an AR process have a root lying within the unit circle, then the process would be unstable, i.e. non-stationary. This type of model gives a function which tends to rise or drop in an exponential manner and is therefore not of much use in describing most non-stationary series encountered. Generally, however, differencing of these series a number of times yields series which are stationary mathematically this can be shown to be equivalent to having a number of roots of the characteristic AR polynomial on the circumference of the unit circle. Thus after obtaining, through differencing a series which is stationary, modelling of the same time series may be continued by the methods already outlined.

2.3.8. Final checking of the model adequacy

Having decided on a structure to represent the process and fitted coefficients to it, it is then necessary to check that the model obtained does indeed give an adequate representation of the series. This is accomplished by using the model as a one step ahead predictor, the autocorrelations of the residual errors are then calculated and examined for indications of non-randomness. Should it be found however that the residuals are not random, then further analysis on them will yield information which can be used for improving the model of the original series.

2.4. Modelling of the System

Here a brief description is given of the Box and Jenkins (B3) formulation of various elements necessary for describing a linear dynamic system.

2.4.1. Transfer functions

The output from a capacitive system can be represented as being dependent on the weighted sum of the past history of inputs. Thus

$$x_t = g \sum_{i=1}^{\infty} w_i \, x^*_{t-i} \qquad (2.4.1)$$

where g is the steady state gain of the system, and w_i one of the weighting coefficients which collectively make up the impulse response function of the system. In the special case of a first order transfer function, which has an exponentially falling impulse response, the system weighting terms are of the type given below.

$$x_t = g\{v \, x^*_{t-1} + v(1-v)x^*_{t-2} \ldots . + v(1-v)^i \, x^*_{t-i-1}\} \qquad (2.4.2)$$

where $v = 1 - e^{-T/\tau}$, T being the sampling interval and τ the time constant. Thus it follows that

$$x_{t+1} = g(v \, x^*_t) + (1 - v) \, x_t \qquad (2.4.3)$$

which after putting $k = \frac{1 - v}{v}$ converts to

$$(1 + k\Delta) \, x^*_{t+1} = g x_t \qquad (2.4.4)$$

If a second order transfer function is to be described, it

could be built up from the first order units

$$(1 + k_1\Delta)y_{t+1} = g_1 x^*_t \qquad (2.4.5)$$

$$(1 + k_2\Delta)x_{t+2} = g_2 y_{t+1} \qquad (2.4.6)$$

On combining one obtains

$$(1 + k_1\Delta)(1 + k_2\Delta)x_{t+2} = gf(x^*_{t+1}, x^*_t) \qquad (2.4.7)$$

where $g = g_1 g_2$ and $f(x^*_{t+1}, x^*_t)$ is a function of the two previous sampled inputs to the system (Appendix 2.1). Equation (2.4.7) can be further generalized for considering oscillating systems which have complex time constants; however, limitations are placed on the development of the difference technique to higher order systems by the increasing complexity of the function on the right-hand side.

$$(1 + \theta_1\Delta + \theta_2\Delta^2)x_{t+2} = gf(x^*_{t+1}, x^*_t) \qquad (2.4.8)$$

2.4.2. Dead times

The mathematical representation of a signal subject to a transport lag, or more generally to a dead time, is based on the assumption that the signal is continuous, and that its trajectory between adjacent sampling points can be described by a straight line.

$$\therefore y_t = (1 - \lambda)x^*_t + \lambda x^*_{t-1} \qquad (2.4.9)$$

λ being the dead time measured as a proportion of the sampling step. Should the dead time be larger than j but less than $j + 1$ sampling steps, then (2.4.9) is modified to

$$y_t = (j + 1 - \lambda)x^*_{t-j} + (\lambda - j)x^*_{t-j-1} \qquad (2.4.10)$$

2.4.3. Limitations

Although the technique described for modelling linear transfer functions appears to be reasonably straightforward, it does suffer from the disadvantage that the right-hand side of (2.4.8) becomes more difficult to formulate as the order of the system increases.

Secondly, when considering systems having discrete inputs, (2.4.10) could in no way be considered as giving a true picture of the delayed input signal; however this does describe adequately what is occurring to the output if used in conjunction with the system's transfer functions.

2.5. Control Application

The application to feedback predictor control of the techniques outlined in (2.3) and (2.4) is given here as a preliminary introduction to their use in the more complex situation of adaptive optimization.

2.5.1. Deriving stochastic predictor

The derivation of the equations necessary for designing a predictor controller is carried out for a general single controllable parameter system as illustrated in Figure (2.1). The process is acted upon by the control signal and the disturbances, thus the output signal is considered to be made up of

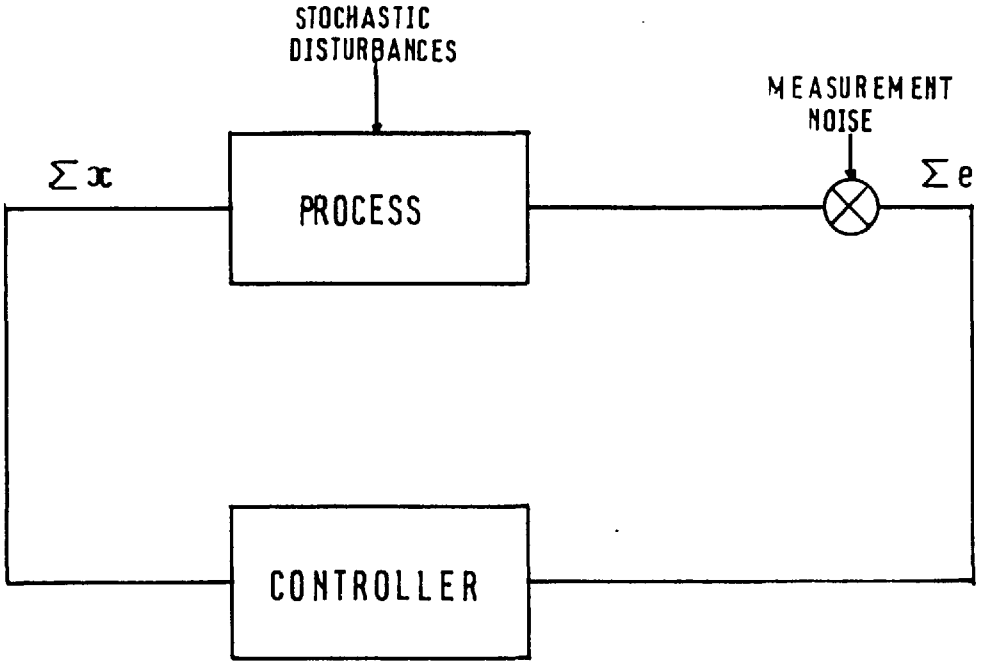

FIGURE 2.1 PROCESS AND CONTROLLER SUBJECT TO RANDOM NDISE

two components: X due to the former, and η due to the latter (the disturbances). There is also a further source of error m, because of the measurement instruments, which is taken to be random. The objective of the controller is to minimize the deviations of the output from a set point, hence knowledge of the resultant effects on the output due to the disturbances is helpful in obtaining the best possible controller design. Because the measurement errors have been assumed random they cannot have any correlation with the disturbances, so it is reasonable to consider the two jointly.

$$\therefore \; n_p = \eta_p + m_p \qquad (2.5.1)$$

It is now possible to specify the changes that take place in the measured deviations from the set point during the interval p to $p + 1$:

$$e_{p+1} - e_p = n_{p+1} + x_{p+1} \qquad (2.5.2)$$

Knowing the dynamics of the system and the history of control increments x^*, the x's can be evaluated and therefore the series of n's isolated.

$$n_{p+1} = e_{p+1} - e_p - x_{p+1} \qquad (2.5.3)$$

The methods outlined in (2.3) can now be used for modelling the time series.

Unfortunately the above algorithm for separating the disturbances depends on knowledge of the system's dynamics, a factor which is not always readily available. In such cases there are two alternatives:

(i) a dynamic model is assumed and used as above in generating a series of effects due to disturbances; this is analysed and the sum of squared random residuals generated. The dynamic model is now readjusted using a non-linear hill-climber and the process repeated until the sum of the squared residuals is considered to be minimized;

(ii) it is assumed that the dynamic and stochastic models have given structures which allow the residuals to be calculated directly. Once again however a hill-climbing programme is necessary to fit the parameters to the combined model which minimize the sum of squares of the errors.

The advantage of the first method is that generally sufficient is known about the system for a reasonable initial dynamic model to be generated, and thus greater analysis of the stochastic process may be carried out. Box and Jenkins (B3) however proposed the latter method on the basis that in many instances very simplified structures are sufficient to describe both system and disturbance. It is this one which is used as the foundation of most work presented here.

Assuming a first order transfer function the effects of the control action are given by:

$$(1 + k\Delta)x_{p+1} = gx^*_p \qquad (2.5.4)$$

However, because there is also a dead time λ this has to be modified to

$$(1 + k\Delta)x_{p+1} = g\left((1-\lambda)x_p^* + \lambda x_{p-1}^*\right) \qquad (2.5.5)$$

$$\therefore\ x_{p+1} = \frac{1}{1+k}\left\{kx_p + g\left((1-\lambda)x_p^* + \lambda x_{p-1}^*\right)\right\} \qquad (2.5.6)$$

Taking the process to be of the type

$$n_{p+1} = \varepsilon_{p+1} + (\gamma_{-1}\Delta + \gamma_0 + \gamma_1 S)\varepsilon_p \qquad (2.5.7)$$

where the ε's are random terms and $S\varepsilon_p = \sum_{i=0}^{\infty} \varepsilon_{p-i}$.
Introducing the backward shift operator B converts (2.5.7) to

$$(1 - B)n_{p+1} = \varepsilon_{p+1} + \left(\gamma_{-1}\Delta^2 + \gamma_0\Delta + (\gamma_1 - 1)\right)\varepsilon_p \qquad (2.5.8)$$

Thus it is seen that the process is being modelled by an integrated MA process of order (1,3).

Combining (2.5.3), (2.5.6) and (2.5.7) now yields

$$\varepsilon_{p+1} = e_{p+1} - e_p - x_{p+1} - (\gamma_{-1}\Delta + \gamma_0 + \gamma_1 S)\varepsilon_p \qquad (2.5.9)$$

The parameters λ, g, k, γ_{-1}, γ_0, γ_1 are now fitted to minimize the sum of squared ε's.

2.5.2. Using stochastic-dynamic model

Assuming that no control action is being taken in the system, the one step ahead predictor of deviations from the set point is obtained from (2.5.2)

$$\hat{e}_{p+1} = e_p + \hat{n}_{p+1} \qquad (2.5.10)$$

the error in the predictor being ε_{p+1} (2.5.7). To minimize the deviations control action should be taken at the sampling time p so that

$$e_p + \hat{n}_{p+1} + x_{p+1} = 0 \qquad (2.5.11)$$

which means that the new deviation at the instant $p + 1$ will in fact be ε_{p+1}. Therefore application of the combined optimal dynamic-stochastic model reduces the deviations of the system to a random sequence, a situation that cannot be improved upon.

Developing (2.5.11),

$$x_{p+1} = - e_p - \hat{n}_{p+1} \tag{2.5.12}$$

$$= - \varepsilon_p - (\gamma_{-1}\Delta + \gamma_0 + \gamma_1 S)\varepsilon_p \tag{2.5.13}$$

which on combining with (2.5.6) gives

$$g\left((1-\lambda)x_p^* + \lambda x_{p-1}^*\right) = (1 + k\Delta)\left(\gamma_{-1}\Delta + (1+\gamma_0) + \gamma_1 S\right)\varepsilon_p \tag{2.5.14}$$

$$x_p^* = \frac{1}{1 - \lambda}\left\{- \lambda x_{p-1}^* + \frac{1}{g}\left(k\gamma_{-1}\Delta^2 + \{k(1+\gamma_0) + \gamma_{-1}\}\Delta + \{k\gamma_1 + (1+\gamma_0)\} + \gamma_1 S\right)\varepsilon_p\right\} \tag{2.5.15}$$

Should it be found necessary, further fitting can be carried out by the same method, after trying the new control scheme on the process.

2.6. Application to Adaptive Optimization

Under certain circumstances, because of the way the disturbances affect the system, the control and adaptive optimization problems can be considered similar. In the control case the output signal is required to be kept as close as possible to a set point, the sampled deviations from this being taken as the error terms; the method assumes, however, that the steady-state gain of the system is constant, i.e. there is a

proportional relationship between the input and output signals. Similarly, in the adaptive optimization problem treated here, the disturbances are considered to move the objective function in a horizontal plane without changing either its shape or the height of its peak. The estimates of the gradient bear a direct relationship with the distance of the current operating point from the optimal one and are therefore taken as the error terms; also, initially at least the steady-state gain is taken as constant. The latter point requires that the surface of the objective function should have a parabolic shape; this limitation is considered further in section (2.6.2) and a method is put forward for reducing errors arising from it. The most serious snag encountered in applying the theory described in (2.5), to questing optimization of the Draper and Li type, is the inability to represent the system dynamics successfully.

2.6.1. Modelling dynamics

Box and Jenkins (B3) showed how three models, namely the steady-state gain, impulse response and dead time were sufficient for modelling a linear dynamic system. Furthermore Kotnour (B4) states that the model obtained by this technique is suitable for describing the dynamics of the same system with an adaptive optimizer included, although he does state that difficulties are encountered when dealing with non-parabolic objective functions. As it has already been stated,

this latter point is dealt with in (2.6.2), and from physical considerations it seems reasonable to assume that the dead time term is readily transferable between the two types of system, therefore they will not be considered further. However, it is not immediately apparent what the transient behaviour of the optimizing system would be to a given disturbance. For intance, if a step change took place in the middle of a perturbing cycle, it could unbalance the sinusoid quite seriously and cause a sharp change in the estimated gradient. Because the mathematics involved in carrying out analytically the equivalent of an impulse response analysis on a system of known modular composition was found to be very complex, it was decided to perform a simulation study instead.

A flow diagram of the system chosen for the study is given in Figure (2.2). The process part is made up of a first order transfer function followed by a non-linear inertialess element representing a parabolic objective function. The optimizing section, seen at the end, consists of high pass filter, correlator and integrator. The process is then perturbed with a sinusoidal signal, the optimally delayed version of which is fed to the correlator. It is also assumed that the optimizer's integrator is sampled and reset once a cycle; this means that under steady-state conditions, the sampled value and the gradient of the objective function at the mean operating point differ only by a multiplying constant. Clearly for a given system, the value of this constant depends solely on the

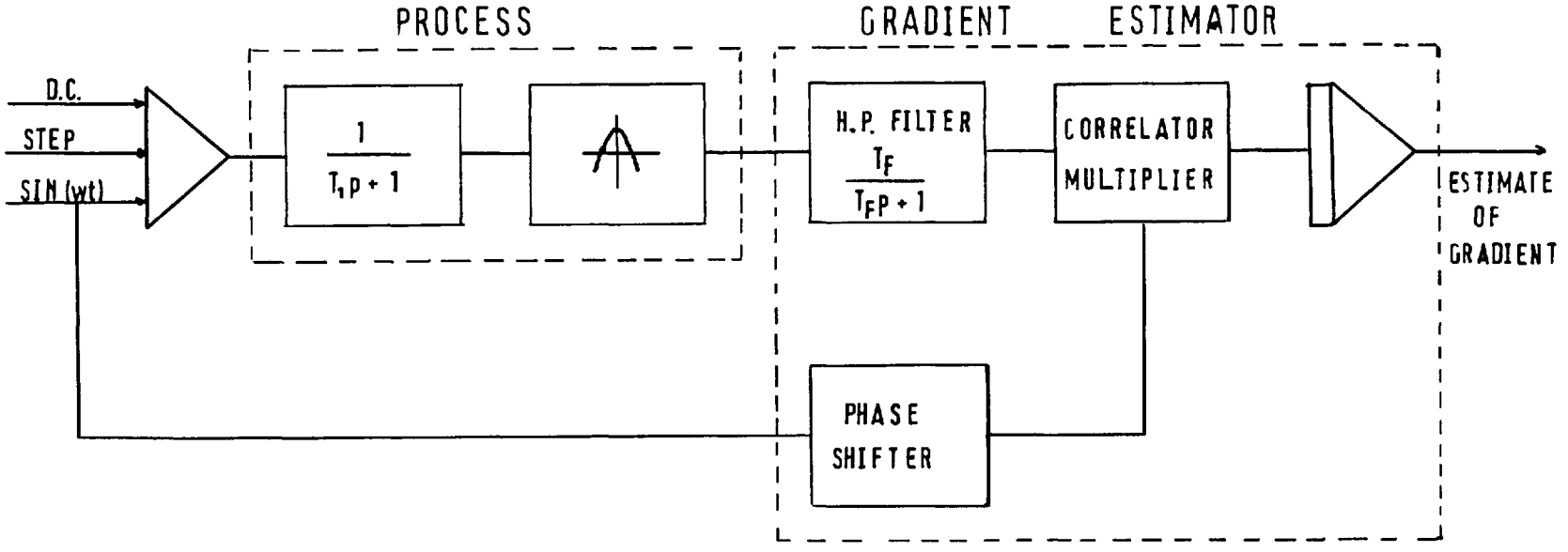

FIGURE 2.2 SYSTEM USED IN TRANSIENT SIMULATION

amplitude and frequency of the perturbing signal.

Analysis of the proposed system was carried out using Laplace transform techniques; this, however, introduced difficulties at points where non-linear operations had to be performed, namely in the objective function and correlator elements. To overcome this hurdle, it was necessary to invert the transforms, carry out the non-linear operation and reformulate the Laplace transform. Having developed the analytical method for dealing with step functions (a detailed description of which is given in Appendix 2.3), a computer programme was written.

Consider a step function entering a system in steady-state; as a result of the dynamics a transient occurs before the new steady-state level is reached. If the system is also considered to be subject to a sinusoidal perturbation which estimates the slope, then at each steady-state condition the correlator will give a value proportional to the true slope, however between the steady-state conditions the transients will affect the value. The object of the simulation was to study the behaviour of this transient.

In a system which is changing level, the transient is generally defined as a dimensionless quantity equal to the change that has taken place up to the time of measurement, divided by the difference between the two steady-state levels. By analogy, here the transient is taken to be the change in

slope measurements divided by the difference between the two steady-state values. Thus if the system were still at its first value, the ratio would be zero, and if at its second steady-state value it would be one.

TABLE 2.1: Parameters describing system used in simulating transient of a step input.

Parameter of parabola	= 1
Distance of mean operating point from optimum	= 4
Time constant of transfer function	= 101
Periods of peturbing sinusoid	= 300
	= 100
	= 10
Time constants of H.P. filters	= 300
	= 100
	= 10
Amplitude of perturbing sinusoid	= 1
Magnitude of step change	= 1

Table 2.1 summarizes the system parameters used in the simulation. Figures (2.3) and (2.4) show the results obtained for a questing sinusoid of unit amplitude and a unit step change. The time along the abscissa defines the

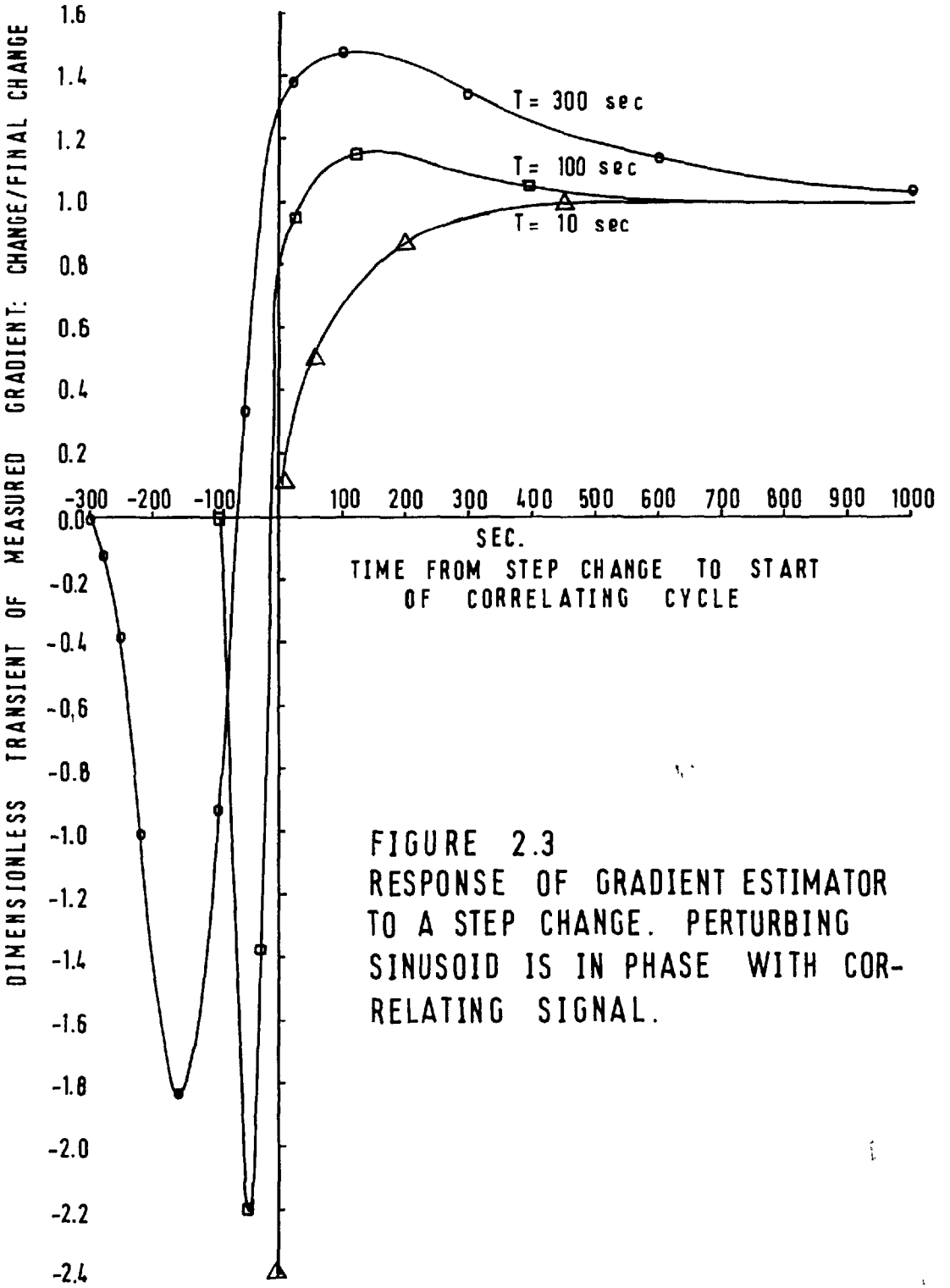

FIGURE 2.3
RESPONSE OF GRADIENT ESTIMATOR TO A STEP CHANGE. PERTURBING SINUSOID IS IN PHASE WITH CORRELATING SIGNAL.

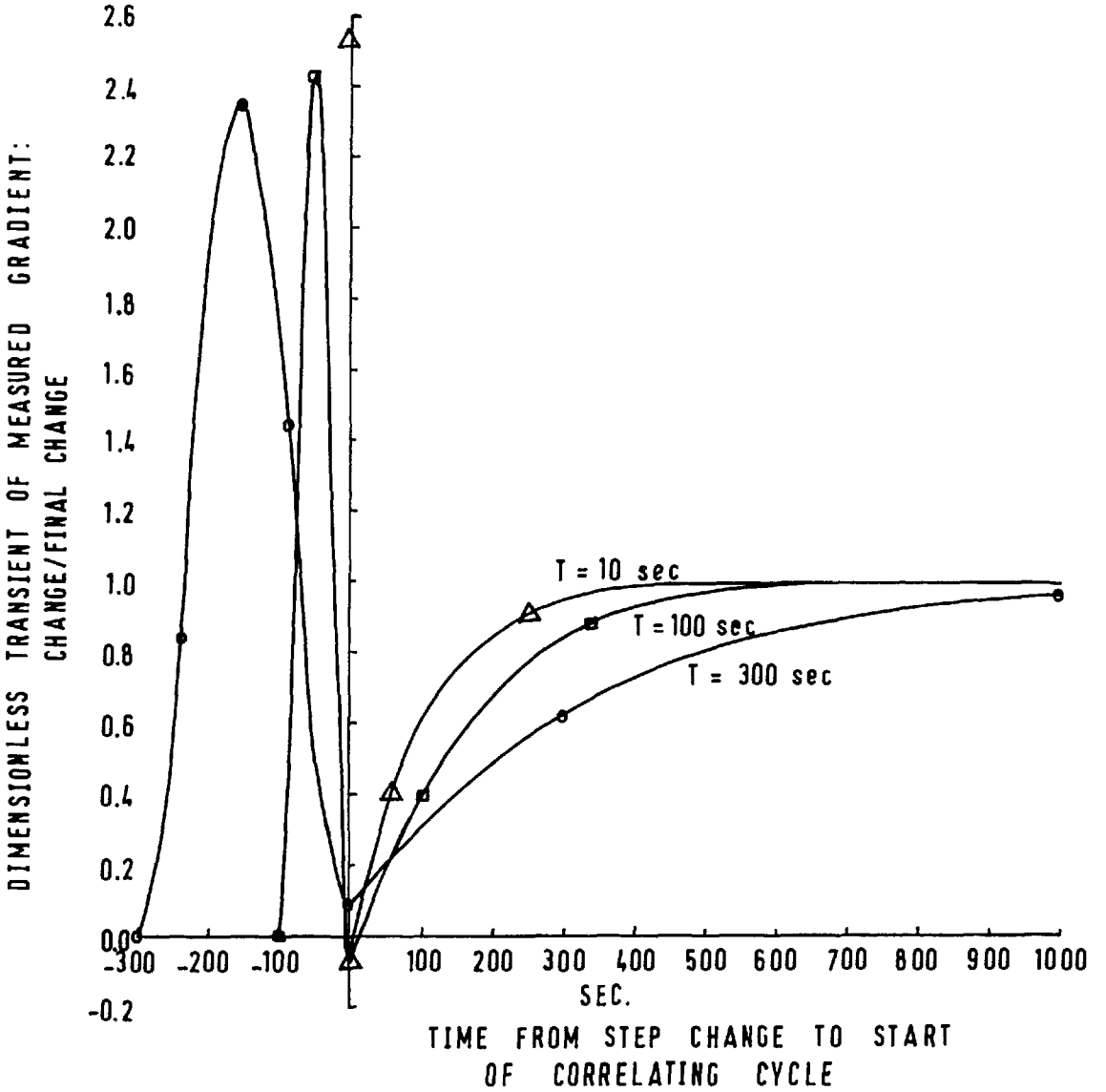

FIGURE 2.4 RESPONSE OF GRADIENT ESTIMATOR TO A STEP CHANGE. PERTURBING SINUSOID IS 180° OUT OF PHASE WITH CORRELATING SIGNAL.

age of the step change at the start of the sinusoid being examined, thus negative times refer to steps entering after the start of this particular sinusoidal cycle, and because this cycle is of only limited duration the curves end at the negative value which gives the magnitude of the sinusoid's period. A point on a graph at a given time t seconds is the transient value of the slope obtained from the interaction of the sinusoidal cycle used in the estimation of the slope and the step change taking place t seconds before the start of the cycle. The difference between (2.3) and (2.4) is that in the first case the amplitude of the perturbing signal was 1 and in the second it was - 1. For the particular conditions set here, the magnitude of the steady-state slope at the initial operating point has a value of 4 when plotted on either (2.3) or (2.4).

To understand better what is being illustrated by Figures (2.3) and (2.4), the components making up the transient for the sinusoid of period 300 seconds were plotted in Figure 2.5. It will be noted that, from Appendix 2.2, the response can be broken down into three components that depend on b^2, bx and ba,

where b = size of step change,

a = amplitude of perturbing sinusoid,

x = distance of mean operating point from the optimum.

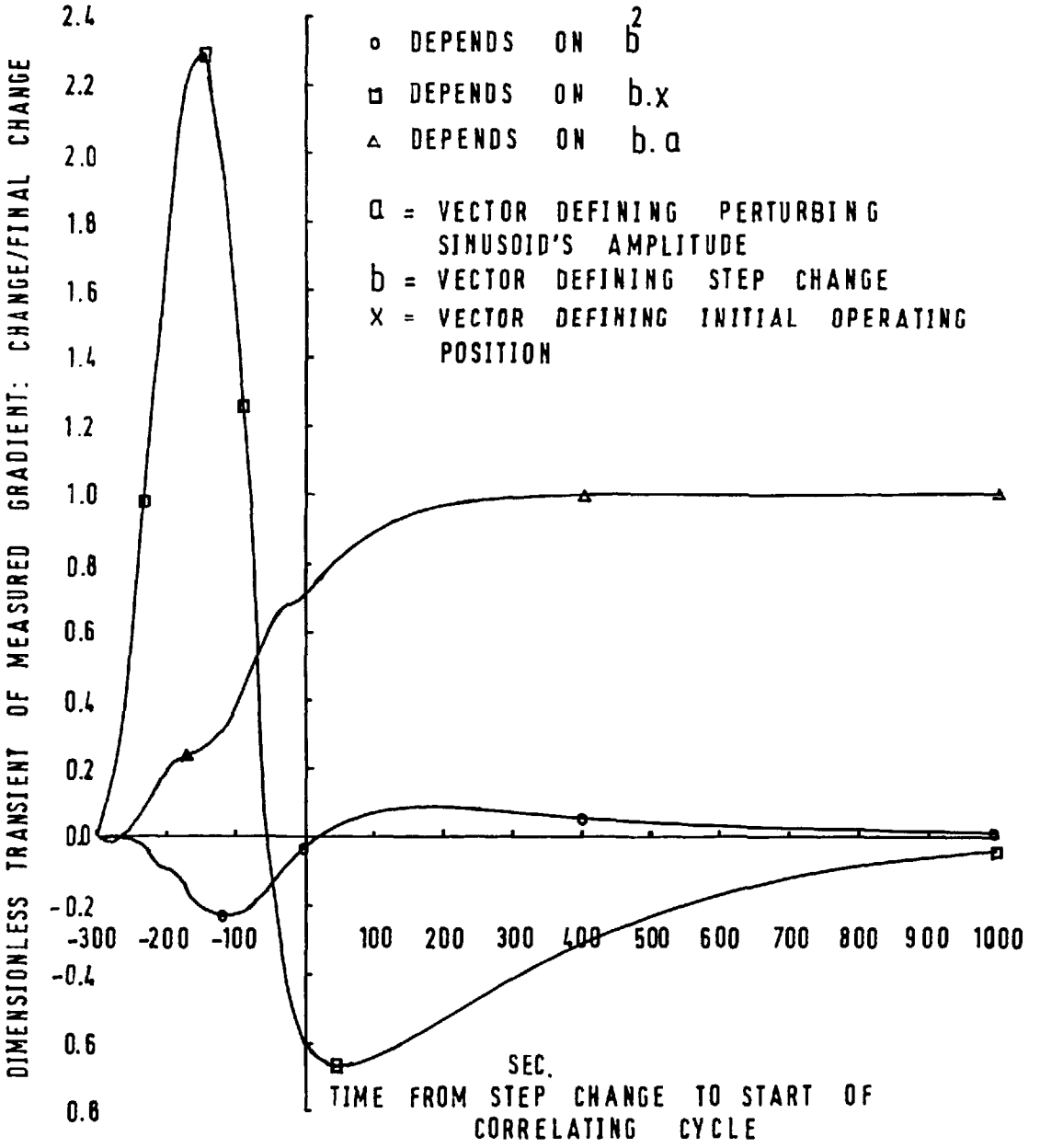

FIGURE 2.5 COMPONENTS MAKING UP THE T = 300 sec. CURVE SHOWN IN FIGURE 2.4

It has already been stated that the transients are made dimensionless by dividing through by the final change, now it happens that this change depends solely on the "ba" component, thus it follows that this is the only component that does not return to zero and also in its dimensionless form it will always have the same sign. However, the "b^2" component will change sign if either a or b change and similarly the "bx" component if either a or x change sign. Hence the conclusion reached is that a change in the sign of one variable must be accomponied by a change in the sign of the other two in order to obtain identical transients.

In normal operation a will remain constant while b and x will be subject to change; these changes will control the relative magnitudes of the peaks of the "b^2" and "bx" components, and it will be noted that as b or x pass through zero so the relevant dependent component will flatten to zero before forming peaks on the other side of the abscissa. Therefore in modelling the transients due to the "b^2" and "bx" components account must be made of the changes taking place in b and x. One possible method is to introduce a gain factor which varies depending on the value of the relevant parameter. Generally, the value of b will be known, but when using a predictor-optimizer as described in the first part of this section, values for x are only found indirectly from the estimates of the slope.

When describing the shape of the components, it would appear that the "ba" component could be modelled by the step response of a first order transfer function. In the case of the other two components the problem is more difficult, though for simplicity the impulse response of a second order transfer function would probably suffice, even though complete damping (as found in Figure 2.5) will not generally occur after the second peak.

On the basis of the present analysis modelling of the transient would require the fitting of one parameter for the "ba" component, and for each of the other two: one parameter for the variable gain and two for the second order transfer function. This means that a total of seven parameters would have to be fitted, although further simplification could possibly be made, by ignoring the "b^2" component, which would reduce the dimensionality to four.

Thus to summarize: the errors encountered in obtaining the estimates of the gradient for a system subject to step changes, depend on the rate at which the changes are entering and the position at which the system is being operated. Also it is found that difficulties encountered in correcting for the errors are due to the large dimensionality of the model describing the dynamics and the need to know the mean operating point.

Although this simulation does not offer an adequate

method of modelling the transients encountered, it does show up the inadequacies of using the same dynamic equations for both the control and optimization problems.

2.6.2. Asymmetric objective functions

Consider a quadratic symmetric objective function of the form:

$$y = \underline{y} - a(x - \underline{x})^2 \qquad (2.6.1)$$

where: y = current profit

$\underline{y}$ = maximum profit for parabolic objective function

x = current operating point

$\underline{x}$ = operating point for maximum profit on parabolic objective function

a = parameter of parabola.

If the system is now assumed to be subject to random Gaussian distributed disturbances having mean μ and variance σ^2, then the probability of operating between the points $x - \frac{dx}{2}$ and $x + \frac{dx}{2}$ is

$$dP_x = \frac{1}{\sigma\sqrt{2\pi}} \exp\{-(x - \mu)^2 / 2\sigma^2\}dx \qquad (2.6.2)$$

and the resulting probability of the loss incurred through operating at that point is

$$dP_{\text{loss}} = a(x - \underline{x})^2 \frac{1}{\sigma\sqrt{2\pi}} \exp\{-(x - \mu)^2 / 2\sigma^2\}dx \qquad (2.6.3)$$

Thus the total expected loss is

$$E\{\text{loss}\} = \int_{-\infty}^{\infty} a(x - \underline{x})^2 \frac{1}{\sigma\sqrt{2\pi}} \exp\{-(x - \mu)^2 / 2\sigma^2\}dx \qquad (2.6.4)$$

Making the substitution

$$z^2 = (x - \mu)^2 \;/\; 2\sigma^2 \qquad (2.6.5)$$

converts (2.6.4) to

$$E\{\text{loss}\} = \int_{-\infty}^{\infty} \frac{a}{2} \{(\mu-x)^2 + 2(\mu-\underline{x})\sigma\sqrt{2}z + 2\sigma^2 z^2\} \frac{2}{\sqrt{\pi}} e^{-z^2} dz \qquad (2.6.\ )$$

Solving

$$E\{\text{loss}\} = a(\mu - \underline{x})^2 + a\sigma^2 \qquad (2.6.7)$$

Thus the minimum expected loss for a parabolic surface is $a\sigma^2$, a result which confirms the findings of Fel'dbaum (F2).

Introduction of a cubic asymmetry gives an objective which would look something like

$$y = \underline{y} - a(x - \underline{x})^2 + b(x - \underline{x})^3 \qquad (2.6.8)$$

which is sketched in Figure (2.6) using the parameters given in Table 2.2.

TABLE 2.2: Parameters of asymmetric objective function

$\underline{y}$	$\underline{x}$	a	b
28.0	5.0	1.0	0.15

$$E\{\text{loss}\} = \int_{-\infty}^{\infty} \left(a(x-\underline{x})^2 - b(x-\underline{x})^3\right) \frac{1}{\sigma\sqrt{2\pi}} \exp\{-(x-\mu)^2 \;/\; 2\sigma^2\}\, dx \qquad (2.6.9)$$

Substituting in (2.6.5) and integrating,

$$E\{\text{loss}\} = a\left((\mu-\underline{x})^2 + \sigma^2\right) - b\left((\mu-\underline{x})^3 + 3(\mu-\underline{x})\sigma^2\right) \qquad (2.6.10)$$

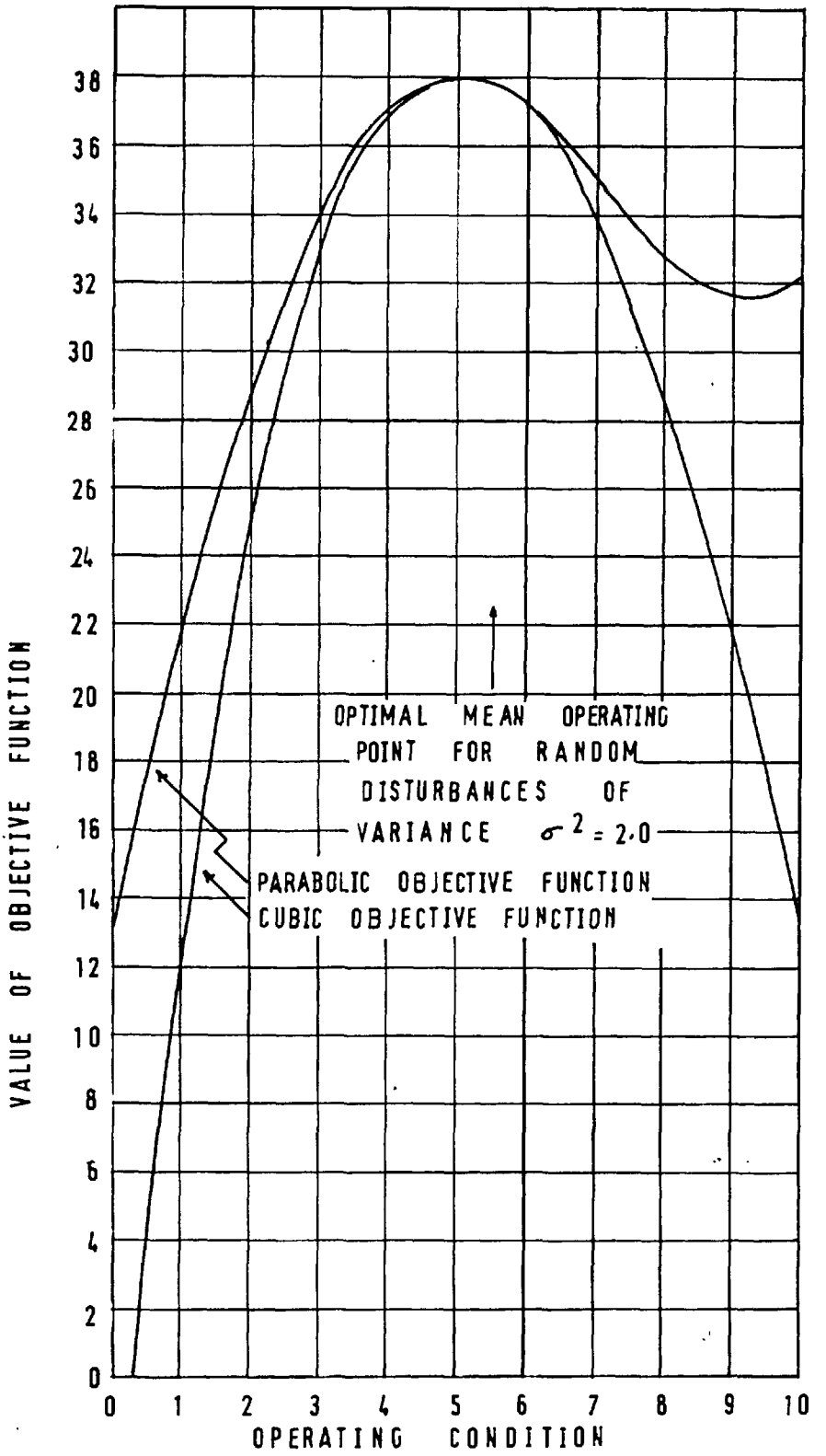

FIGURE 2.6 ASYMMETRIC OBJECTIVE FUNCTION

$$\frac{dE\{\text{loss}\}}{d(\mu-\underline{x})} = 2a(\mu - \underline{x}) - 3b\left((\mu - \underline{x})^2 + \sigma^2\right) \qquad (2.6.11)$$

$$\frac{d^2E\{\text{loss}\}}{d(\mu-\underline{x})^2} = 2a - 6b(\mu - \underline{x}) \qquad (2.6.12)$$

From (2.6.11) the stationary values are shown to exist at

$$\mu = \underline{x} + \frac{2a \pm \sqrt{4a^2 - 36b^2\sigma^2}}{6b} \qquad (2.6.13)$$

Now it can be verified that the maximum point on the objective function is $\underline{x}$. Hence it has been shown that on an asymmetrical surface the mean point of operation for minimum loss when disturbances are taking place does not coincide with the optimum point.

Usually, however, an analytical description of the surface is not available, in which case an alternative procedure of finding the optimal mean operating point is:

(1) break the surface down into discrete sections,

(2) choose a value for the mean operating point μ,

(3) calculate the probability p of being in a given section, and the loss l incurred through being there,

(4) find the expected losses through operating at μ by summing the product pl over the whole surface,

(5) repeat from (2) until the minimum value for the expected losses has been found.

Finally, in order to use this method in conjunction

with a predictor optimizer, the estimates of gradient obtained by the correlator must be converted into estimates of deviations of the controllable variable from the optimal operating point. The predictor regulator is then fitted and the variance of the random errors calculated. A bias term for operating away from the steep side of the response surface may then be evaluated using the algorithm given above.

CHAPTER 3

THE EXPERIMENTAL APPARATUS

3.1. Introduction

In this chapter a description of the process used is given. Although most of the construction was originally done by Price (P6) and Kisiel (K4), and therefore reported by them, for the purpose of completeness a summary of the design and construction of the apparatus is made. Finally, a brief account of how the instruments were calibrated is also included.

3.2. Overall Description of Process and Equipment

The water gas shift reaction entails the combination of steam and carbon monoxide to give carbon dioxide and hydrogen as shown by equation 3.1.1.

$$CO + H_2O \text{ (gas)} \rightleftarrows H_2 + CO_2 - 9.83 \text{ Kcals} \qquad (3.1.1)$$

A flow diagram of the process together with the instrumentation employed is given in Figure 3.1.

Pure dry gases were fed from cylinders at a pressure of 15 psig, through rotameters where the flow was measured, to a mixer. So as to simplify the operation of the system, the total dry gas flow rate was always maintained constant. Although industrial dry gas compositions were simulated as far as possible, it was considered to be more important to operate at an average molecular weight equal to that of water.

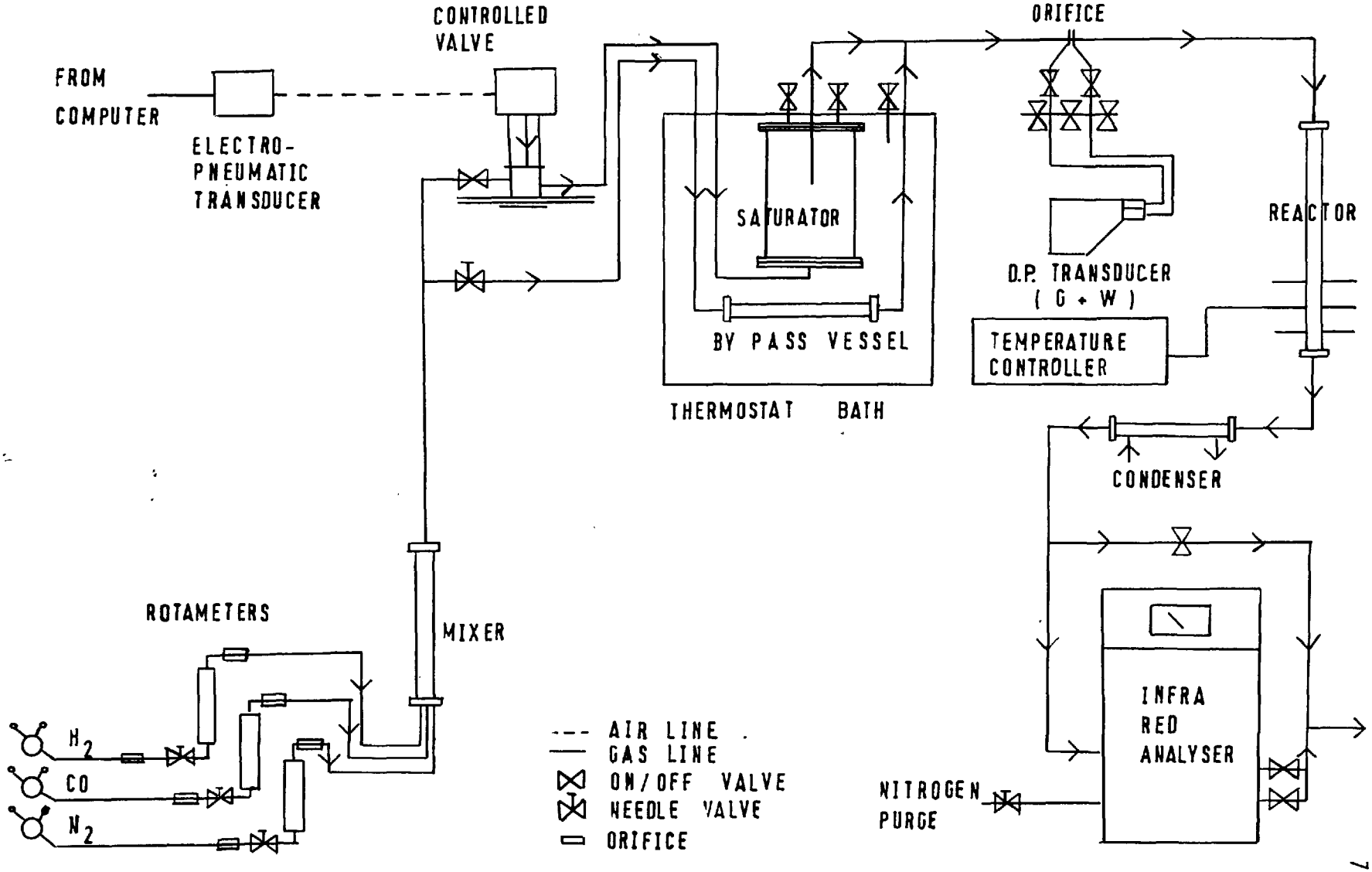

FIGURE 3.1 FLOW DIAGRAM OF PLANT

The combination of flow rates used to give this were:

Carbon monoxide	9.0 l/hr
Hydrogen	20.8 l/hr
Nitrogen	23.2 l/hr

Saturator

After passing through the mixer, which was a cylindrical copper tube 1' long and 1" diameter packed with 550 micron sand, the gases were split into two streams. One stream flowed through the saturator, a vessel 12" high and 6" in diameter, filled with water and immersed in a constant temperature oil bath maintained at 100°C; the other went through a 650 cc empty vessel also immersed in the bath; this allows some time for the gases to heat up and because of the added capacity reduces any surging that might occur due to changes in the relative flow through each branch. The above arrangement is a novel technique for introducing accurately small quantities of steam, the ratio of dry gas flowing through each branch being varied by using the pneumatic control valve placed just upstream of the saturator; when this was half open the upstream pressure was adjusted to 4 psig by a needle valve in the by-pass line. Unfortunately the upstream pressure would vary by as much as ± ½ psig over the range of operation of the pneumatic valve; however, the anticipated variations in rotameter and other flow meter calibrations were not as important as at first expected.

Beyond the saturator the two gas streams were reunited and heated to prevent condensation, before having their combined flow rate measured.

Reactor

The gases were now ready for feeding to the reactor (Figure 3.2) which was a 2' long, 1" diameter cylindrical copper tube vertically mounted. 6" from the bottom and at successive 2" intervals were pairs of thermowells placed diametrically opposite each other. Starting at the bottom there was first 69 cc of 1100 micron sand, followed by 40 cc of 650 micron ICI CO shift catalyst sandwiched between two layers of 7.5 cc of sand also of 650 micron nominal diameter, and finally there was a top stratum of 72 cc of 1100 micron sand. The whole packing was kept in position by a stainless steel gauze at the bottom of the tube.

In order to carry out isothermal operation of the reactor it was necessary to supply heat to the system. This was done by three heaters mounted in parallel. The first, which consisted of nichrome ribbon wound directly on to the tube, acted basically as a preheater getting the gases up to the reaction temperature. The next section was heated using the same element material wound separately onto two half-cylinder formers which were clamped in position around the catalyst and connected in series. Finally the end effects heater was of the same design as the preheater. To ensure

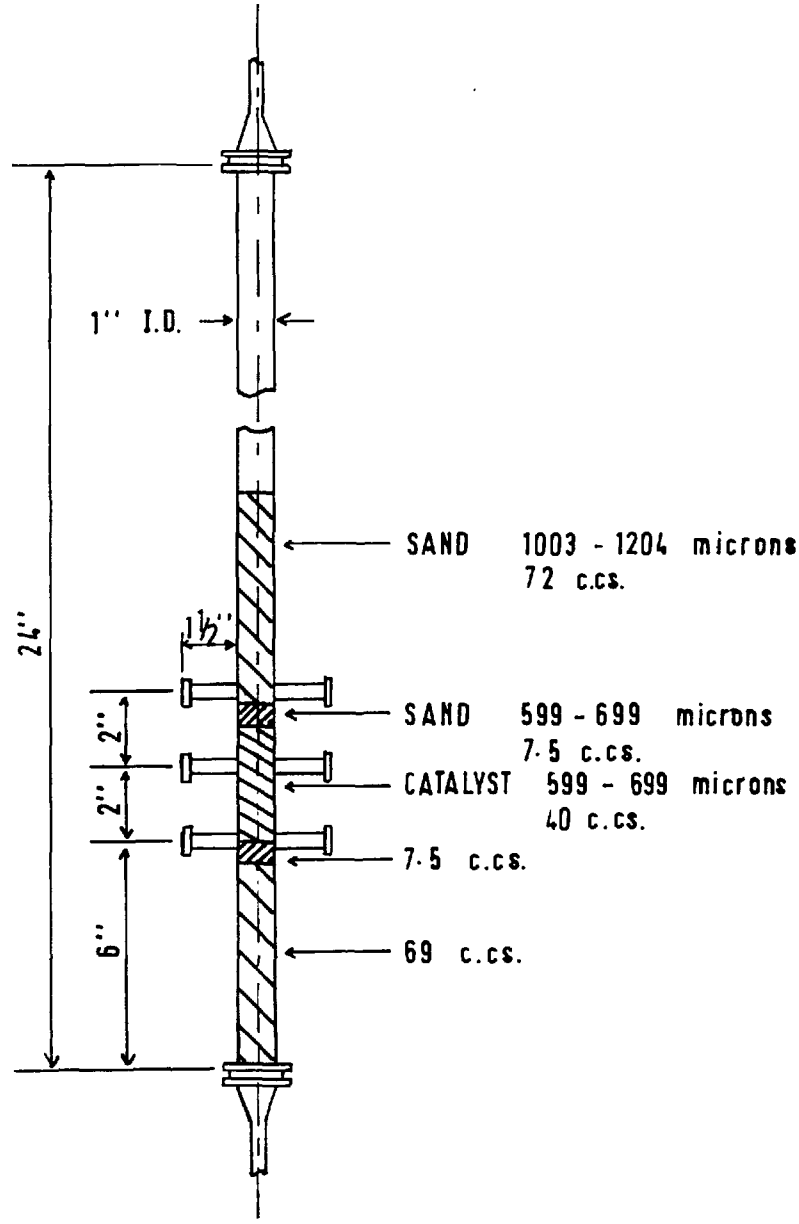

FIGURE 3.2 REACTOR

an equal temperature throughout the catalyst bed, balancing of the power output of the heaters to obtain a constant longitudinal temperature was effected by incorporating rheostats in the pre- and end effects heater circuits.

Analyser

On leaving the reactor the gases were cooled to approximately room temperature by passing through an 8" long, 1" diameter water cooled condenser; final chemical drying was obtained by pushing them through a glass tube containing silica gel. The concentration of carbon monoxide in the dried exit gases was then measured continuously in an infra-red analyser from whence the gases were disposed of.

3.3. Instrumentation

Pressure upstream of the rotameters was measured and maintained at the cylinder reducing valves; downstream of the mixer this was measured with a straightforward Bourbon gauge; in no case was it possible to record these readings automatically.

Temperature was measured at the exit from the saturator, just after the orifice and in the reactor by chromel/alumel thermcouples. The reactor thermocouples were arranged so that at each level one read the temperature at the wall, and the other at the centre. An iron/constantan thermocouple placed on the wall of the reactor, but electrically insulated from it,

was used as a sensor for the temperature controller.

The pneumatic control valve was an Audco Annin type supplied by Gloucester Controls. The initial voltage signal fed to the system was converted via an electro-pneumatic transducer to a pressure signal in the range 3 - 15 psig.

The flow of steam and dry gas was measured before entering the reactor by throttling through an orifice plate; using a differential pressure transducer the pressure drop across the orifice was converted to an electrical signal. In order to get an approximately linear relationship with the flow rate being measured, the output signal was put through a square-rooting board before finally being recorded.

Control of the reactor temperature was effected using a proportional controller designed and built in the departmental electronic workshop. The error signal was provided by the difference between an input control signal, which could vary continuously, and the output from the iron/constantan sensor which had been suitably amplified. In this case of course, only the outside skin temperature of the reactor wall was controlled; however, measurements made later confirmed this to be sufficient for maintaining the same constant temperature throughout. As a safety precaution, the bottom wall thermocouple was connected to an on-off circuit, which would not allow the temperature there to rise above 510^{o}C.

All electric outputs and control signals were such that they could be measured or generated on a PACE analogue

computer. This required that the signal be a potential in the range 0 - 10 volts. Although it was possible to read thermocouple signals on the analogue computer, it was not advisable because of the errors introduced by the necessarily large magnifications. The PACE analogue equipment available was made up of a TR10, a TR20 and a HYBRID 48.

In order to be able to record accurately the state of the system, in a form ready for data processing, facilities were made for the inclusion of an Electronic Associates MDP 200 data logger in the recording equipment. Again, error was introduced in the reading of thermocouples; some was due to the system not having a high enough impedance and the rest, which only occurred sporadically, was because of bad common mode rejection in the case of low level signals. The former could be corrected for, because it was fairly constant throughout the range of operation. In the latter case, although it could be recognised, correction after the event was not generally possible. Accurate thermocouple measurements were always carried out with a potentiometer. The remaining recording equipment consisted of a variable speed 4-channel strip chart recorder with an acceptable input signal of 0 - 10 volts, and an Electronic Associates X-Y plotter.

Generation of the sinusoidal perturbation signal was carried out using an adjustable constant speed motor, and a sine-cosine potentiometer. By providing the latter with constant references of + 10 V, - 10 V and earth, it was

possible to obtain a sine and a cosine signal of amplitude 10 volts and mean zero. The frequency of the sinusoid was of course determined by the speed of rotation of the motor.

3.4. Calibration

Although Price (P6) had already calibrated the intrumentation used, it was decided to repeat his work because in some cases the conditions were slightly altered, and in others there appeared to be some inconsistencies present.

The rotameters were calibrated individually, with conditions being kept as close as possible to those at normal operation. The inlet pressure to the particular rotameter was set to 15 psig at the cylinder head. At the same time the gas was made to flow through the system as usual, with the pressure just before the saturator being maintained at 4 psig. On exiting from the plant, the total volume of gas was measured with a wet-gas flow meter. In order to ensure that the calibrations were consistent at all times, corrections had to be made for variations in atmospheric pressure and ambient temperature. Calibration runs were also carried out at pressures of 3.6 and 4.4 psig; they showed that an error of 3% was introduced per ½ psi deviation. Another inconsistency noted was that when there was more than one rotameter in operation the actual flow rate was higher than that predicted by the rotameter readings. This follows from the fact that a higher pressure differential is required

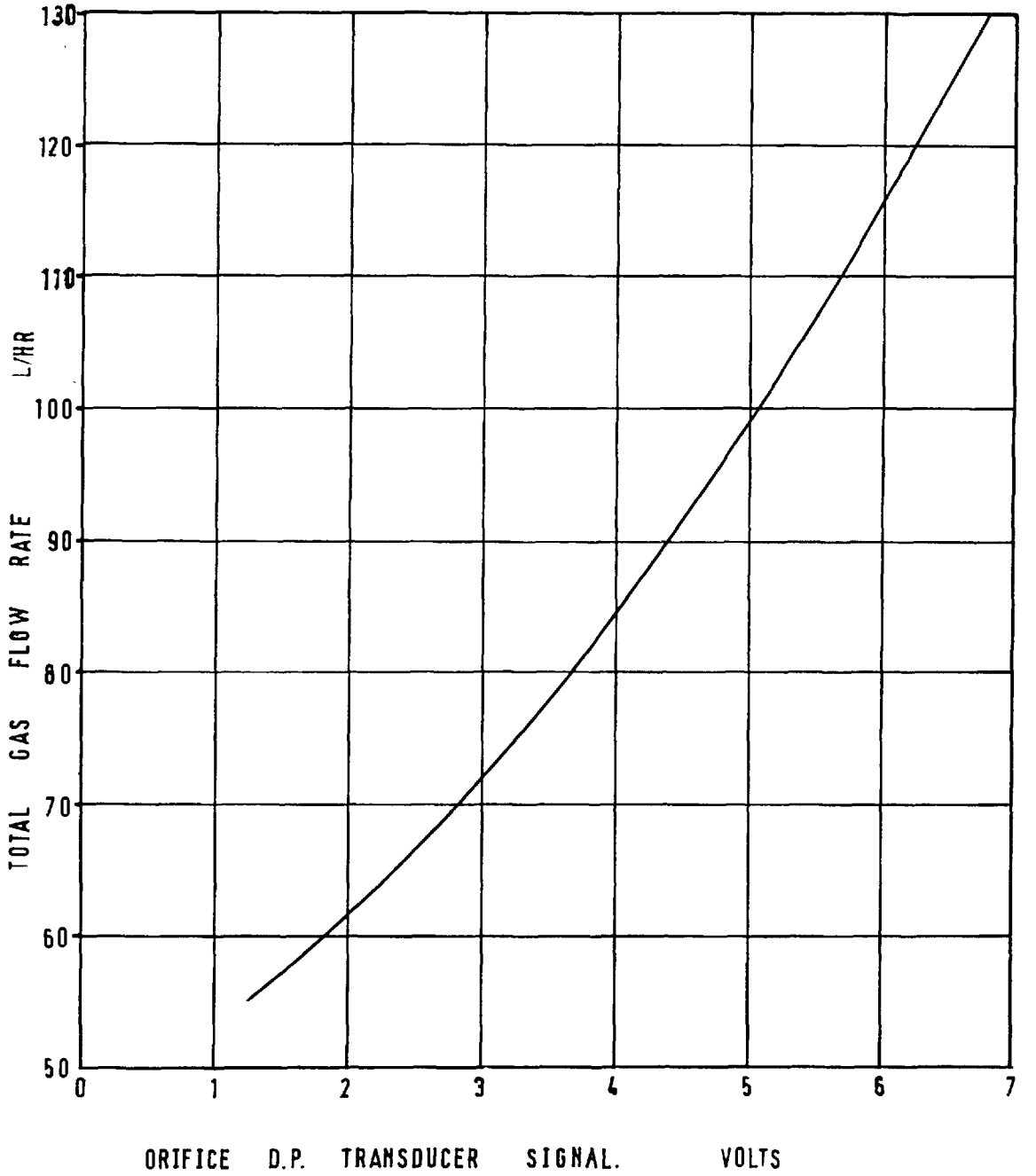

FIGURE 3.3 ORIFICE CALIBRATION

between the rotameter outlets and the point at which the pressure is being maintained at 4 psig; therefore the density is higher in the rotameters and the gases require a smaller area for flowing through. The simplifying assumption made for dealing with this case was that the increase in total flow rate over that predicted by the rotameter readings was due to equal proportional increases in the individual flow rates.

In the measurement of flow rates, two other sets of instruments required to be calibrated. Firstly, the orifice and differential pressure transducer placed just after the saturator were calibrated using nitrogen. Again the normal operating conditions were reproduced as closely as possible, both in respect of pressure and temperature. In the latter case adjustment of the power input to the heating tape was made to maintain the orifice temperature at 190^{o}C. The characteristic curve then had to be converted for dealing with a gas of the same average molecular weight as steam. This was easy, since for a given pressure drop across an orifice the flowrate is inversely proportional to the square root of the density. For purposes of simplification Price (P6) assumed the calibration curve to be linear throughout its range. Although this assumption is valid at the high end, it was felt to be erroneous in the lower part of the range, hence it was represented by the second order polynomial:

$$y = 47.28 + 5.14x + 1.03x^2$$

where y = total flow rate; x = orifice reading.

Table 3.1: Total steam and dry gas flow rates for different input voltages to the pneumatic control valve.

Signal to control valve volts	Total flow rate l/hr	Signal to control valve volts	Total flow rate l/hr	Signal to control valve volts	Total flow rate l/hr
9.58	71.64	5.27	50.61	3.75	30.45
7.85	63.10	9.32	70.05	3.14	24.44
5.73	51.99	3.11	21.82	7.38	68.21
6.95	59.96	7.04	61.01	8.63	73.93
4.97	44.41	4.98	46.61	6.46	61.62
8.61	66.35	8.64	67.53	9.50	76.80
4.93	44.43	6.39	57.25	4.86	49.26
6.42	55.90	9.52	70.53	7.37	67.28
9.51	67.28	3.77	27.82	5.97	57.41
8.96	66.94	7.85	64.04	6.57	65.12
9.35	68.14	5.62	52.07	9.56	79.71
4.34	39.12	3.11	21.78	7.14	68.05
7.58	60.47	8.33	67.09	3.39	29.74
6.83	57.54	9.87	70.79	5.63	58.85
3.16	21.52	3.74	27.21	8.92	76.90
3.94	30.14	4.95	45.64	3.14	24.84
5.75	52.71	9.72	71.41	4.29	43.71
9.42	67.96	7.68	62.14	5.02	52.04
4.18	36.24	7.04	60.22	7.01	68.59
6.01	53.50	6.01	55.86	6.00	58.47
7.82	64.12	5.16	52.39		

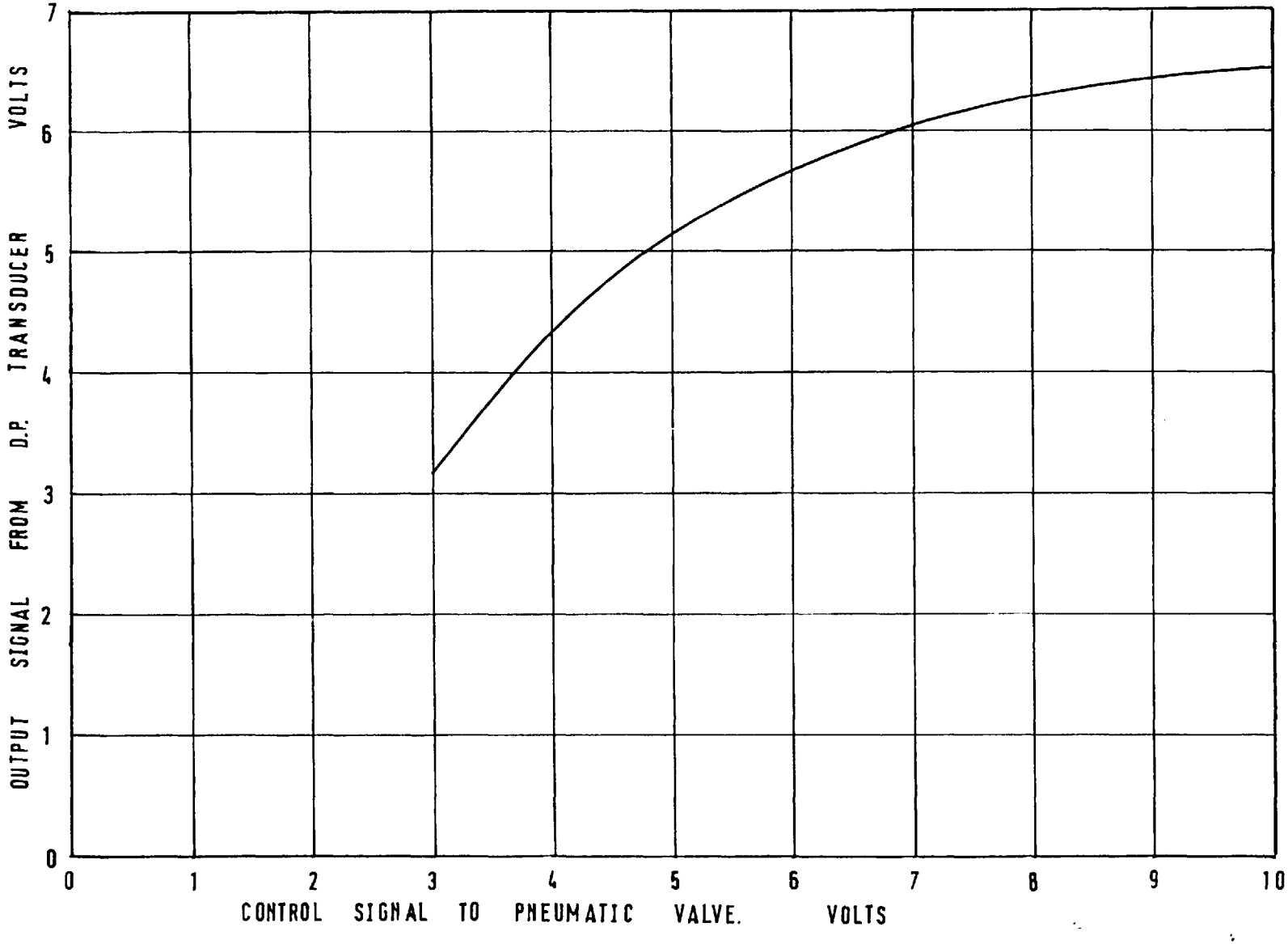

FIGURE 3.4 ORIFICE SIGNAL v VALVE CONTROL

Finally for use in a simulation model of the system, a knowledge of the relationship between the input signal to the pneumatic valve and the resulting output signal from the differential pressure transducer at the saturator orifice is needed. This characteristic was very dependent on the settings of the other valves in the by-pass and saturator lines. Because of this, once they were set the valves were never touched throughout the course of the experimental runs.

The infra-red analyser was an instrument which needed constant checking. Although calibration curves were provided by the manufacturers, the zero and sensitivity settings had to be continuously updated. In the latter case a mechanical obstruction was used for short term calibration work; however, even this device had to be checked over longer intervals by using a sample gas with a known carbon monoxide concentration.

CHAPTER 4

MODELLING THE SYSTEM

4.1. Introduction

In order to verify and extend any results obtained experimentally, it was found necessary to derive a dynamic simulation model of the plant together with its associated measurement and control instrumentation. Here the method in which it was done is described, and the differences arising between this and previous work are pointed out.

Former experimenters (K4, P6) have shown that the system may be broken down into blocks that consist either of linear intertial elements or non-linear inertialess elements, as shown by Fig. 4.1. Thus the development of the simulation model was carried out in three basic stages:

(i) steady-state studies to investigate the non-linear elements,

(ii) dynamic studies to obtain transfer function descriptions of the intertial blocks,

(iii) final assembly of the information produced to give the simulation model.

4.2. Steady-State Modelling

Figure 4.1 illustrates the fact that most of the non-linear blocks are essentially characteristics of measurement or control equipment, hence their modelling has been dealt with in the preceding chapter. However, some sort of model

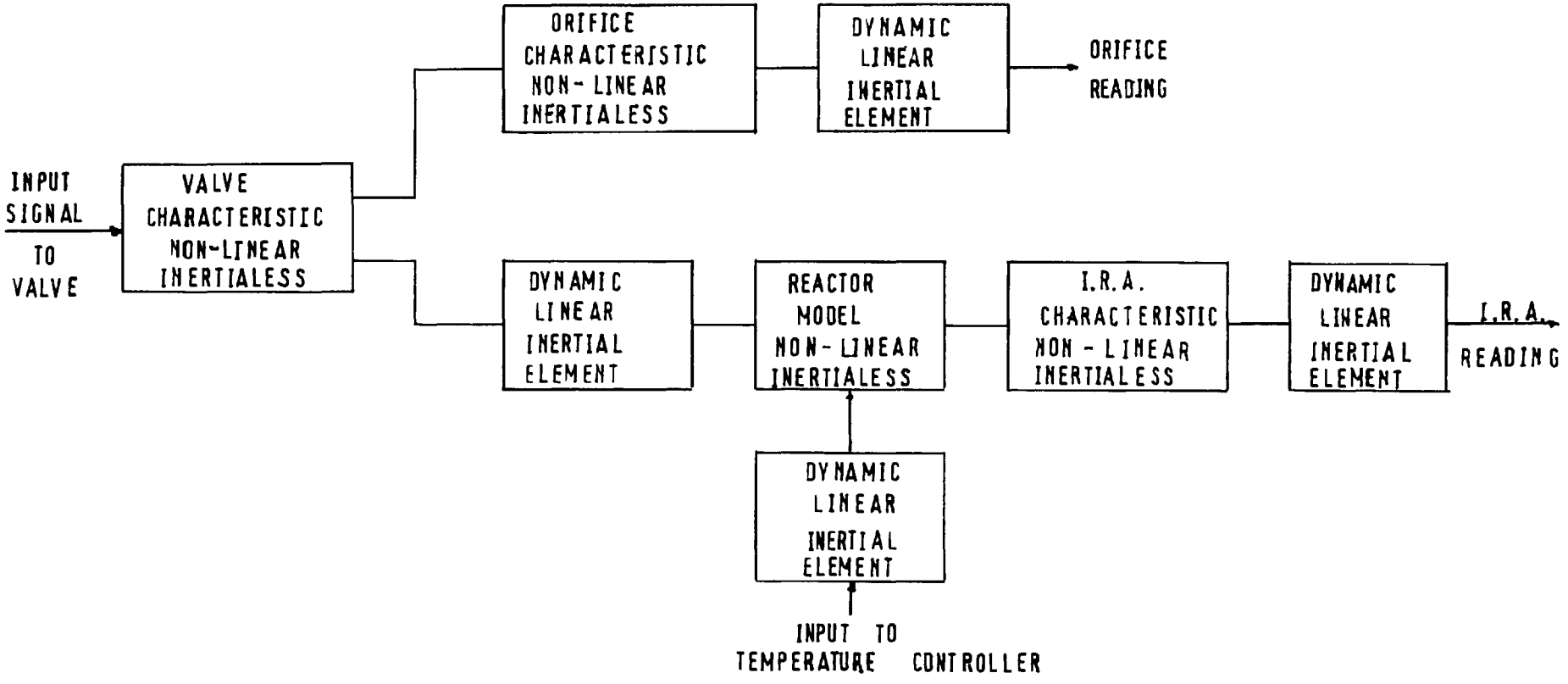

FIGURE 4.1 BLOCK DIAGRAM ILLUSTRATING STRUCTURE OF SYSTEM

of the reactor itself was still necessary for obtaining an overall steady-state description of the system. Kisiel (K4) and Price (P6) have already dealt extensively with this, but nevertheless the rebuilding of the system and replacement of the catalyst brought with them changes in conditions as a result of which re-evaluation of the parameters in the model was required. On this occasion the steady-state runs were also repeated at the end of the experimental programme to obtain a quantitative assessment of the change in catalyst activity. The section ends with a discussion on the objective function used in the later optimization work.

4.2.1. Reactor

Given an accurate description of the transport properties of the reactants, the structure and dimensions of the catalyst bed, both on the macro- and microscale, together with information regarding the thermodynamic and kinetic aspects of the reaction, it is possible to develop an accurate, but highly complex, dynamic model of the reactor (H2, M1). In the present instance a lot of information was still unavailable or dubious, also the dynamics of the rest of the system considerably outweighed those of the reactor, for which reason it was decided that a simpler steady-state model would suffice.

The basic assumptions made in deriving such a steady-state model were:

(i) that the plug flow state existed,

(ii) that the conditions were isothermal.

Although the first assumption is only valid for packed tubular reactors in which the particle to reactor diameters ratio is very small, it was felt to be adequate, providing a modification was made to account for the looser packing at the wall. The reactor was originally designed for isothermal operation, hence its small diameter and low mass of catalyst. However, apart from the thermocouples giving the same reading at different points in the bed, there is no other evidence to support the assumption of isothermal conditions; doubts arise here because of the possibility of heat conduction down the thermocouple sheaths from or to the wall of the reactor. Nevertheless, in the absence of concrete evidence to the contrary, the second assumption was also taken to be correct.

4.2.2. Plug flow model

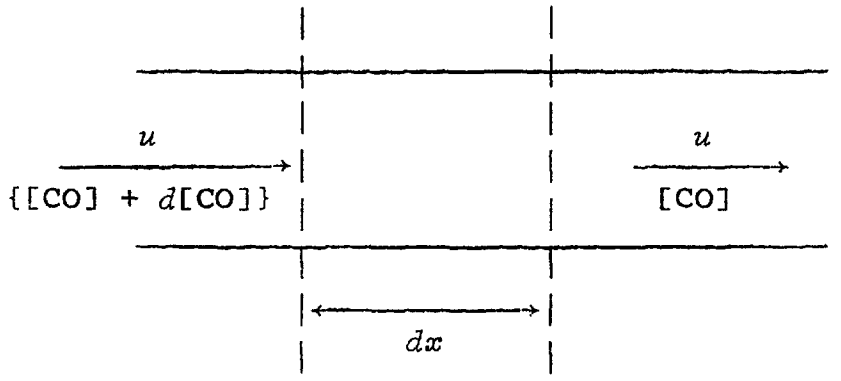

Figure 4.2: Longitudinal element of reactor

Consider a longitudinal element of the reactor of length dx, with reactants entering at a velocity u. Since

there is no change in volume due to either the stochiometry of the reaction, or changes in temperature or pressures, the velocity of the gases leaving should also be u. As shown in Figure 4.2, the difference in concentration of carbon monoxide entering and leaving the element is $d[CO]$. Carrying out a mass balance on the element one obtains

$$ua[CO] = ua\{[CO] + d[CO]\} + ra.dx \qquad (4.2.1)$$

where:

a = cross-sectional area of reactor,

r = moles of carbon monoxide produced per unit time and unit volume of the reactor.

$$\therefore \frac{d[CO]}{dx} = -\frac{r}{u} \qquad (4.2.2)$$

At this stage a decision had to be made on how the rate constant was to be defined. Kisiel (K4) compared three models of the kinetics, namely a first order model by Mars (M2), a pseudo second order one put forward by Moe (M3), and finally a log kinetic model which lay somewhere between the first two. He found that the fits given by Mars' and Moe's kinetic models were considerably better than that of the log model, but not significantly different from each other. On the basis of these results and because of its slightly greater simplicity, Mars' model has since been used in describing the steady-state response surface of the reactor.

4.2.3. Mars' kinetic model

Mars assumed the shift reaction to have such an excess

of steam present that the kinetics could be considered as being first order with respect to the concentration of carbon monoxide present. Because it is also a reversible reaction, the driving force is taken to be the difference between the actual concentration and that at equilibrium, the latter factor being calculated from the relationship

$$K_e = \frac{[CO]_{eq}\ [H_2]_{eq}}{[CO]_{eq}\ [H_2O]_{eq}} \qquad (4.2.3)$$

where:

K_e = equilibrium constant of the reaction,

$[A]_{eq}$ = concentration of component A at equilibrium. g. mole/cc.

Therefore the rate equation may be re-stated as:

$$\frac{d[CO]}{dx} = -\frac{k}{u}\{[CO] - [CO]_{eq}\} \qquad (4.2.4)$$

which after integrating gives

$$[CO]_{out} = [CO]_{eq} + \{[CO]_{in} - [CO]_{eq}\}e^{-(\frac{k}{u}x_o)} \qquad (4.2.5)$$

where:

k = kinetic constant,

x_o = length of catalyst packed bed.

4.2.4. Correction to plug flow model

It has already been stated that the plug flow assumption is only really applicable in cases where the reactor diameter to particle diameter ratio is large. Schwartz and Smith (S3) discovered that the greatest fluid velocity, which

was approximately twice that at the centre, was found at about one particle diameter from the wall, and this they considered to be due to the lower density of packing in that region. The model they suggested to describe this phenomenon, and which was used by both Kisiel and Price, involved breaking up the velocity profile into two regions; a central core and an annulus at the wall of about one particle thickness, the velocity in the annulus being taken as twice that in the central core.

The outlet carbon monoxide concentration predicted by the new model is obtained by solving the two sections as if they were independent reactors, and then averaging the results arithmetically.

4.2.5. Fitting model

Before any modelling of the reactor could be done, it was necessary firstly to reduce the freshly introduced catalyst, by the ICI recommended method, and then to operate with it until such time as its activity was considered to lie on the flat section of the ageing curve. It was hoped that after this stage, the catalyst activity would not change appreciably during the period in which it was required. Nevertheless, in order to gain some idea of its deterioration, the steady-state model was refitted after the experimental programme had been completed.

The system was now operated at different conditions of

constant temperature and flowrate, these being predetermined by a grid set up in the region of interest, i.e. 370 - 470°C and 20 - 80 l/hr of steam. After reaching equilibrium on each occasion, the outlet concentration of carbon monoxide together with other parameters describing the state of the system were recorded on the data logger. So as to reduce systematic error creeping in, the order in which experiments were carried out should have been randomized. However, because of the large time involved in allowing the system to come to equilibrium after changing the operating temperature, it was decided to carry out all runs at a given temperature sequentially. The order in which the temperatures were chosen and the setting of the steam flow rates was randomized however.

The fitting of parameters to Mars' kinetic model was carried out using Powell's (P7) non-linear hill-climber without derivatives, to minimize the sum of squared differences between values of outlet carbon monoxide concentration predicted by the model, and those obtained experimentally. A final check was made on the parameters fitted, using a hill-climber due to Marquardt (M4) and features present in this programme were used to generate both linear and non-linear confidence limits for the parameters. The variables that were thought reasonable to optimize were two defining the kinetic constant (4.2.6), two defining the thermodynamic constant (4.2.7), and possibly one specifying the thickness of the annulus in the reactor model:

$$k = \exp\left(a_k - \frac{E_k}{RT}\right) \qquad (4.2.6)$$

TABLE 4.1: Values and confidence limits of parameters for the four term model fitted to the first set of data

Parameters	Best values of parameters	Linear confidence limits			Non-linear confidence limits			
		std. error	lower param. value	upper param. value	lower param. value	lower s.s.	upper param. value	upper s.s.
E_k	26927.	2387.	22154.	31700.	26394.	1.42	26974.	1.46
a_k	30.4	1.86	26.7	34.1	30.4	1.34	30.5	1.87
E_K	10459.	867.	8724.	12194.	10398.	1.44	10557.	1.60
A_K	5.31	0.61	4.09	6.52	5.22	1.75	5.36	1.52
min s.s. = 1.33				variance = 0.021				

TABLE 4.2: Values and confidence limits of parameters for the four term model fitted to the second set of data

Parameters	Best values of parameters	Linear confidence limits			Non-linear confidence limits			
		std. error	lower param. value	upper param. value	lower param. value	lower s.s.	upper param. value	upper s.s.
E_k	6600.	831.	4938.	8263.	6420.	3.66	6663.	2.28
a_k	14.7	0.61	13.5	15.9	14.7	2.06	14.7	2.48
E_K	12110.	1279.	9552.	14668.	12032.	2.13	12260.	2.44
A_K	6.02	0.89	4.24	7.80	5.88	2.83	6.10	2.28
min s.s. = 2.00				variance = 0.033				
variance of experimental error = 0.0055								

TABLE 4.3: Values and confidence limits of parameters for the five term model fitted to the first set of data

Parameters	Best values of parameters	Linear confidence limits			Non-linear confidence limits			
		std. error	lower param. value	upper param. value	lower param. value	lower s.s.	upper param. value	upper s.s.
E_k	26889.	3414.	20061.	33716.	25750.	1.81	26948.	1.49
a_k	30.4	2.50	25.4	35.4	30.4	1.31	30.5	1.85
E_K	10561.	1002.	8558.	12564.	10496.	1.42	10671	1.63
A_K	5.38	0.70	3.98	6.78	5.28	1.86	5.44	1.53
Annulus	2.38	8.50	0.00	21.4	2.38	1.29	8.28	1.57
min. s.s. = 1.24				variance = 0.021				

TABLE 4.4: Values and confidence limits of parameters for the five term model fitted to the second set of data

Parameters	Best values of parameters	Linear confidence limits			Non-linear confidence limits			
		std. error	lower param. value	upper param. value	lower param. value	lower s.s.	upper param. value	upper s.s.
E_k	6566.	1170.	4226.	8906.	6263.	2.83	6642.	2.38
a_k	14.7	1.23	12.2	17.2	14.7	2.00	14.8	2.81
E_K	12116.	1536.	9044.	15188.	12038.	2.10	12287.	2.53
A_K	6.02	1.08	3.85	8.19	5.83	2.24	6.11	2.32
Annulus	1.81	1.21	0.00	26.2	1.81	1.97	8.10	2.42
min. s.s. = 1.97				variance = 0.032				

TABLE 4.5: Experimental data used in fitting first model together with CO concentration predicted by 4 and 5 parameter fits

Temp. of reaction °C	Steam flow rate l/hr	Measured % conc. of CO	Predicted % CO by 4 term model	Error in prediction	Predicted % CO by 5 term model	Error in prediction
373.75	77.4	2.06	2.37	- 0.31	2.34	- 0.29
373.75	54.6	1.87	1.89	- 0.02	1.89	- 0.02
374.00	40.4	1.89	1.71	0.18	1.72	0.17
374.25	68.9	1.98	2.11	- 0.13	2.10	- 0.12
374.00	51.8	1.90	1.82	0.08	1.83	- 0.07
374.00	63.5	1.97	2.03	- 0.07	2.02	- 0.06
373.75	60.8	1.96	1.99	- 0.03	1.98	- 0.02
373.50	37.0	1.91	1.72	0.18	1.74	0.17
373.50	30.9	2.11	1.77	0.33	1.78	0.32
373.00	46.1	1.96	1.81	0.14	1.82	0.14
468.25	50.9	1.67	1.46	0.21	1.46	0.21
468.25	73.0	1.32	1.01	0.31	1.01	0.31
468.50	41.1	1.95	1.83	0.12	1.83	0.12
469.25	64.4	1.36	1.16	0.20	1.16	0.20
469.50	69.7	1.35	1.07	0.28	1.07	0.28
469.00	35.25	2.09	2.16	- 0.07	2.16	- 0.07
470.00	47.2	1.67	1.61	0.06	1.61	0.06
470.50	44.3	1.79	1.72	0.06	1.72	0.06
470.50	62.5	1.43	1.21	0.22	1.21	0.22
408.00	60.7	0.82	0.76	0.06	0.76	0.06
408.25	32.0	1.33	1.43	- 0.10	1.42	- 0.10
408.25	35.8	1.17	1.26	- 0.09	1.26	- 0.08
408.25	50.4	0.92	0.90	0.02	0.89	0.03
408.25	40.6	1.08	1.11	- 0.03	1.10	- 0.02
408.50	55.0	0.86	0.83	0.04	0.82	0.04
408.50	46.4	0.99	0.97	0.02	0.96	0.02
409.00	64.4	0.77	0.73	0.04	0.73	0.05

TABLE 4.5 .... continued

409.00	76.4	0.72	0.66	0.06	0.66	0.06
409.25	71.3	0.73	0.68	0.05	0.68	0.05
429.00	76.3	0.83	0.68	0.16	0.67	0.16
433.40	56.1	1.01	0.97	0.04	0.97	0.04
433.75	46.4	1.17	1.19	- 0.02	1.19	- 0.02
430.75	60.4	0.94	0.87	0.06	0.87	0.07
430.50	65.5	0.89	0.80	0.09	0.80	0.09
430.50	31.7	1.49	1.75	- 0.26	1.75	- 0.26
430.25	28.1	1.72	2.00	- 0.28	2.00	- 0.28
430.50	41.0	1.21	1.32	- 0.11	1.32	- 0.10
430.50	71.2	0.85	0.73	0.12	0.73	0.12
430.75	36.3	1.32	1.51	- 0.19	1.51	- 0.19
430.75	51.7	1.06	1.03	0.03	1.03	0.03
431.00	74.2	0.85	0.71	0.14	0.70	0.15
431.00	55.6	1.01	0.95	0.05	0.95	0.05
431.00	47.1	1.15	1.14	0.01	1.14	0.02
452.75	55.7	1.14	1.16	- 0.02	1.16	- 0.02
454.50	30.4	1.82	2.24	- 0.42	2.24	- 0.42
455.50	45.3	1.36	1.48	- 0.13	1.48	- 0.13
455.50	41.2	1.43	1.64	- 0.21	1.64	- 0.21
454.50	49.9	1.26	1.33	- 0.06	1.33	- 0.06
455 00	76.0	1.01	0.86	0.15	0.86	0.15
453.50	61.7	1.12	1.04	0.08	1.04	0.08
451.75	66.6	1.05	0.96	0.09	0.96	0.09
452.00	70.7	1.02	0.90	0.12	0.90	0.12
451.75	36.3	1.63	1.82	- 0.20	1.82	- 0.19
393.00	59.7	0.89	0.93	- 0.05	0.95	- 0.06
392.75	51.3	0.95	0.97	- 0.02	0.98	- 0.03
392.75	32.2	1.41	1.33	0.08	1.33	0.08
393.00	70.2	0.87	0.94	- 0.07	0.96	- 0.09
393.00	64.9	0.89	0.93	- 0.03	0.94	- 0.05
393.00	74.7	0.88	0.96	- 0.08	0.98	- 0.10
392.75	35.6	1.27	1.22	0.05	1.22	- 0.05
392.75	54.2	0.98	0.95	0.03	0.96	- 0.02
392.60	40.1	1.11	1.11	0.00	1.11	0.00
392.75	44.9	1.06	1.03	0.03	1.04	0.03

TABLE 4.6: Experimental data used in fitting second model with CO concentration predicted by 4 and 5 parameter fits

Temp. of reaction °C	Steam flow rate l/hr	Measured % conc. of CO	Predicted % CO by 4 term model	Error in prediction	Predicted % CO by 5 term model	Error in prediction
491.25	71.6	1.33	1.19	0.14	1.19	0.13
491.50	63.1	1.39	1.25	0.14	1.26	0.13
492.00	52.0	1.59	1.42	0.17	1.42	0.18
492.25	60.0	1.42	1.29	0.13	1.30	0.13
491.50	44.1	1.73	1.61	0.12	1.61	0.12
491.25	66.4	1.35	1.22	0.12	1.23	0.12
481.75	44.4	1.72	1.50	0.22	1.49	0.23
491.25	55.9	1.50	1.35	0.16	1.34	0.16
492.00	67.3	1.35	1.22	0.12	1.22	0.12
434.50	66.9	0.96	1.13	- 0.17	1.14	- 0.18
434.50	68.1	0.97	1.14	- 0.17	1.14	- 0.18
434.50	39.1	1.33	1.23	0.10	1.24	0.09
434.50	60.5	1.01	1.10	- 0.09	1.11	- 0.10
434.50	57.5	1.06	1.10	- 0.04	1.11	- 0.04
434.50	21.5	1.90	2.09	- 0.19	2.08	- 0.19
434.50	30.1	1.55	1.49	0.06	1.49	- 0.06
434.25	52.7	1.11	1.10	0.00	1.11	0.00
434.25	68.0	0.96	1.14	- 0.18	1.14	- 0.19
434.25	36.2	1.38	1.29	0.09	1.29	0.09
443.75	53.5	1.20	1.11	0.08	1.12	0.08
407.00	64.1	1.01	1.24	- 0.23	1.24	- 0.23
407.25	50.6	1.08	1.13	- 0.04	1.13	- 0.05
408.25	70.1	0.99	1.30	- 0.31	1.30	- 0.31
409.75	21.8	1.59	1.71	- 0.12	1.70	- 0.12
410.00	61.0	0.98	1.19	- 0.21	1.19	- 0.22
410.75	46.6	1.09	1.11	- 0.02	1.12	- 0.03
411.50	67.5	0.93	1.25	- 0.31	1.25	- 0.31
411.50	57.3	1.01	1.15	- 0.14	1.15	- 0.14

Table 4.6 (continued)

412.00	70.5	0.94	1.28	- 0.34	1.28	- 0.34
410.00	27.8	1.39	1.37	0.02	1.37	0.02
455.50	64.0	1.10	1.11	- 0.01	1.12	- 0.02
456.25	52.1	1.23	1.17	0.06	1.18	0.06
456.00	21.8	2.07	2.44	- 0.37	2.43	- 0.36
457.00	67.1	1.07	1.11	- 0.04	1.12	- 0.05
460.25	70.8	1.05	1.11	- 0.06	1.12	- 0.07
461.50	27.2	1.81	2.01	- 0.21	2.01	- 0.20
461.25	45.6	1.34	1.29	0.06	1.29	- 0.05
461.75	71.4	1.04	1.12	- 0.08	1.12	- 0.08
462.50	62.1	1.13	1.13	0.00	1.14	- 0.01
461.75	60.2	1.14	1.14	0.00	1.14	0.00
444.25	55.9	1.06	1.11	- 0.05	1.12	- 0.06
475.75	52.4	1.40	1.28	0.12	1.28	0.12
476.00	30.5	1.86	2.02	- 0.16	2.01	- 0.15
475.75	24.4	2.12	2.52	- 0.40	2.50	- 0.38
465.25	68.2	1.21	1.12	0.09	1.13	0.08
476.00	73.9	1.16	1.13	0.03	1.14	0.02
476.50	61.6	1.29	1.19	0.10	1.19	0.10
477.00	76.8	1.15	1.13	0.01	1.14	0.01
476.75	49.3	1.49	1.34	0.15	1.34	1.48
476.50	67.3	1.23	1.15	0.08	1.16	0.01
477.00	57.4	1.36	1.23	0.13	1.23	0.13
393.00	65.1	1.59	1.38	0.21	1.37	0.22
392.50	79.7	1.59	1.64	- 0.05	1.62	- 0.03
392.75	68.1	1.62	1.43	0.19	1.42	0.20
393.00	29.7	1.72	1.23	0.50	1.23	0.49
393.75	58.9	1.51	1.28	0.23	1.28	0.23
396.50	76.9	1.46	1.54	- 0.08	1.52	- 0.06
397.00	24.8	1.74	1.40	0.34	1.40	0.34
395.75	43.7	1.49	1.14	0.35	1.14	0.34
395.50	52.0	1.49	1.19	0.30	1.19	0.29
395.75	68.6	1.44	1.41	0.04	1.40	0.04
444.75	58.5	1.14	1.10	0.03	1.11	0.03

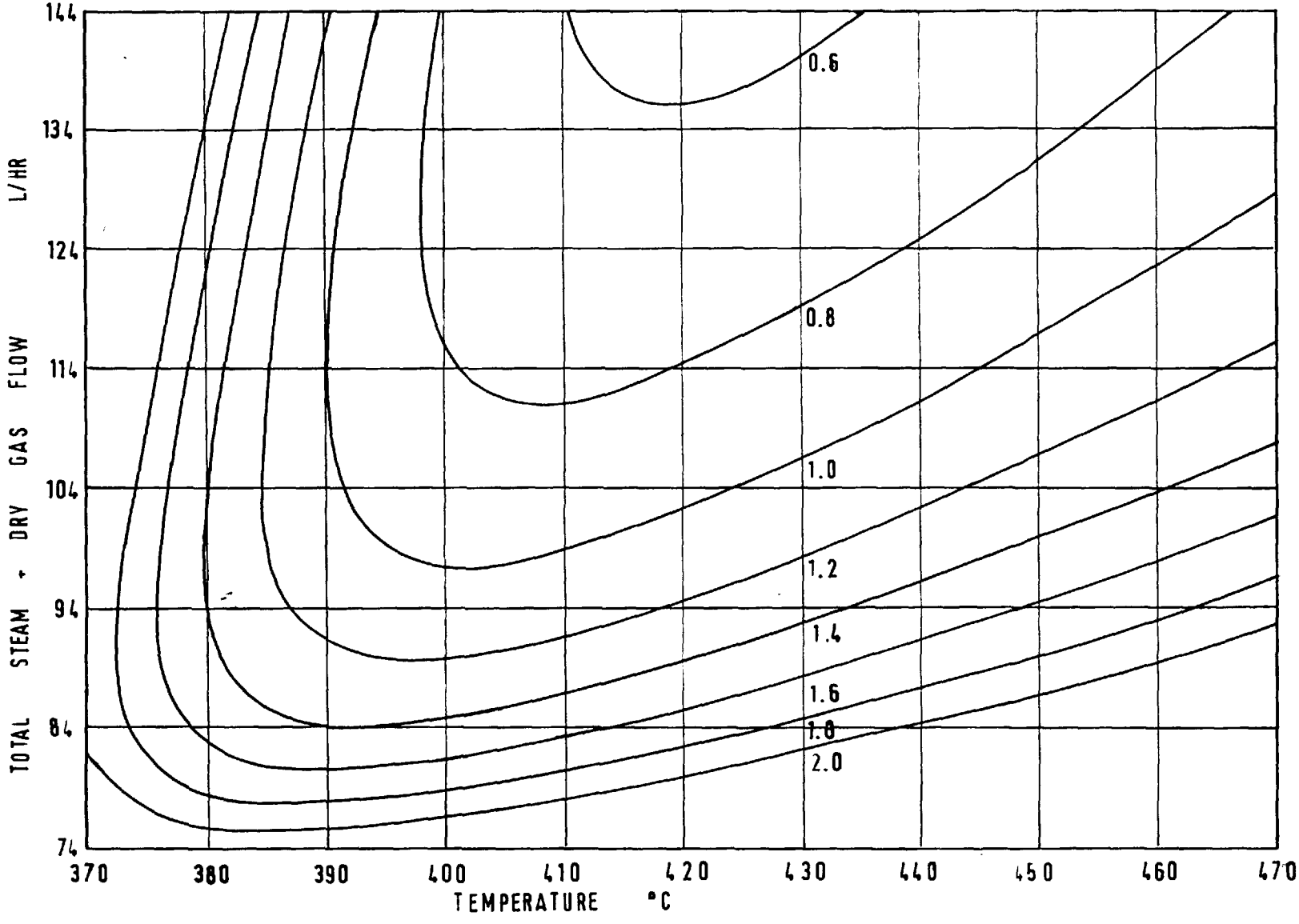

FIGURE 4.3 RESPONSE SURFACE FOR PERCENT CO IN OUTLET WITH NEW CATALYST

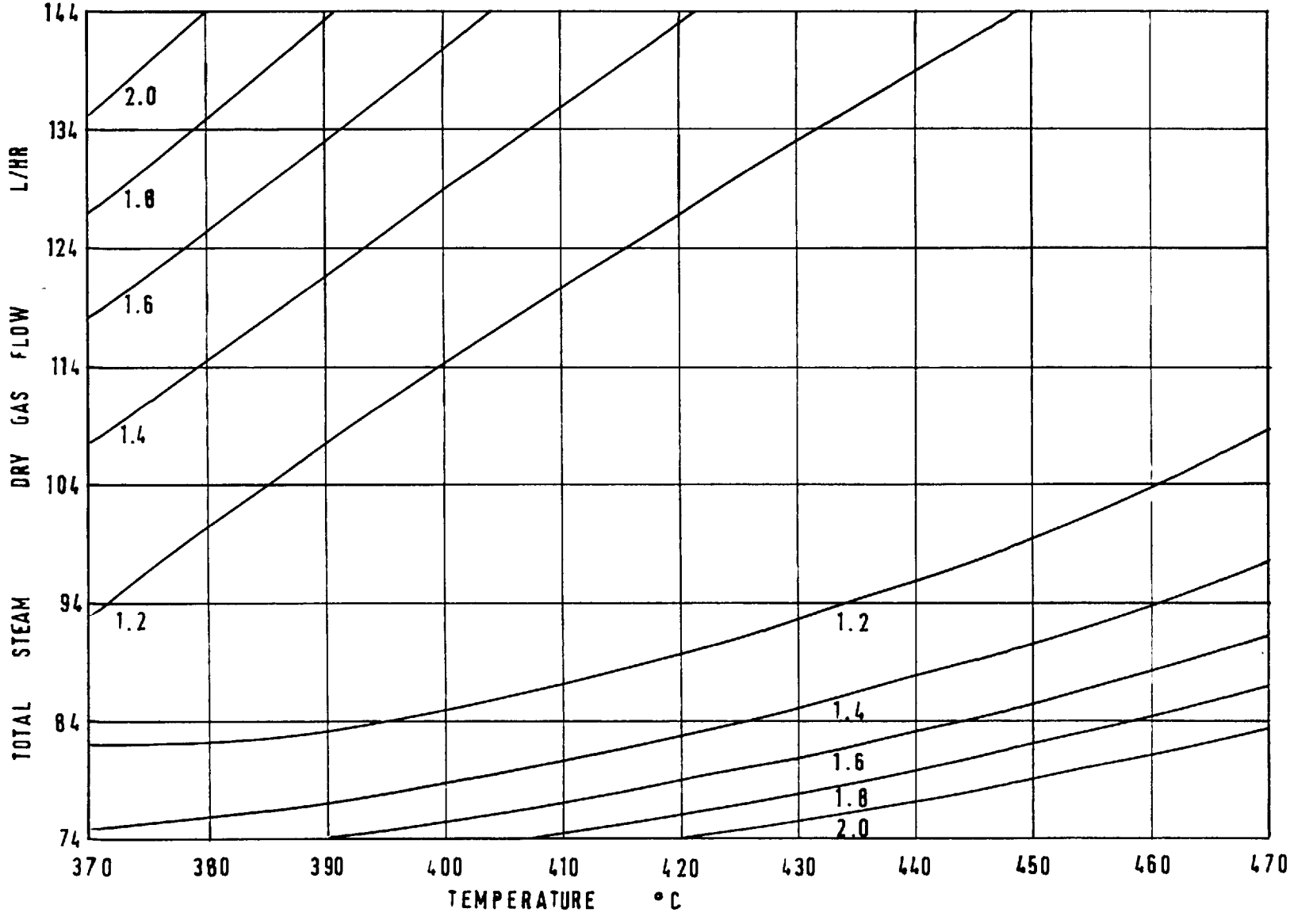

FIGURE 4.4 RESPONSE SURFACE FOR PERCENT CO IN OUTLET WITH OLD CATALYST

$$K_e = \exp\left(\frac{E_K}{RT} - A_K\right) \qquad (4.2.7)$$

Price, however, showed that the latter parameter gave no improvement in the closeness of fit, a fact which has also been verified here. In Tables 4.1 and 4.3 are given the parameters fitted to the four term models, while those fitted to the other models are given in 4.2 and 4.4. Tables 4.5 and 4.6 give the experimental data used in the fitting of the models together with the outlet concentrations predicted by the models, and the difference between these and the observed results. Contour maps of the steady-state reactor response surfaces are given in Figures 4.3 and 4.4.

4.2.6 Statistical confidence limits

If it is assumed that one is dealing with a linear model in which the random errors are independent and normally distributed, then Scheffé (S7) states that the confidence region may be defined as a k-dimensional ellipsoid, where k is the number of parameters in the model. Under these conditions, one parameter confidence limits are evaluated in Marquardt's programme using the following expression:

$$b_j \pm \left(t_{1-a'}, (n - k)\right) S_o \sqrt{c_{jj}}$$

where b_j = the j^{th} parameter.

n = total number of data points,

$(1-a')$ = confidence probability

$\left(t_{1-a'},(n - k)\right)$ = two-tailed $(1-a')$ point of Student's t distribution,

S = standard error of the estimate of the minimum sum of squares,

$S_o^2 \, c_{jj}$ = j^{th} diagonal element of the variance-covariance matrix.

Should the parameters prove to be not uncorrelated, then the above expression will be an underestimate of the interval in which the parameter j may lie and still remain within the ellipsoid.

The Marquardt hill-climber assumes that the nonlinear model may be replaced by a linear form in the region surrounding the best parameter values; it is therefore reasonable to expect this to break down outside a given space surrounding the minimum. Thus the non-linear confidence limits of the parameters are an indication of the extent of non-linearity in the confidence regions. Assuming the non-linear model is correct and the deviations of the parameters from their correct values are due to normally distributed experimental errors, Beale (B6) states that the most natural confidence region is the set of parameter values for which

$$\Phi_{critical} - \Phi_{optimum} = kS_o^2 \, F_{a,(k,n-k)} \qquad (4.2.9)$$

where $\Phi_{optimum}$ = sum of squared errors at the optimal fit,

$\Phi_{critical}$ = sum of squared errors at the edge of the confidence region.

Using (4.2.9) Marquardt calculates the non-linear confidence limits for a given parameter by varying it until two evaluations of Φ straddle Φ_c and then carrying out a quadratic interpolation; the inefficiency of this latter technique is shown up by the

variations in the sum of squares at the calculated limits.

4.2.7. Adequacy of model

Three times throughout the second set of steady-state runs tests were repeated at the same conditions of temperature and steam flow-rate to check the reproducibility of the results. The operating conditions themselves were not reproducible enough to obtain the same observations of outlet carbon monoxide concentration; they were however close enough together to expect the same difference between predicted and observed outlet concentrations. Assuming this inference to be correct, variations in the error will be due solely to lack of experimental reproducibility. The unbiased estimate of variance for the differences calculated on these points (bottom of Table 4.3) is considerably smaller than those calculated for the total set of experimental observations. At first sight this would suggest that the model proposed did not quite fit the data; however, an alternative explanation is that a proportional bias existed in one or more of the measuring instruments. Correlation analysis between the errors and measured variables was therefore carried out to check for this. Jackson (J3) had already found that a correlation did exist between the error and the steam flowrate in the case of Price's results; this has since been confirmed, but it was also found that a higher correlation existed between the observed carbon monoxide concentration and the error (Appendix 4.1). In the case of data

presented here, the correlation between the outlet CO concentration and the error was only noted after breaking the latter down into smaller groups, the division taking place at those points where the infra-red analyser had been recalibrated for its zero and sensitivity settings. The conclusion drawn was that the sensitivity setting on the analyser did not quite correspond with that required for using the provided calibration curve, and as a result errors proportional to the observed carbon monoxide concentration were being introduced. Removal of the error due to incorrect IRA sensitivity could be carried out to reduce the variance of Price's differences from 0.0134 to 0.0061 and for the first group of data in Table 4.1 from 0.0388 to 0.0036. However, this is a remedy which can only be obtained with quite a lot of data, and is therefore only useful to prove the adequacy of the model employed and not for making corrections during the main experimental programme.

Finally, a quantitative test of adequacy was made on the basis that should the model describe accurately the actual conversion taking place, then the variance of the residual errors would equal the variance of the experimental errors, hence leading to the conclusion that their ratios would be distributed as the F-statistic.

Table 4.7: Analysis of variance for the steady-state model.

Models	Differences between observed and predicted results		Experimental error		Statistic
	Variance S_o^2	No. of degrees of freedom	Variance S_1^2	No. of degrees of freedom	$F = \frac{S_o^2}{S_1^2}$
1st data, 4 parameter	.021	59	.0055	2	3.82
2nd data, 4 parameter	.033	58	.0055	2	6.0
$F_{0.95}(60,2) = 19.48$			$F_{0.99}(60,2) = 99.48$		

Since in each case $F < F_{0.95}$ the differences are not found to be significant at the 5% level, thus the hypothesis put forward is accepted and the models are considered to be adequate.

4.2.8. Objective function

For purposes of this study it was desired to have an objective function which would have both an optimum and be subject to reasonably large changes within the operating range of the parameter being varied. Price found that in the case of optimization with respect to temperature a suitable function was provided using the IRA reading in the form:

Objective function = $c_1 - c_2$ x (IRA reading) (4.2.10)

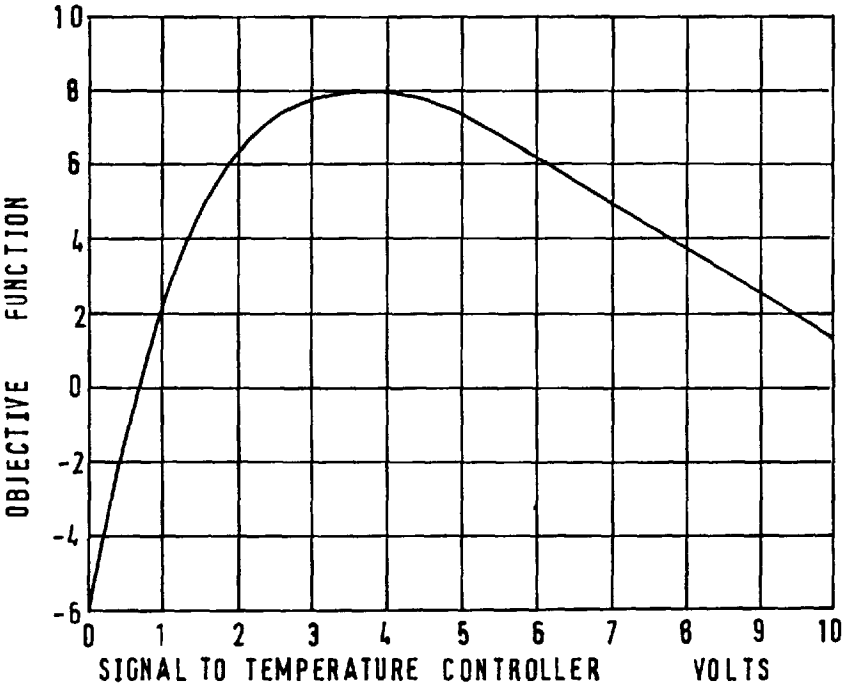

FIGURE 4.5 OBJECTIVE FUNCTION FOR NEW CATALYST

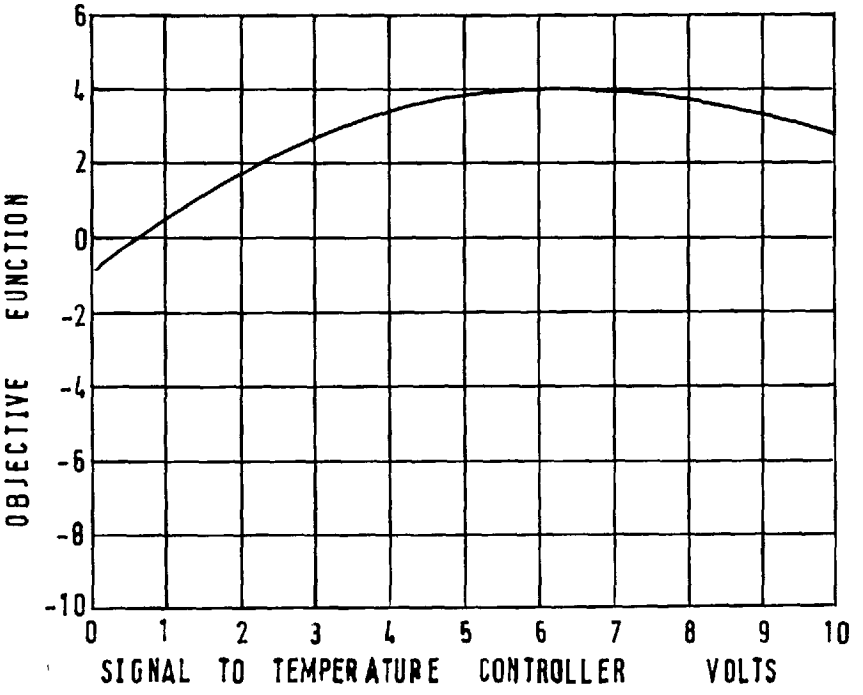

FIGURE 4.6 OBJECTION FUNCTION FOR OLD CATALYST

A glance at Figures 4.3 and 4.4 confirms the fact that at most steam flow rates this is indeed the case, hence the same type of objective function is used here. On the basis of the first steady state data it was therefore decided to operate the system at a mixed dry gas-steam flow rate of 115 l/hr and to use parameters of value:

$$c_1 = 18.0$$

$$c_2 = 52.5$$

This gave an objective function having the characteristic shown in Figure 4.5, and for the case of the spent catalyst that shown in Figure 4.6.

4.2.9. Performance criterion

In order to assess the effectiveness of the optimization procedure some form of performance criterion requires to be evaluated as the experiments proceed. The simplest one possible is to track the losses incurred through not operating at the optimum point all the time; this was used effectively both by Price and Kisiel and, since thre is no reason for doing otherwise, it is also used in this work. The criterion consists in integrating continuously the difference between the actual value of the objective function and some constant greater than the optimal value of the objective function.

$$\text{Performance criterion} = \int_0^t (\text{constant} - \text{objective function})\,dt \qquad (4.2.11)$$

In this case the constant was taken to have a value of 9.

4.2.10. Comments on changes in catalyst activity

In order to put forward possible explanations for the changes that occurred in catalyst activity, it is first necessary to have some understanding of the mechanism whereby catalysts influence a reaction. It is generally thought that in heterogeneous systems gaseous reactants are adsorbed on the surface of the catalyst. This adsorption may take place either as a monolayer or as a relatively thick film. In the first case the bonding between the catalyst and adsorbate is chemical in nature, while with multimolecular layer adsorption the bonding is probably physical of the van der Waal type.

In most cases physical adsorption is not involved in catalysis, but can provide a low energy path to chemisorption. Though chemisorption appears to take place all over the surface, it is found that there are centres where a greater amount of reaction occurs. These centres, known as active sites, vary relative to each other and it is found that they are in constant flux of being created and destroyed.

The temperature dependence of the reaction rate is explained by the concept of activation energy and is represented by a variation of equation (4.2.6), namely,

$$k = A \exp\left(-\frac{E_k}{RT}\right) \qquad (4.2.12)$$

Changes in catalyst activity will frequency indicate changes

in the activation energy. However, it is found that these changes of activation energy can be partially or fully compensated for by accompanying changes in the pre-exponential term A. This phenomena, normally referred to as the "compensating effect", although as yet not fully understood, has been explained in a number of ways. The most likely interpretation due to Kemball (K5) is now given.

According to Eyring's absolute rate theory (4.2.12) may be expressed as

$$k = \left(\frac{KT}{h}\right) \exp\left(\frac{\Delta S^{\dagger}}{R}\right) \exp\left(-\frac{\Delta H^{\dagger}}{RT}\right) \qquad (4.2.13)$$

where K = Boltzmann's constant

h = Plank's constant

$\Delta S^{\dagger}$ = entropy

$\Delta H^{\dagger}$ = enthalpy

= E_k for single reactions.

Kemball suggested that the enthalpy and entropy terms were related and thus changes occurring in one could be compensated for by accompanying changes in the other.

Comparison of the kinetic constants for the used and unused catalyst does suggest the occurrence of compensating effects, although within the limits of the investigation this was difficult to prove. Since examination of the catalyst had shown no obvious changes of the particle size on the macroscale, it was decided to examine the surface by taking electron micrographs and electron diffraction pattern analysis.

†Surface replicas of the original samples were made by evaporating carbon on to them and then etching away the body with hydrochloric acid. Plates 1 and 2 show the pictures obtained of the surface replicas using a magnification of 16 000. It is noticed that there is no real difference between the two apart from the slightly smoother appearance of the used catalyst, and this could be due entirely to differences in chemistry between the new and reduced catalyst. The electron diffraction studies were equally disappointing in their results, although they did confirm the presence of chromium oxides in both cases.

††Measurement of the specific surface of the catalyst was also made using the BET method. This technique estimates the area by measuring the quantity of gas (in this case nitrogen) required to cover the surface with a monolayer; its advantage is that it also corrects for errors introduced by the formation of additional layers. Comparison with data supplied by ICI showed that the catalyst had a surface area of 6.5 m^2/g where it should have been 13.0 m^2/g, i.e. a total drop of 50%.

Another possible cause of catalyst decay could have been due to poisoning. Dowden (D5) suggested that likely poisons were H_2S or CO. The first was never present so can be discounted immediately while precautions were always taken

† Carried out by electron microscope service.

†† Carried out at Catalyst Research Labs, Johnson Matthey & Co.

PLATE 1: Micrograph of fresh catalyst

(Magnification x 16 000)

PLATE 2: Micrograph of used catalyst

(Magnification x 16 000)

to prevent CO entering without steam so the second should never have arisen. Had CO poisoning taken place the catalyst would have been reduced to iron, which on re-oxidising would have caused sintering. This would have been shown up as a break down in particle size which did not appear to have occurred.

Thus in conclusion it is surmised that the changes that took place in the activity of the catalyst were probably due to compensation effects occurring as the result of a reduction in the specific surface of the catalyst, rather than to poisoning.

4.2.11. Conclusions

According to Mars' (M2) the equilibrium constant, derived from free energy data, is well described in the range being operated in, by

$$K_e = \exp\left(\frac{9220}{RT} - 4.45\right) \qquad (4.2.14)$$

where T is the temperature in ^{o}K and R the universal gas constant. Price obtained values for E_K and A_K of the order of 2000 and - 0.2, thus in comparison it is seen that in all cases the results presented in Tables 4.1 - 4.4 show that the equilibrium parameters lie very close to Mars' prediction. At the same time the kinetic constants fitted for the fresh catalyst showed good agreement with those values estimated by Price and Kisiel.

The present work also confirmed Price's findings that a one particle thickness for the annulus used in the correction to the plug flow model was reasonable.

Finally it was pointed out that the main remaining source of error was due to the sensitivity setting of the infra red analyser.

4.3. Dynamic Modelling

Although sometimes a general description of a system will yield sufficient information for deriving an adequate dynamic model, more frequently this is not enough, and direct experimentation has to be resorted to. In the present instance, since accurate knowledge was required regarding the influence of the dynamics, an experimental programme was necessary.

There are a large number of methods available for experimental dynamic analysis; all involve comparison of system inputs and outputs, but unfortunately not all may be applied in a given situation. Hougen (H3) has written a very good critique on the majority of methods available, and since most of these are well tried no more need be said.

Price (P6) originally carried out a frequency response analysis of the system and formulated a dynamic model. However, in certain instances it was found that the model did not represent the dynamics; also the technique proved to be

very slow. It was therefore hoped that by using a pseudo-random binary noise signal to excite the system, an improved model might be obtained reasonably quickly. A direct comparison has in fact been made between the two methods, and the results reported at the 5th AICA Congress (W1). A summary of Price's work, followed by a description of the method using pseudo-random binary noise, and a comparison of the two is given in the rest of this section.

4.3.1. Sinusoidal forcing

The system was perturbed continuously about a mean point by a low amplitude sinusoidal signal; assuming its linearity, the output of the system would be expected to oscillate at the same frequency sinusoidally, and because of the dynamics, the degree of attenuation and the phase differences between these signals would vary with their frequency. These two factors were used to derive the dynamic model. After transients had died out the constant peak to peak height was measured. It was also necessary to record the constant peak to peak height for zero frequency which corresponded to the steady-state values of the outputs at the upper and lower limits of the perturbing signal. The ratio $G_{\omega}/G_{\omega=0}$ represented a dimensionless evaluation of the gain of the system at the particular frequency. For each frequency the gain was determined and the overall phase shift between input and output sinusoids noted. The latter measurement represented

the summation of the distance velocity lag or dead time and the phase shift associated with the assumed first, second or third order lag.

Initial analysis of the ensuing results was carried out by means of Bode plots. From a graph of gain against frequency on log-log paper not only was the approximate order of the system determined but also estimates of the corresponding time constants were made (E1). Final fitting of the time constants of a particular transfer function were carried out by hill-climbing to minimize the sum of squared differences between the predicted and observed gain.

At each frequency, the phase shift due to the fitted transfer function was evaluated, and from differences between this and the observed phase shift an estimate of the dead time was obtained.

Recordings of the input and output sinusoids were made on a four-channel chart recorder. When measuring the phase lag between two signals, it was found necessary to run the chart at a very high speed for several cycles. This latter method of measuring the phase lag, although the best one available, does introduce considerable error on the results.

The sinusoidal forcing method does however suffer from a number of disadvantages. It is slow as for each frequency the transients caused by initiating the sinusoids have to be allowed to die out; this generally takes several cycles. In addition, because of limitation in hardware, it is not always

always possible to introduce a sinusoidal disturbance into a process.

4.3.2. Random noise forcing

The output $y(t)$ from a linear system may be described in terms of a weighting function $h(\nu)$ and the past history of inputs $x(t - \nu)$:

$$y(t) = \int_0^\infty h(\nu)\ x(t - \nu)\ d\nu \qquad (4.3.1)$$

Cross-correlation of the input and output signals automatically leads to the Weiner-Hopf equation:

$$\phi_{xy}(\tau) = \int_0^\infty h(\tau)\ \phi_{xx}(\nu - \tau)\ d\nu \qquad (4.3.2)$$

To obtain the weighting function of the system from knowledge of the input and output signals by solving this integral equation is difficult, although Goodman and Reswick (G4) did a considerable amount of work on this problem. If white noise however is used as the input signal, then because its auto-correlation function is one at a lag of zero and zero elsewhere, the problem simplifies considerably and equation (4.3.2) reduces to:

$$\phi_{xy}(\tau) = h(\tau) \qquad (4.3.3)$$

Unfortunately, it is not always possible to guarantee that a particular length of random signal is white noise, so it is necessary to run an experiment for much longer than the minimum time required to generate the weighting function.

Hoffman (H4) has given a comprehensive description of a class of binary sequential filters which, by their nature, may be transformed to generate long strings of binary digits possessing quasi-random properties. Such generators are made up from memory units, which may be shift registers, and modulo two adders. Also required is a synchronous driving source, usually a clock pulse. Modulo two addition is a binary operation in which two equal inputs give an output of 0 and two different inputs give an output of 1, as shown below.

$\oplus$	0	1
0	0	1
1	1	0

(4.3.4)

Because the networks are sequential, the output from a filter may be considered as the modulo two addition of a number of delayed inputs and the present input. Therefore, defining D as that operator which delays a signal by one discrete interval of time, it is possible to describe the output as a polynomial of D operating on the input; this is known as the characteristic polynomial of the system (B5):

$$Z_{out} = \theta(D)\ Z_{in} \tag{4.3.5}$$

By judiciously choosing the characteristic polynomial of a shift register generator, it is possible to have a system of N shift registers switch through $2^N - 1$ of its 2^N different states before repeating the sequence. It is under these conditions that the output of any of the shift registers is

found to approximate to a white noise signal. Such an output is normally referred to as a maximal length null sequence or briefly an m-sequence. Those characteristic polynomials which describe this type of network are called primitive and possess two necessary properties:

(i) they must be irreducible,

(ii) they must not be divisors of any polynomial $D^k \oplus I$, where $k < 2^N - 1$.

Peterson (P8) gives a list of primitive polynomials up to degree 34.

The main property of interest associated with m-sequences is that if the two states are + 1 and - 1, then the auto-correlation of the sequence is of the form shown in Figure 4.7 and is periodic with the same period as the sequence. Thus it is seen that the auto-correlation of m-sequences approximates very closely to that of white noise, hence it should be possible to use them in dynamic analysis. One serious disadvantage arises from the fact that in any sequence there are more + 1's than - 1's, thus biasing the weighting function. A method of correcting for this is to average the tail (usually the last third) of the weighting function after it has settled out and to subtract this over the whole length of the function (G5).

In the analysis of the results obtained, the weighting function not only gives a good indication of the order of the system together with estimates of the time constants, but also

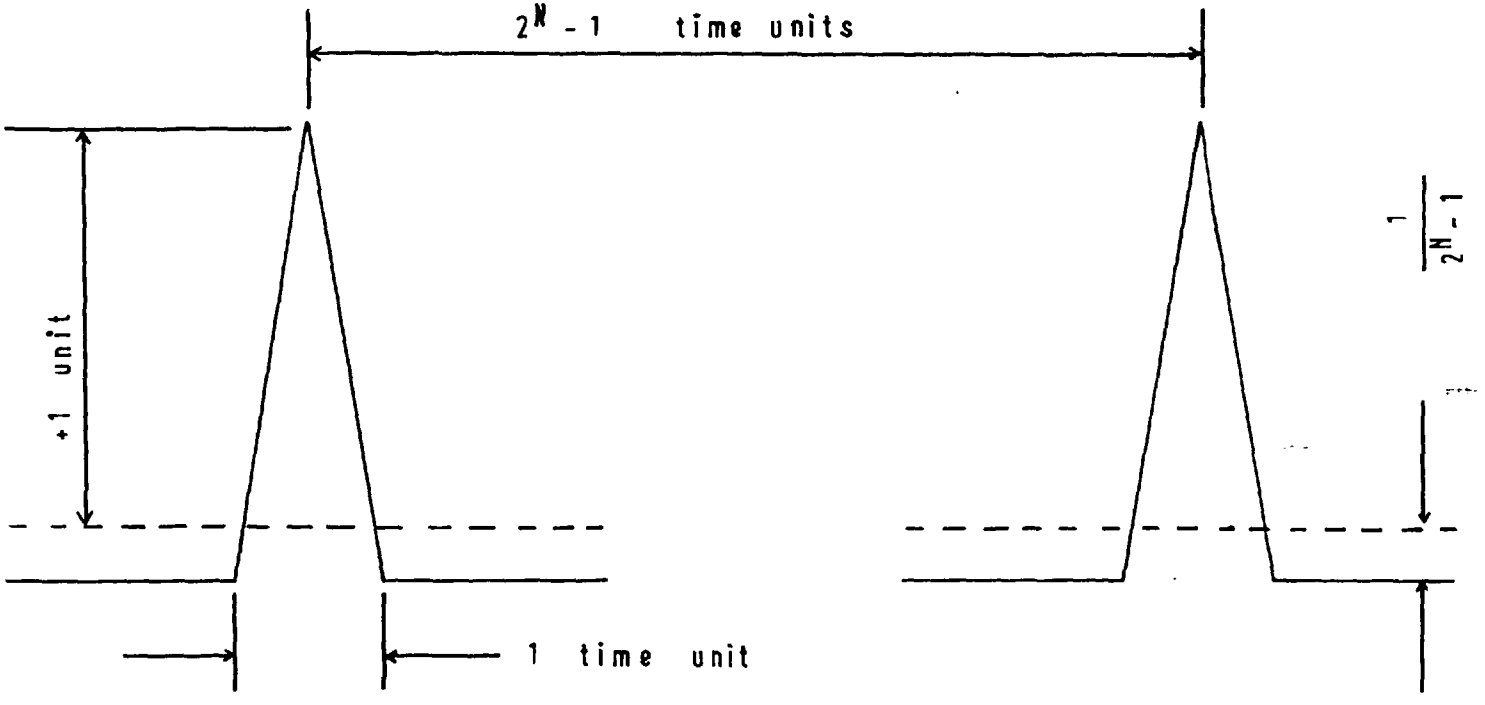

FIGURE 4.7 AUTOCORRELATION FUNCTION OF AN M-SEQUENCE

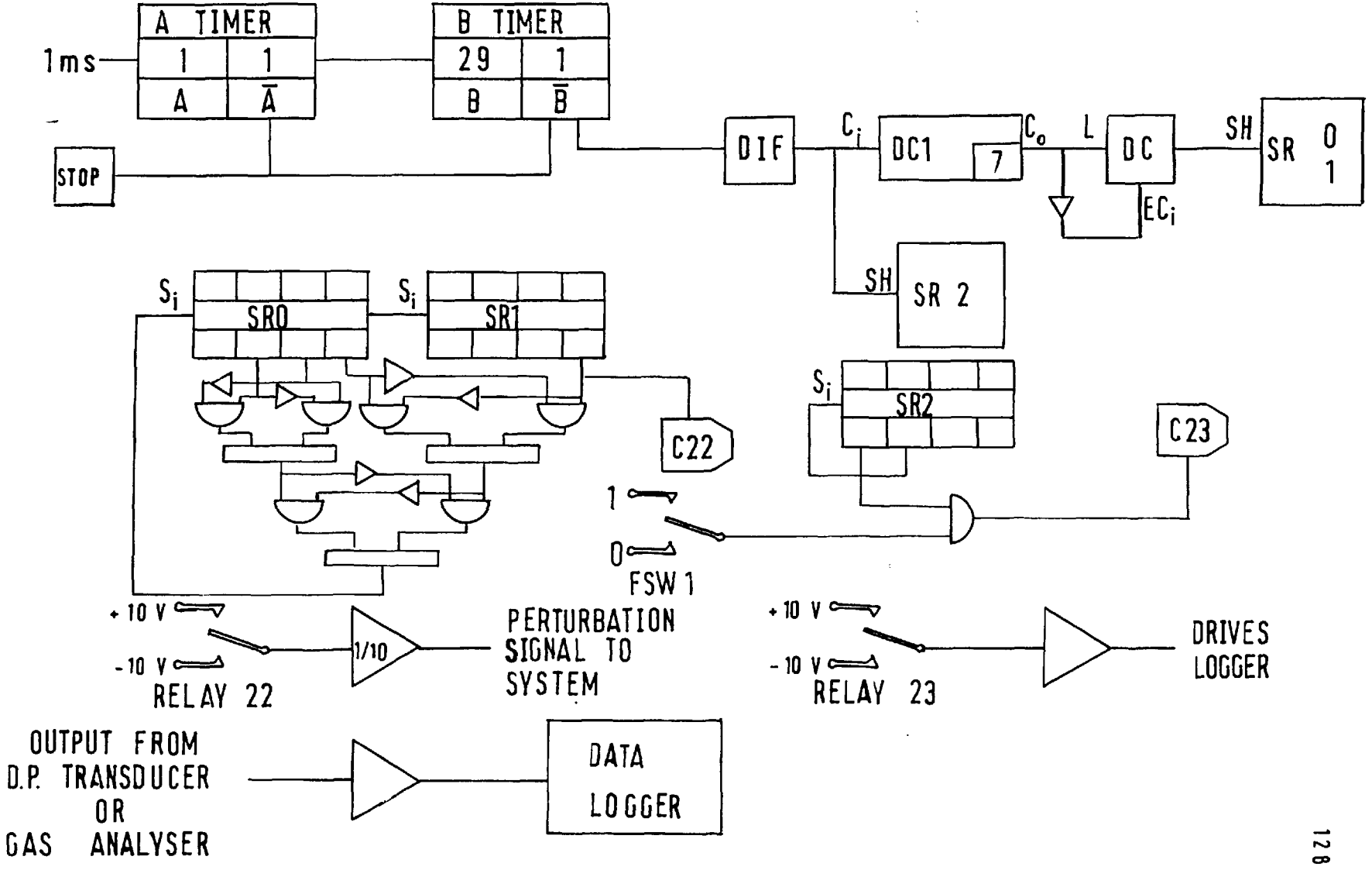

FIGURE 4.8 CIRCUIT USED IN M-SEQUENCE FORCING METHOD

fixes directly the distance-velocity lag. Final fitting of parameters is carried out using a hill-climbing routine to minimize the sum of squares of the differences between the experimentally obtained and predicted weighting functions.

4.3.3. Auxilliary equipment

The auxilliary equipment required for carrying out the m-sequence tests is shown in Figure 4.8. The m-sequence was generated in the logic section of the PACE HYBRID 48, the last of the shift registers being used to switch the perturbing signal from positive to negative and vice-versa. All important inputs and outputs of the system could be controlled or measured from the PACE TR10 analogue computer; when necessary recording of the signals on the paper was made with the EAL MDP 200 data logger. In order to ensure that the logger always made the same number of scans per bit of the m-sequence, it was found necessary to use the same clock to drive the noise generator and the logger.

4.3.4. Experimental investigations

The dynamic characteristics of the process which were of interest are shown schematically in Figure 4.9.

Frequency response measurements with respect to temperature were made by Price using about 30 different sinusoidal perturbations of amplitude 1 volt, ranging in period from 20 to 2000 sec. On the steam side the pneumatic control valve was perturbed also by about 30 different sinusoids, but the

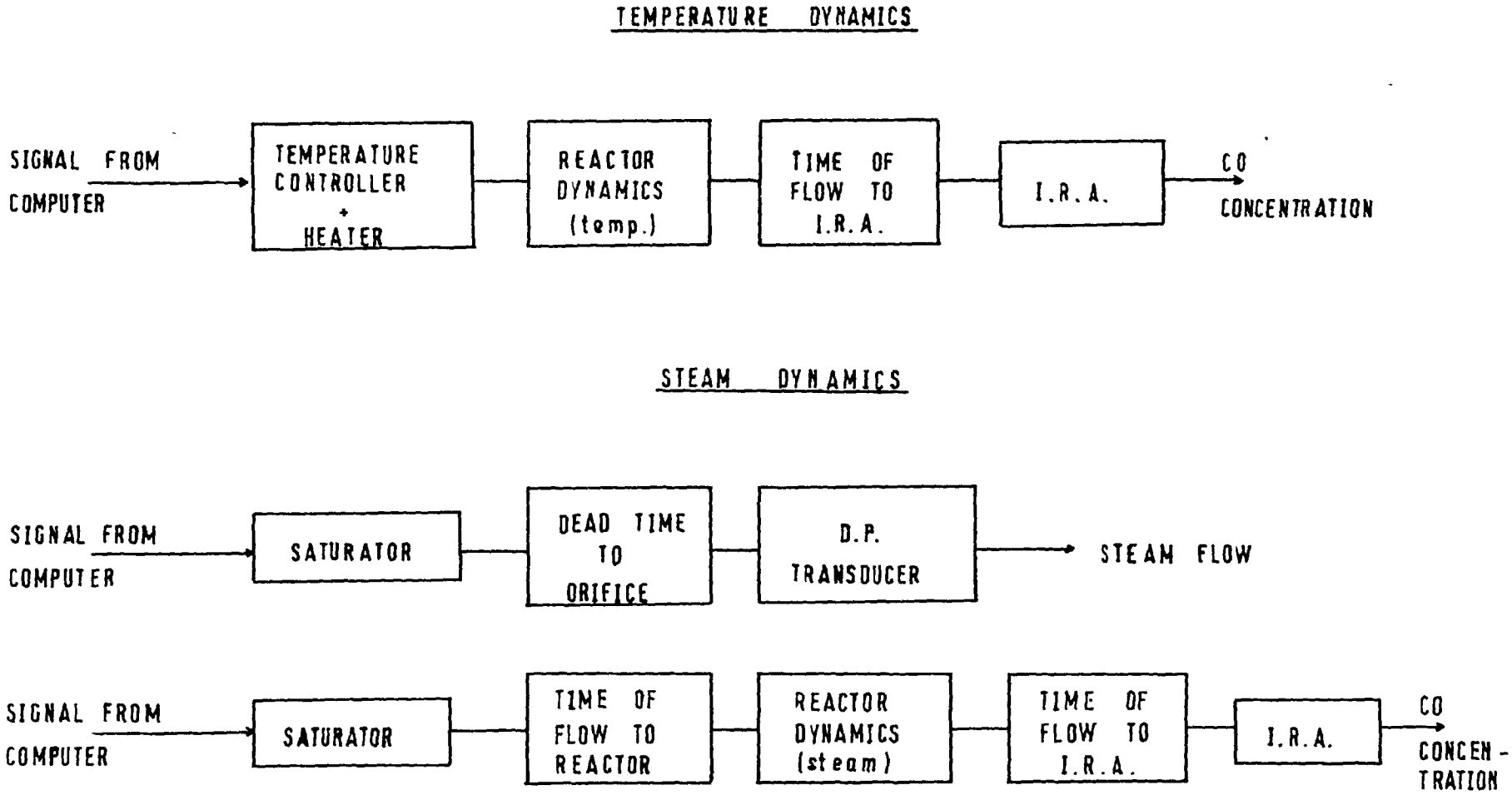

FIGURE 4.9 DYNAMICS OF PROCESS

amplitude was only ¾ volt and the total range covered was of periods 20 to 210 sec. In each case the runs were randomized to reduce any biasing which could have arisen.

An eight-stage shift register was used to generate the m-sequence which was adjusted to give an amplitude of 1 volt on all occasions. When studying the temperature side the bit period was 1.92 sec and the logger was driven at a rate of 4 scans per bit period. In the case of steam side dynamics, however, the bit period was reduced to 0.48 sec and because of limitations in the logger this could only do 2 complete scans per bit period. For each dynamics experiment four runs of the m-sequence were recorded to reduce experimental error.

Fitting the 1st, 2nd and in some cases 3rd order transfer functions was carried out as described in section 4.3.2. The hill-climbing routines used were again Powell's (P7) and Marquardt's (M4).

When it was found necessary to decide between two models which were not apparently equivalent, then the statistical test of significance known as the general linear hypothesis was applied. This is discussed by Mandel (M5) and Davies (D4).

Finally, having obtained the best possible model to describe the system dynamics, it was necessary to ascertain whether this was adequate. In the cases of Price's frequency response experiments three near frequencies in each set of runs were taken as being the same and used to evaluate the variance of experimental error; for the case of the m-sequence

tests, this variance was calculated from the tail of the weighting function which should have been zero.

4.3.5. Results of dynamic modelling

The results obtained by the two methods are summarized in Tables 4.8 - 4.12. Plots of the experimental impulse responses found, together with curves generated from the best fitted transfer functions, were shown in Figures 4.10 - 4.12. Also plotted on each figure is a dotted curve obtained from the transfer function produced by Price's method.

It is clear from Table 4.8 - 4.10 that both methods give constants of the same order of magnitude. In most cases, however, not even the confidence limits of the time constants obtained overlap. Hence it is necessary to decide which method gives the more reliable information. In the case of temperature dynamics, a first order model, because it gave a smaller sum of squared deviations, was found to adequately fit the data obtained by sinusoidal forcing; the m-sequence data, however, called for a second order transfer function. On considering the apparatus it was reasonable to assume that the latter would be the truer result. In cases that could be compared the sinusoidal forcing method produced narrower confidence regions for time constants, therefore greater weighting should be given to results produced by it. However, in Figures 4.10 and 4.12 there is little scatter of the experimental points on the leading edge of the weighting function

TABLE 4.8: Time constant fitting results for the temperature dynamics

Temperature controller to outlet concentration CO, sinusoidal forcing method						
transfer function fitted	fitted time constants		residual sum of squares	standard error	dead time	
	T_1	T_2			(secs)	standard deviation
$\frac{1}{(1+pT_1)}$	98.72		0.157	0.0724	7.23	6.82
$\frac{1}{(1+pT_1)\ (1+pT_2)}$	101.20	0.06	0.158	0.0739	6.6	-

Confidence limits for the transfer function giving an adequate fit							
transfer function	one parameter confidence intervals			non-linear confidence intervals			
	standard error	lower value T	upper value T	lower value T	lower residual S.S.	upper value T	upper residual S.S.
$\frac{1}{(1+pT_1)}$ T_1	4.95	88.81	108.62	88.53	0.179	110.26	0.179
critical sum of squares $SS_{(critical)}$ = 0.178							

TABLE 4.8 (continued)

Temperature controller to outlet concentration CO, m-sequence method

transfer function fitted	fitted time constants		residual sum of squares	standard error	dead time (secs)	steady state gain
	T_1	T_2				
$\frac{1}{(1+pT_1)}$	76.33	-	0.4447 x 10^{-3}	.1329 x 10^{-2}	32.3	.951
$\frac{1}{(1+pT_1)\ (1+pT_2)}$	50.73	15.39	0.2374 x 10^{-3}	.9725 x 10^{-3}	24.13	.928

Confidence limits for the transfer function giving an adequate fit

transfer function	one parameter confidence intervals			non-linear confidence limits			
	standard error	lower value T	upper value T	lower value T	lower residual	upper value T	upper residual
$\frac{1}{(1+pT_1)\ (1+pT_2)}$ T_1	3.78	43.44	58.27	46.64	.247 x10^{-3}	55.59	.247 x10^{-3}
T_2	2.07	11.25	19.36	13.16	.247 x10^{-3}	17.71	.247 x10^{-3}

critical sum of squares SS (critical) = .247 x10^{-3}

TABLE 4.9: Time constant fitting results for the control valve to steam flowrate dynamics

Valve to steam measurement, sinusoidal forcing method						
transfer function fitted	fitted time constants		residual sum of squares	standard error	dead time	
	T_1	T_2			(secs)	standard deviation
$\frac{1}{(1 + pT_1)}$	13.22		0.0696	0.0490	0.80	1.96
$\frac{1}{(1+pT_1)(1+pT_2)}$	13.19	0.48	0.0695	0.0499	0.35	-

Confidence limits for transfer function giving an adequate fit							
transfer function	one parameter confidence intervals			non-linear confidence limits			
	standard error	lower value T	upper value T	lower value T	lower residual S.S.	upper value T	upper residual S.S.
$\frac{1}{(1+pT_1)}$ T_1	0.38	12.46	13.98	12.47	0.0794	14.01	0.0793

Critical sum of squares $SS_{(critical)} = 0.0792$

TABLE 4.9 (continued)

Valve to steam measurement, m-sequence method						
transfer function fitted	fitted time constants		residual sum of squares	standard error	dead time (secs)	steady state gain
	T_1	T_2				
$\frac{1}{(1+pT_1)}$	9.20		0.4100 x 10^{-3}	0.1276 x 10^{-2}	0.04	0.1016
$\frac{1}{(1+pT_1)(1+pT_2)}$	12.57	0.10	0.4642 x 10^{-3}	0.1360 x 10^{-2}	0.0	0.1175

Confidence limits for transfer function giving an adequate fit							
transfer function	one parameter confidence intervals			non-linear confidence limits			
	standard error	lower value T	upper value T	lower value T	lower residual S.S.	upper value T	upper residual S.S.
$\frac{1}{(1+pT_1)}$ T_1	0.498	8.33	10.28	8.67	0.4138 x 10^{-3}	10.07	.4139 x10^{-3}

critical sum of squares $SS_{(critical)} = 0.4138 \times 10^{-3}$

TABLE 4.10: Time constant fitting results for the control valve to CO concentration measurement dynamics

Valve to outlet CO concentration measurement sinusoidal forcing method						
transfer function fitted	fitted time constants		residual sum of squares	standard error	dead time	
	T_1	T_2			(secs)	standard deviation
$\frac{1}{(1 + pT_1)}$	13.49		0.789	0.0522	25.96	
$\frac{1}{(1+pT_1)(1+pT_2)}$	11.98	3.54	0.0630	0.0474	23.31	2.0

Confidence limits for the transfer function giving an adequate fit							
transfer function	one parameter confidence intervals			non-linear confidence limits			
	standard error	lower value T	upper value T	lower value T	lower residual S.S.	upper value T	upper residual S.S.
$\frac{1}{(1+pT_1)(1+pT_2)}$ T_1	1.14	1.27	5.81	2.13	0.0807	4.82	0.0809
T_2	0.90	10.19	13.78	10.96	0.0810	13.07	0.0811
Critical sum of squares $SS_{(critical)} = 0.810$							

TABLE 4.10 (continued)

Valve to outlet concentration CO measurement m-sequence method						
transfer function fitted	fitted time constants		residual sum of squares	standard error	dead time (secs)	steady state gain
	T_1	T_2				
$\frac{1}{(1+pT_1)}$	18.97		.8499 x 10^{-4}	.5807 x 10^{-3}	21.83	.055
$\frac{1}{(1+pT_1)(1+pT_2)}$	8.47	4.6	.5638 x 10^{-4}	.4739 x 10^{-3}	20.66	.053

Confidence limits for the transfer function giving an adequate fit

transfer function	one parameter confidence intervals			non-linear confidence intervals			
	standard error	lower value T	upper value T	lower value T	lower residual S.S.	upper value T	upper residual S.S.
$\frac{1}{(1+pT_1)(1+pT_2)}$ T_1	1.05	6.39	10.55	6.28	.5892 x 10^{-4}	9.70	.5893 x 10^{-4}
T_2	1.31	2.01	7.2	2.97	.5890 x 10^{-4}	6.24	.5892 x 10^{-4}

Critical sum of squares $SS_{(critical)}$ = .5893 x 10^{-4}

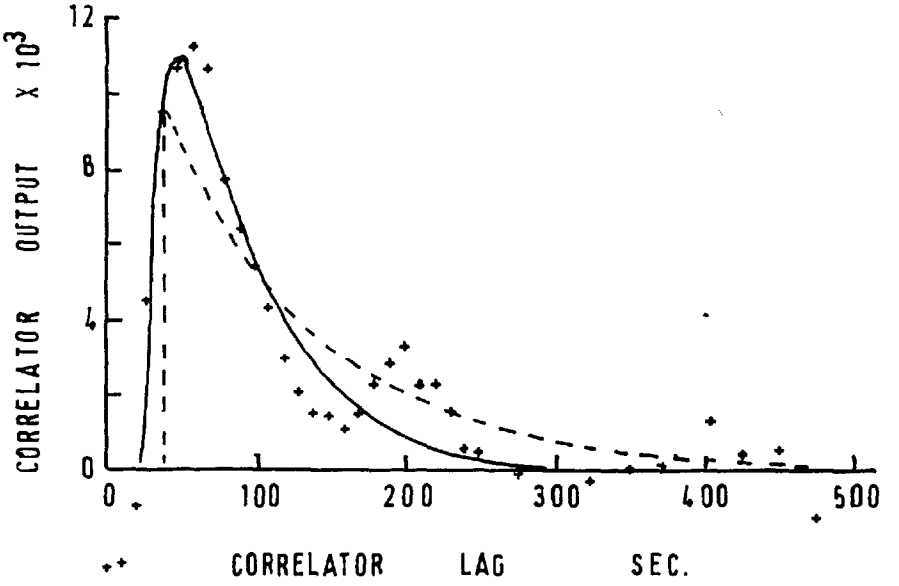

FIGURE 4.10 TEMPERATURE DYNAMICS: CO MEASUREMENT

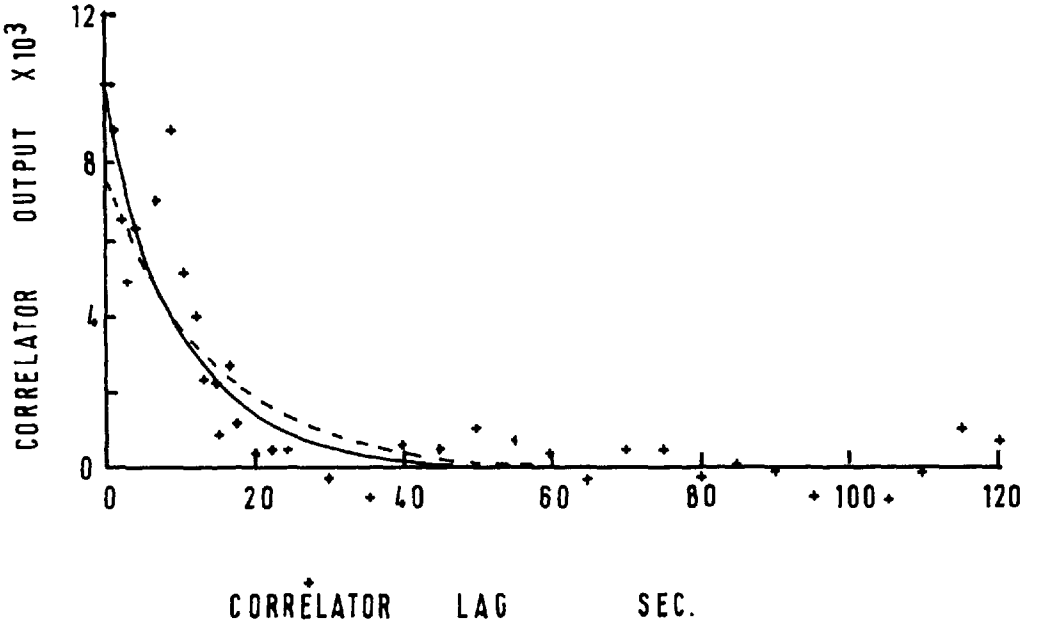

FIGURE 4.11 STEAM DYNAMICS: FLOW MEASUREMENT

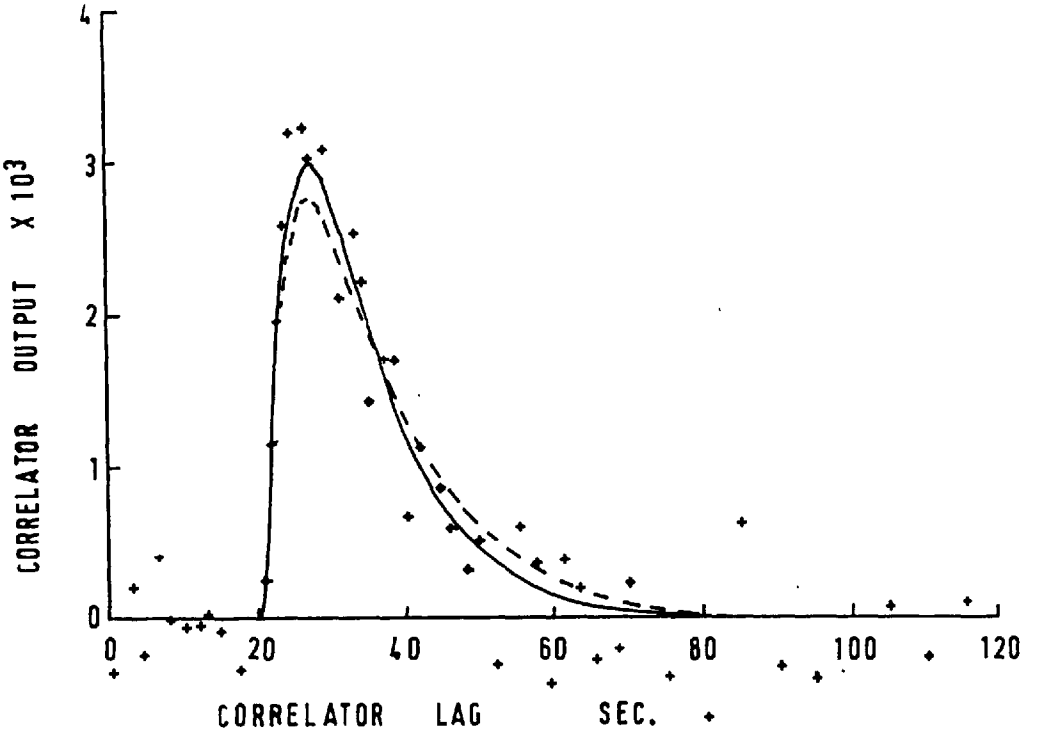

FIGURE 4.12 STEAM DYNAMICS:
CO MEASUREMENT

and these agree well with the predicted results. It is therefore assumed that a better estimate of the dead time is obtained, especially as the frequency response method did not yield this directly in the fitting. If 95% confidence limits are evaluated for the dead times obtained from sinusoidal forcing, it is found that all the dead times calculated by the m-sequence method lie within or very close to these limits.

Table 4.11 summarises the cases in which it is shown that a second order transfer function represents the dynamics significantly better than a first order one. The null hypothesis assumed that first order dynamics fitting was the correct one. After generating $F_{1,2}$ (M5) a comparison was made with the F-distribution. $F_{1,2}$ was found to lie outside the 95% and 99% levels in all cases except one, and then it was almost significant at the 99% level. Hence in these cases the null hypothesis was considered to be unacceptable and the second order dynamics assumed to give the better fit.

In Table 4.12 adequacy of each model is analysed by means of the F-test. In the case of temperature dynamics by the frequency response method and steam to steam flowrate dynamics by the m-sequence method, an inadequate fit of the data has been made.

Finally, in assessing the methods, notice should also be taken of the presence of an extra peak in Figure 4.10. This would be a reasonable occurrence if there were feedback in the

TABLE 4.11: Analysis of variance to choose between alternative models

Temperature controller to outlet concentration CO m-sequence method **				
No. of parameters	Remaining degrees of freedom	Sum of squares of residuals	Mean square	$F_{1,2} = \frac{M_{1-2}}{M_2}$
3	252	$SS_1 = .4447 \times 10^{-3}$	$M_1 = .1765 \times 10^{-5}$	
4	251	$SS_2 = .2374 \times 10^{-3}$	$M_2 = .9458 \times 10^{-6}$	$.2192 \times 10^{3}$
1	1	$SS_{1-2} = .2073 \times 10^{-3}$	$M_{1-2} = .2073 \times 10^{-3}$	
Valve to outlet concentration CO sinusoidal forcing method				
No. of parameters	Remaining degrees of freedom	Sum of squares of residuals	Mean square	$F_{1,2} = \frac{M_{1-2}}{M_2}$
1	29	$SS_1 = 0.079$	$M_1 = .00273$	
2	28	$SS_2 = 0.063$	$M_2 = .00225$	7.1
1	1	$SS_{1-2} = 0.016$	$M_{1-2} = .016$	
	$F_{0.95}(1,28) = 4.2$			
	$F_{0.99}(1,28) = 7.6$			

TABLE 4.11 (continued)

No. of parameters	Remaining degrees of freedom	Sum of squares of residuals	Mean square	$F_{1,2} = \frac{M_{1-2}}{M_2}$
3	252	SS_1 = $.8499 \times 10^{-4}$	M_1 = $.3373 \times 10^{-6}$	
4	251	SS_2 = $.5638 \times 10^{-4}$	M_2 = $.2246 \times 10^{-6}$	126.5
1	1	SS_{1-2} = $.2861 \times 10^{-4}$	M_{1-2} = $.2861 \times 10^{-4}$	
** $F_{0.95}(1,251) = 3.92$ $F_{0.99}(1,251) = 6.85$				

TABLE 4.12: Analysis of variance for the temperature dynamics

Comparison of the estimated variance for the temperature dynamics

	Differences between observed and predicted results		Experimental error		
Dynamics	Standard deviation S_o	No. of degrees of freedom N_o	Standard deviation S_1	No. of degrees of freedom N_1	$F = \frac{S_o^2}{S_1^2}$
Outlet concentration sinusoidal	0.072	30	0.47×10^{-2}	2	230.5
Outlet concentration m-sequence	$.9725 \times 10^{-3}$	251	0.1175×10^{-2}	84	.685
$F_{0.95}(30.2) = 19.46$			$F_{0.95}(251,84) = 1.25$		
$F_{0.99}(30.2) = 99.47$			$F_{0.99}(251,84) = 1.38$		

TABLE 4.12 (continued)

Comparison of the estimated variances for the steam dynamics					
	Differences between observed and predicted results		Experimental error		
Dynamics	Standard deviation S_o	No. of degrees of freedom N_o	Standard deviation S_1	No. of degrees of freedom N_1	$F = \frac{S_o^2}{S_1^2}$
Steam measurement sinusoidal	0.049	29	0.053	2	0.85
Steam measurement m-sequence	$.1276 \times 10^{-2}$	252	$.9192 \times 10^{-3}$	84	1.926
Outlet concentration sinusoidal	0.047	28	0.026	2	3.39
Outlet concentration m-sequence	$.4739 \times 10^{-3}$	251	$.6726 \times 10^{-3}$	84	.4965
$F_{0.95}(29,2) = 19.46$ $F_{0.99}(29,2) = 99.46$			$F_{0.95}(252,84) = 1.25$ $F_{0.99}(252,84) = 1.38$		

system or two parallel branches between input and output, but neither of these appeared to be present in the system so it is questionable how it arose.

4.3.6. Conclusions

From the experiments carried out it has been found that the sinusoidal forcing method is probably more reliable for generating the time constants. Although possibly if a shorter m-sequence were to be run for the same time, a lot of scatter obtained would be reduced and therefore this method improved. However, it is felt that dead times are more accurate when found by the use of pseudo-random binary sequence perturbation.

Both methods are easy to implement using commercially available equipment although care has to be taken in the case of m-sequence forcing to synchronize the recording equipment and the noise generator. The amount of on-line experimental work is considerably greater for the sinusoidal forcing which means the plant is being disturbed for longer periods, resulting in equivalently greater operating losses. The relative time required for off-line analysis is approximately proportional to the number of data points available. In each case a hill-climber is used to fit the transfer function, but in one the cross-correlation function over all lags must first be prepared and in the other the dead time has to be calculated separately. For the case of m-sequence forcing the steady state gain of the system is also fitted, which naturally

increases the time required in hill-climbing. Hence for this particular case about ten times more off-line computing was required in the analysis of the m-sequence forcing results. Therefore in making an estimate of the relative costs involved, the loss in operating efficiency associated with the sinusoidal method must be balanced against the requirements of more sophisticated equipment and greater data processing of the other method.

4.4. Simulation Model

Figure 4.13 shows how the non-linear inertialess blocks and the linear inertial blocks combine together to describe the system. Dealing with the inertialess elements is relatively simple as, provided the input parameters to an element are known, the output ones can be calculated by one of the algebraic manipulations given in either Chapter 3 or Section 4.2. In the case of the inertial elements, however, the modelling is complicated by the differential equation relationship between inputs and outputs, which necessitate continuous solution in order to describe the changing state of the system. Although dead times are comparatively easily dealt with in the digital simulation by storing, care still has to be taken to ensure that the signals maintain the same relative position with respect to each other as they had in the system being modelled. Also because what is essentially a sampled data system is being dealt with, the required value

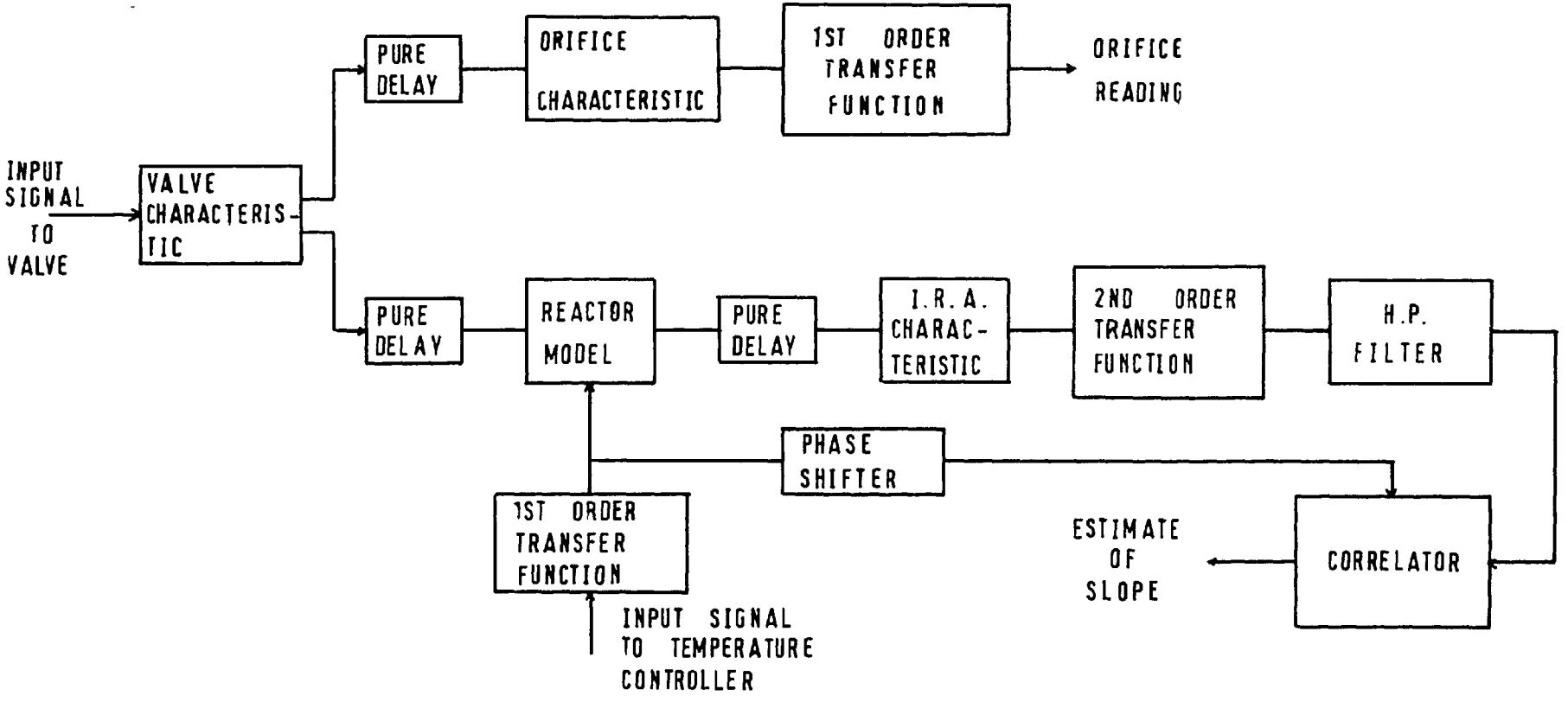

FIGURE 4.13 BLOCK DIAGRAM OF SYSTEM FOR OPTIMIZATION WITH RESPECT TO TEMPERATURE

is not always readily available and therefore a method of interpolating is needed.

4.4.1. Differential equations

The differential equations necessary for describing what occurs when optimization with respect to temperature is carried out are given below. In some cases equations of higher degree are reorganized into two or more first order equations.

Reactor temperature:

$$\frac{d}{dt}\ (\text{temperature}) = \frac{1}{T_{TR}}\ (\text{temperature specified by controller - actual temperature}) \qquad (4.4.1)$$

Output from IRA:

$$\frac{d^2}{dt^2}\ (\text{IRA reading}) = \frac{1}{T_{IR1}\ T_{IR2}}\ (\text{reading specified by non-linear characteristic - IRA reading}) - \left[\frac{1}{T_{IR1}} + \frac{1}{T_{IR2}}\right] \frac{d}{dt}\ (\text{IRA reading}) \qquad (4.4.2)$$

which after substituting

$$Z = \frac{d}{dt}\ (\text{IRA reading})$$

converts to

$$\frac{d}{dt}\ (Z) = \frac{1}{T_{IR1}\ T_{IR2}}\ (\text{reading specified by non-linear characteristic - IRA reading}) - \left[\frac{1}{T_{IR1}} + \frac{1}{T_{IR2}}\right] Z \qquad (4.4.2a)$$

and

$$\frac{d}{dt} \quad \text{(IRA reading)} \quad = \quad Z \qquad (4.4.2b)$$

High pass filter:

$$\frac{d}{dt} \quad \text{(output)} = \frac{d}{dt} \quad \text{(input)} - \frac{1}{T_{HP}} \quad \text{(output)} \qquad (4.4.3)$$

Correlator:

$$\frac{d}{dt} \quad \text{(correlated signal)} = \text{H.P. filter output} \times \text{phase shifted sinusoid} \qquad (4.4.4)$$

Penalty function:

$$\frac{d}{dt} \quad \text{(total loss)} = \text{constant} - \text{value of objective function} \qquad (4.4.5)$$

The numerical integration of these equations on a digital computer requires the breaking down of the problem into finite steps, solutions at the boundaries of which are obtained by the use of a variety of formulae. By their nature these step-wise calculations are open to two sources of error. Firstly the formulae are based on the assumption that the state at a certain point in the step prevails throughout the step. The error arising from this is normally referred to as 'truncation error' and can usually be reduced by decreasing the step size. The other, known as 'round-off' error, generally arises after operations like multiplication, division, etc., where the results are always rounded off to a constant number of digits; this is a non-systematic type of error which should not magnify if the programme formulation is a good one; if it

does influence the results however, improvement can be obtained by increasing the step length and therefore decreasing the number of calculations. Thus it is noted that since these two errors work against each other, a balance would have to be struck in choosing the step length.

The integration method used in the simulation model is Merson's (L1) modification of the classical fourth order Runge-Kutta algorithm; like the latter, this also uses the first four terms of a Taylor series expansion to approximate the integration over one step.

$$y_{n+1} = y_n + hy'_n + \frac{h^2}{2!} y''_n + \frac{h^3}{3!} y'''_n + \frac{h^4}{4!} y''''_n + O(h^5) \qquad (4.4.6)$$

where: y_n = value of integral at n^{th} stage,

h = step length.

Merson's modification does, however, have the advantage over the original Runge-Kutta method in that it is very much easier to estimate the 5th order error term $O(h^5)$ thus making it possible to keep a record of the truncation error. In the routine used accumulation was carried out in double precision thus resulting in, virtually, the complete elimination of 'round-off' error. Because of these two factors it was possible to reduce the step-length choosing procedure to one of running a typical problem with a given step-length and then halving this and re-running until such a stage that the difference between two successive final results was of no engineering consequence. A final check was made by ensuring that the

truncation errors were reasonable.

4.4.2. Programme

The programme for the simulation model was written in FORTRAN IV for running on the Imperial College IBM 7090 Computer. The flow diagram in Figure 4.14 illustrates how the magnetic tape facilities have been used for storing data either for safe keeping or further processing. The diagram shows the care taken to simulate dynamic conditions existing in the real system before initiating optimization and the inputting of noise. It is also seen how correlation is started before optimization so as to account for the dead time; for the same reason sampling of the correlator output is made at this same time interval before the end of each cycle.

FIGURE 4.14: Flow diagram of digital simulation model

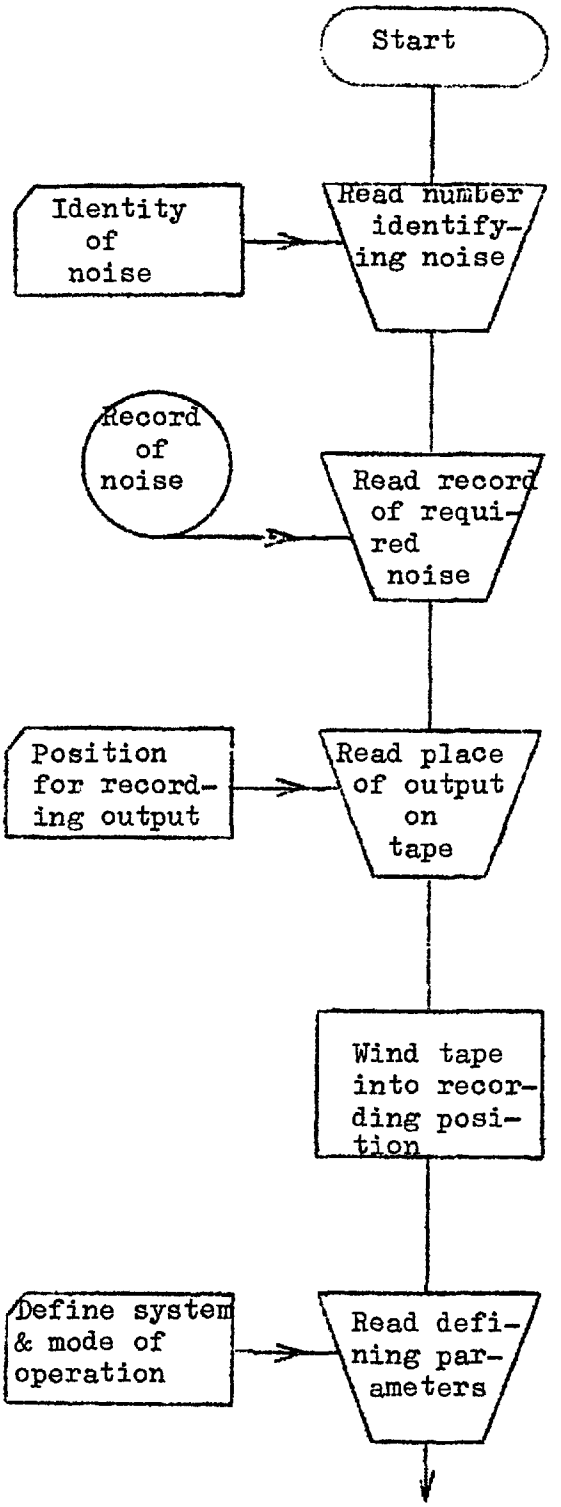

FIGURE 4.14 (continued)

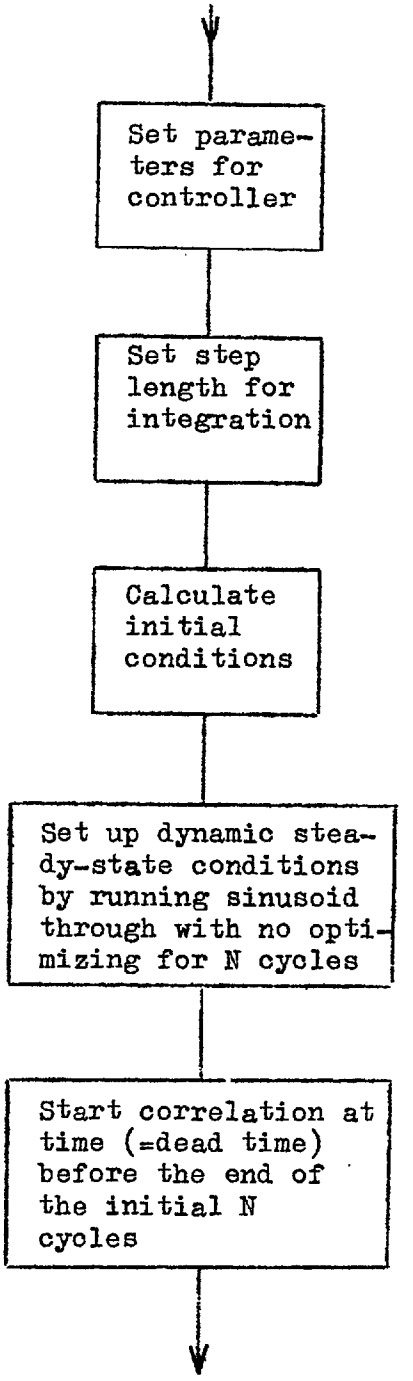

FIGURE 4.14 (continued)

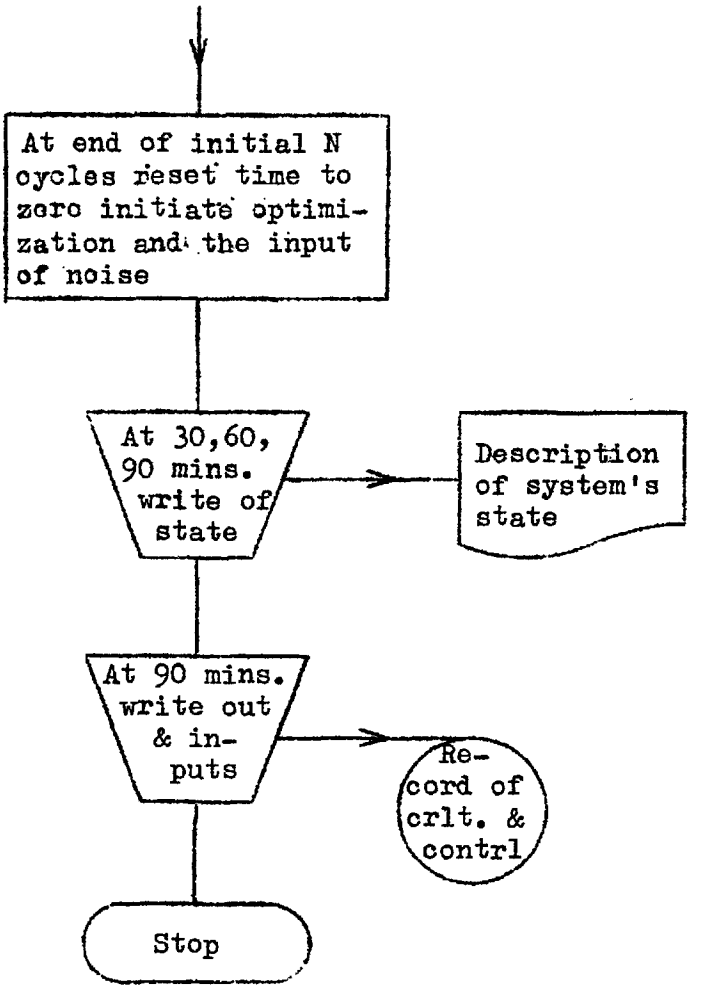

CHAPTER 5.

Application of the Predictor Regulator

5.1. Introduction

This chapter gives a description of the experiments carried out on the temperature side of the process to assess the feasibility of combining a Box and Jenkins predictor regulator with the Draper and Li adaptive optimizer; statistical analysis of the results suggest that improvements can indeed be obtained for cases where the rate of noise change is not too great. The second part of the chapter deals with a number of computer experiments that were carried out using the digital simulation model described in Chapter 4; the programme was partly a repeat of the experiments performed on the pilot plant and partly an extension of this work. The results obtained confirmed that improvements were possible but showed that difficulties which arise in fitting the parameters to the controller could lead to worse rather than better control.

5.2. Experimental Investigation

Optimization with respect to temperature was carried out for two reasons: firstly the system was found to behave better and more consistently on this side, hence greater reproducibility would be possible; and secondly the objective function that could be used was simple, involving only one measurement, and therefore avoiding the necessity of having to make phase compensations for measurements made at different points in the system.

5.2.1. Experimental programme

Kisiel and Price considered in their investigations into one variable optimization five parameters which influence the performance of the optimizer, namely: the amplitude and frequency of the perturbation, the phase shift of the correlating signal, the time constant of the high pass filter and the gain of the feedback loop. In this investigation only two of these were studied: the amplitude and frequency of the perturbing signal, while the remaining parameters were maintained either constant or at what Price had found to be their optimal values. A set of factorial experiments, designed to study the influence of the parameters on the optimizer when working in the presence of disturbances, was carried out for each of three noise signals. The required runs per factorial experiment were:

Period:	180 sec		180 sec
Amplitude:	5°C		10°C
		120 sec 7.5°C	
	60 sec		60 sec
	5°C		10°C

The middle point was included so as to obtain information about the curvature of the surface. Each individual experiment was run for a period of 1½ hrs; in the case of experiments which used the Draper and Li controller, the estimates of slope that were produced at the end of each questing cycle were

employed in designing the Box and Jenkins predictor regulator required for the re-run. Thus it was hoped that, by comparing the last half hour of each run, the new controller could still maintain an improvement in the presence of noise that had not influenced its design.

At each frequency the phase shift of the correlating sinusoid was adjusted so that this signal would be in phase with the high pass filter output, while the time constant of the latter was set to the period of the questing signal. The proportion of feedback was maintained constant at a value at which there would not be an uncontrollably large change in the set point when operating on the steep side of the hill. This was found to give ample feedback when climbing on the flat side of the hill at low frequencies, although it proved to be less satisfactory at the higher frequencies.

5.2.2. Analogue circuit

Figure 5.1 shows the analogue circuit used in the first part of the experimental work, where the straight forward Draper and Li optimizer was applied, and Figure 5.2 shows the additional circuit used when the predictor regulator was incorporated. The components are shown as numbered in two parts, the first number indicates which computer the component is from while the second specifies the actual location on the computer. Each multiplier has numbers on it specifying the module used and the amplifier associated with it. To aid in the understanding

of the circuits broken lines have been used to box individual pieces of circuitry and a list of the amplifier employed together with a description of their purpose is given below. Finally the potentiometers used are listed in two sections, one in which the settings remain constant throughout all the experiments and the other in which the settings are those used when the amplitude of perturbation was 1 volt ($10^{o}C$) and the period 3 minutes.

When operating the computers care had to be taken to ensure that all three chassis were connected with copper wire, and that their mains supplies came from the same source. If these precautions were not taken, it was found that amplifiers could go into a high state of oscillation or overload.

The source of the sinusoidal signals entering amplifiers 2.11 and 2.12 was from a sine-cosine potentiometer mounted on an adjustable constant speed motor. Also on the shaft of the motor was attached a magnetic switch which every cycle made and broke a circuit for a period ranging from 1 to 5 seconds; it was this signal fed to a comparator which was used to control the sample and hold circuit. The remaining integrators in the circuit were operated in one of two ways, either continuously like 2.5 in the high pass filter, or from the operate button as was the case with the others. Arrangements were made with comparator II so that whenever integrator 2.1 reached the overload point of 10 volts it could be reset to 1 volt; thus at any one time,reading the value of the performance criterion

involved counting the number of times amplifier 2.1 had overloaded and taking the current value of the amplifier.

In Figure 5.2 it is seen that some additional sample and hold circuits have been incorporated to allow calculation of terms needed for the Box and Jenkins predictor regulator.

List of amplifiers used:

Amplifier	Purpose
1.1	Signal to e/p transducer which drives pneumatic valve
1.3	Receives signal from steam orifice
1.4	Inverter
1.5	Amplifies signal from I.R.A.
1.6	Forms objective function
1.7	Forms penalty function
1.8	Inverter
1.15	Prepares sinusoid for recording on chart
1.19	Limits the combined noise and control signal
1.20	Feeds signal to temperature controller
2.1	Integrator for performance criterion
2.2	Inverter
2.3	Integrator for correlating circuit
2.4	Prepares H.P. filter output for recording
2.5	Integrator in H.P. filter
2.6	Summer in H.P. filter
2.7	Sampling integrator
2.8	Holding integrator

Amplifier	Purpose
2.9	Inverter
2.10	Inverter
2.11	Inverter
2.12	Inverter
2.13	Inverter
2.14	Inverter
2.19	Inverter
2.20	Inverter
2.22	Inverter
2.23	Amplifier for servo-multiplier SM1
2.24	Summer for phase shifting the perturbing signal
3.20	Summer for terms in $\Sigma\epsilon$ and ϵ
3.21	Summer to calculate x^*
3.24	Sampling integrator
3.26	Summer to calculate ϵ
3.27	Summer to calculate $\Delta\epsilon$
3.28	Summer to calculate $\Delta^2\epsilon$
3.29	Summer for terms in $\Delta\epsilon$ and $\Delta^2\epsilon$
3.30	Sampling integrator
3.31	Sampling integrator
3.32	Sampling integrator
3.33	Sampling integrator
3.34	Summer to calculate Σx^*
3.36	Holding integrator
3.42	Holding integrator

Amplifier	Purpose
3.43	Holding integrator
3.44	Holding integrator
3.45	Holding integrator
3.82	Inverter
3.93	Inverter
3.94	Inverter
3.97	Inverter
3.98	Inverter

Potentiometer with fixed settings:

Potentiometer	Purpose	Setting
1.1	Control signal to e/p transducer which drives pneumatic valve	.500
1.5	Multiplying parameter for objective function	.525
1.6	D.C. term of objective function	.180
1.7	D.C. term of penalty function	.090
1.8	Multiplying parameter for penalty function	.100
1.14	Sets level at which switch operates	.700
1.15	Changes mean level of oscillation	.500
1.16	Attenuates correlating sinusoid	.500
1.18	Sets limit beyond which control plus noise signal must not go	.150
1.19	Sets initial mean operating level of temperature controller	.300
1.20	Sets limit beyond which control plus noise signal must not go	.550

Potentiometer	Purpose	Setting
2.4	Changes mean operating level of signal from H.P. filter	.500
2.13	Attenuates signal to correlating integrator	.200
2.14	Attenuates signal to multiplier	.020

Potentiometers which are set specifically for perturbing signal of 1 volt (10°C) amplitude and 3 minutes period:

Potentiometer	Purpose	Setting
2.5	Feedback gain on H.P. filter	.006
2.8	Sets amplitude of perturbing signal	.100
2.11	Attenuates sinusoid for phase-shifting	1.000
2.12	Attenuates cosinusoid for phase-shifting	0.000

Potentiometers used in implementing Box and Jenkins predictor; no settings are given.

Potentiometer	Purpose
3.35	Multiplies $\Sigma\varepsilon$ by $\frac{\gamma_1}{g(1-\lambda)}$
3.36	Multiplies ε by $\frac{1 + \gamma_0 + k\gamma_1}{g(1-\lambda)}$
3.37	Multiplies $\Delta\varepsilon$ by $\frac{\gamma_{-1} + k(1+\gamma_0)}{g(1-\lambda)}$
3.38	Multiplies $\Delta^2\varepsilon$ by $\frac{k\ \gamma_{-1}}{g(1-\lambda)}$
3.39	Multiplies x^* by $\frac{\lambda}{1-\lambda}$

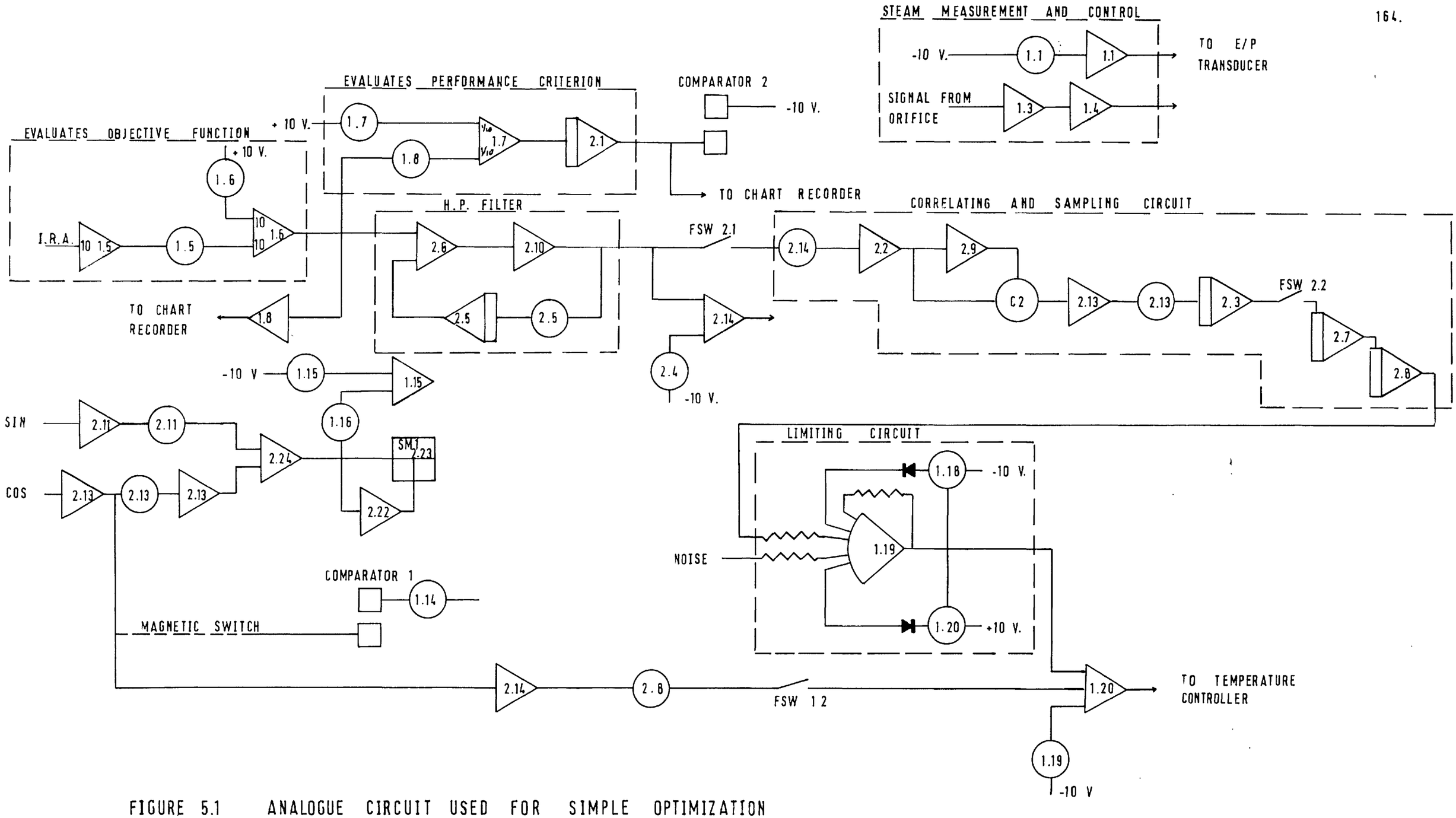

FIGURE 5.1 ANALOGUE CIRCUIT USED FOR SIMPLE OPTIMIZATION

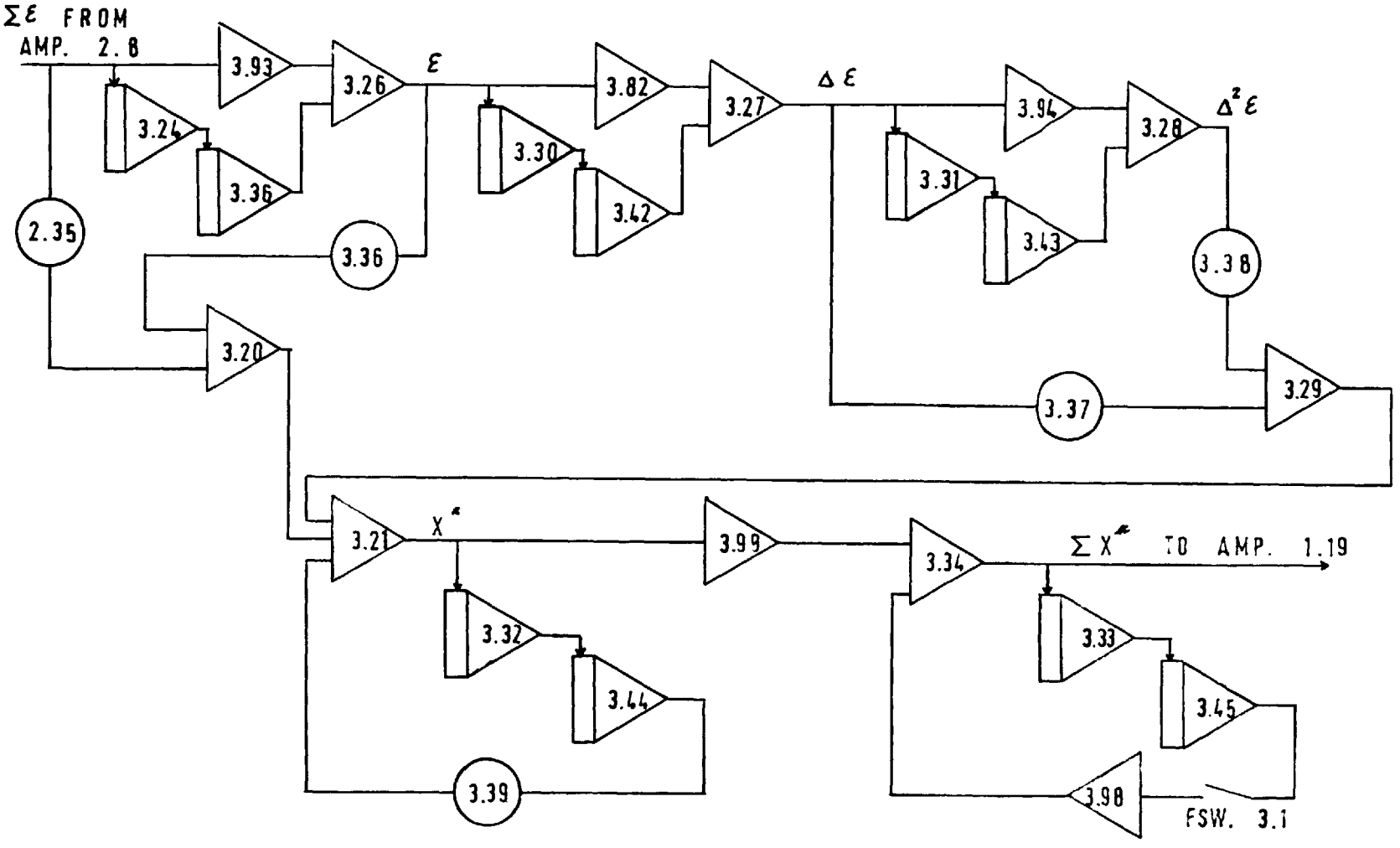

FIGURE 5.2 ANALOGUE CIRCUIT USED TO IMPLEMENT PREDICTOR OPTIMIZER

5.2.3. Description of noise

At first, the disturbance signals used in the experiment were generated automatically. A ten stage shift register, patched as an m-sequence generator, was cycled at a rate of 10 bits/sec., the last stage was sampled and put through a linear filter. Once every 90 seconds the signal from the filter was sampled and held; gaussian distributed random noise, from which a stochastic signal of given structure could be built up, was now available (E2). It was decided to use three different types of noise, namely:

(a) $z_p = a_p$ (0,0,0)

(b) $z_p - z_{p-1} = a_p$ (1,0,0)

(c) $z_p - 2z_{p-1} + z_{p-2} = a_p$ (2,0,0)

A list of the three noise signals used is given in Table 5.1. It will be noted that (a) only varies by ± 3 volts whereas the other two go up to ± 5 volts.

Originally these noise signals were to be generated on the Hybrid 48 (Figure 5.3), but it was found that although (a) and (b) were fairly reproducible, small errors were propagated into (c) causing large variations between successive runs. As a result of this, and because the analogue equipment was required for other purposes, the noise signal was introduced by hand (Figure 5.4).

Operation of the circuit shown in Figure 5.4 is controlled by the B timer, which switches the shift register block SRO

TABLE 5.1: Disturbances used to move the optimal operating point.

Time mins	Series I volts	Series II volts	Series III volts	Time mins	Series I volts	Series II volts	Series III volts
0.0	0.0	0.0	0.0	46.5	- 2.034	+ 2.318	0.924
1.5	- 2.648	0.930	0.466	48.0	2.390	1.564	1.303
3.0	0.872	0.683	0.776	49.5	1.512	1.103	1.438
4.5	- 2.087	1.405	1.441	51.0	2.925	0.170	1.088
6.0	1.558	0.933	1.850	52.5	- 2.280	0.955	1.126
7.5	- 2.027	1.634	2.604	54.0	- 1.466	1.471	1.412
9.0	2.480	0.861	2.951	55.5	- 2.284	2.259	2.084
10.5	- 2.114	1.590	3.656	57.0	1.630	1.750	2.490
12.0	0.907	1.332	4.220	58.5	- 1.226	2.192	3.111
13.5	1.641	0.833	4.515	60.0	1.041	1.182	3.564
15.0	0.885	0.582	4.671	61.5	- 2.235	2.652	4.395
16.5	2.773	- 0.291	4.371	63.0	2.358	1.906	4.838
18.0	2.321	- 1.013	3.694	64.5	1.019	1.602	5.120
19.5	2.484	- 1.708	2.614	66.0	2.919	0.661	4.914
21.0	2.384	- 2.534	1.144	67.5	2.717	- 0.211	4.260
22.5	- 0.727	- 2.258	- 0.199	69.0	- 2.055	0.504	3.954
24.0	- 2.826	- 1.293	- 1.065	70.5	- 2.345	1.309	4.045
25.5	- 1.294	- 0.832	- 1.712	72.0	0.899	1.045	3.992
27.0	2.795	- 1.709	- 2.820	73.5	1.123	0.706	3.753
28.5	- 2.303	- 0.922	- 3.536	75.0	0.840	0.461	3.385
30.0	- 0.974	- 0.567	- 4.080	76.5	- 2.277	1.250	3.404
31.5	- 2.320	+ 0.232	- 4.236	78.0	1.550	0.767	3.171
33.0	- 0.803	+ 0.530	- 4.252	79.5	2.440	- 0.015	2.533
34.5	- 2.349	+ 1.333	- 3.875	81.0	2.669	- 0.872	1.453
36.0	1.038	+ 1.028	- 3.667	82.5	1.493	- 1.326	0.126
37.5	- 2.534	+ 1.893	- 3.035	84.0	- 2.606	- 0.437	- 0.756
39.0	- 2.613	+ 2.787	- 1.963	85.5	- 1.204	- 0.006	- 1.433
40.5	0.851	+ 2.542	- 1.028	87.0	0.899	- 0.273	- 2.254
42.0	2.947	+ 1.610	- 0.577	88.5	0.896	- 0.058	- 2.924
43.5	0.959	+ 1.329	- 0.280	90.0	-	-	-
45.0	- 0.756	+ 1.613	0.150				

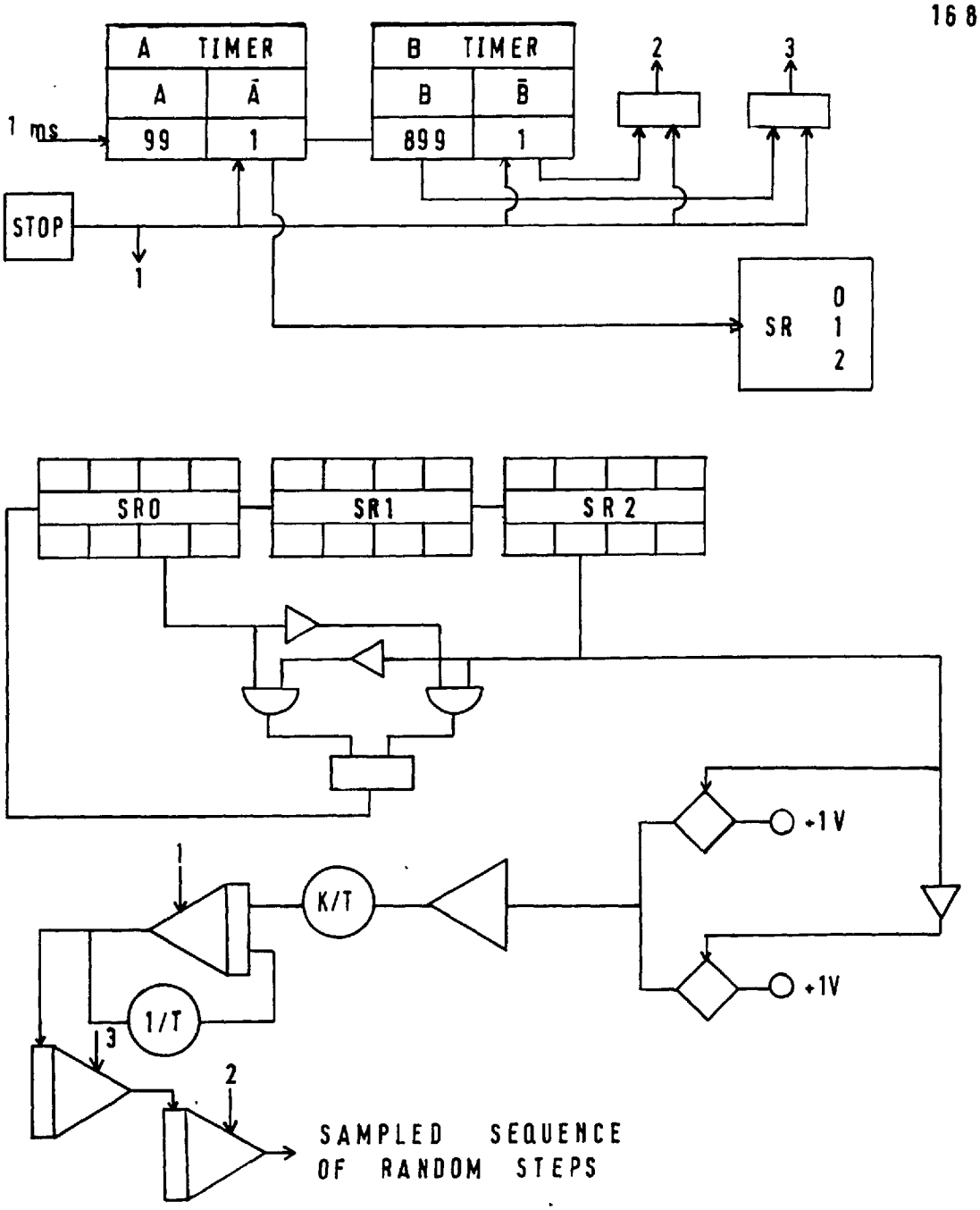

FIGURE 5.3 AUTOMATIC RANDOM NOISE GENERATOR

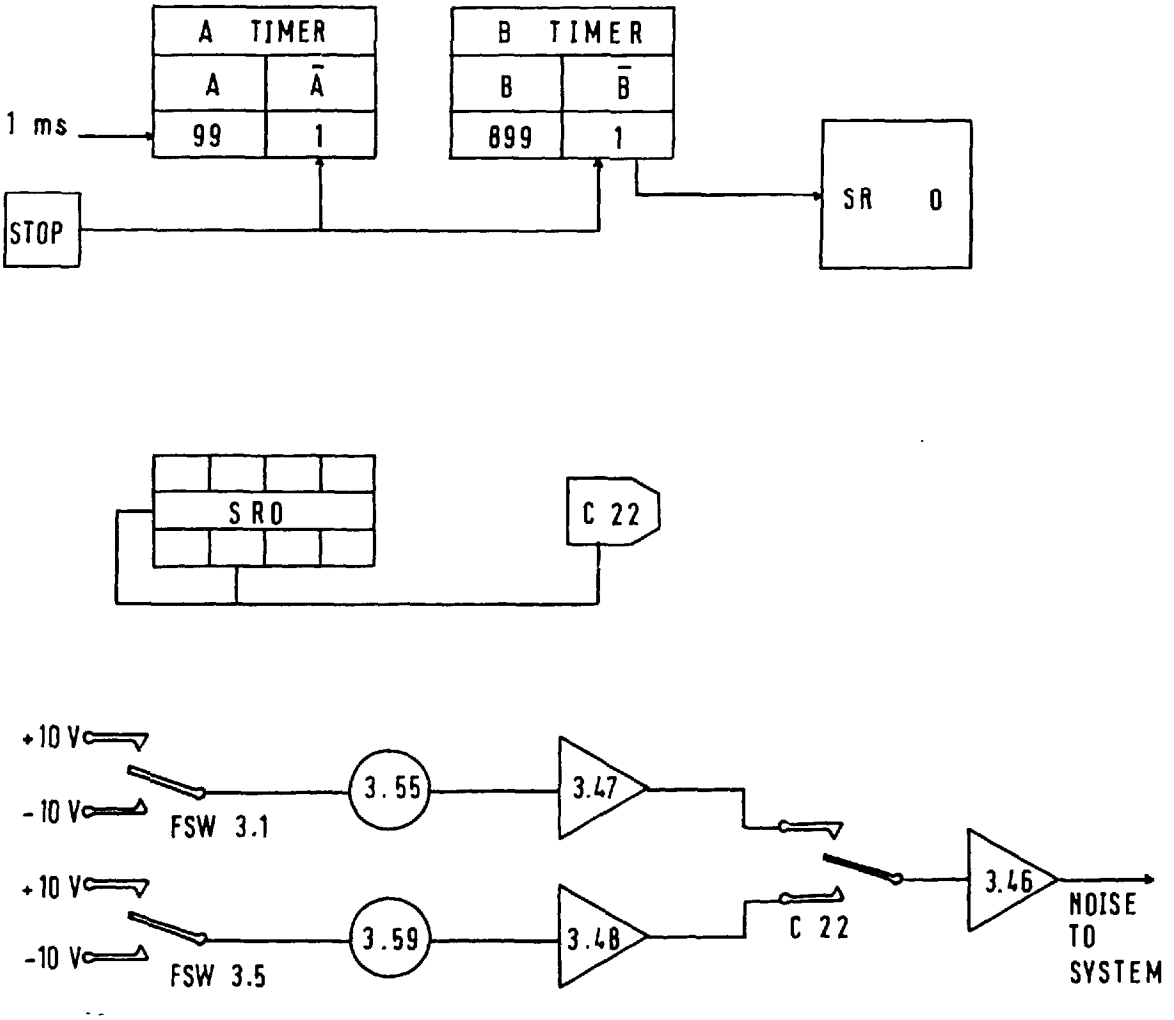

FIGURE 5.4 CIRCUIT TO INTRODUCE NOISE BY HAND

once every 90 secs. The latter in turn changes the position of relay 22. Thus after the relay has for instance switched to the downward position, there is a 90 second interval, during which the next value of the stochastic disturbance may be set up by means of FSW 3.1 and pot 3.55.

5.2.4. Experimental technique

The plant was started with a steady flow of dry hydrogen and nitrogen passing through the reactor, part of the stream was then diverted to the saturator where moisture was picked up. After operating like this for ten or fifteen minutes the arms on each side of the orifice plate were bled to remove any condensed water present. Carbon monoxide was then introdocued slowly, and the rotameters were adjusted to give the required readings. Lastly a fine adjustment was made to the level of the control valve (pot. 1.1) so that the total stream and dry gas flow was 115 l/hr.

The system, which was now ready for operation, had its mean operating temperature set on the left hand side of the optimum (Figure 4.5) and the potentiometer in the high pass filter adjusted to $\frac{1}{T}$, where T was the period of the perturbing signal. Perturbation was then initiated with the signal of required amplitude and frequency by closing function switch 1.2, and the optimality of the phase shifted sinusoid was checked by closing function switch 2.1 and putting integrator 2.3 into the operate mode; at this stage function switch 2.2 was of course kept open. If the phase shift were correct the

slope of the integrator output would always be greater than or equal to zero.

Having checked the phase shift of the correlating signal, integrators 2.1 and 2.3 were reset, the mean operating point of the temperature controller moved to the optimal operating point, and the system was allowed to reach steady state conditions. The point in the perturbing cycle at which the magnetic switch closed was taken as a reference with which to start all experiments; at this stage the function switch was closed, integrators 2.1 and 2.3 put into the operate mode, and the clock and noise inputting started. At the end of each cycle the output from the correlating integrator was sampled and the control signal updated; in the case of the straight Draper and Li optimizer these two values were the same. The signal from the magnetic switch which indicated the end of the cycle was also used to initiate a scan by the MDP 200 data logger; thus a complete recording of all parameters necessary to define the state of the system was made once a cycle. The outputs from amplifiers 1.8, 2.1, 2.3 and 2.4 were also plotted continuously on the four channel recorder. At times 30, 60 and 90 minutes after starting each experiment the value of the performance criterion was read off the chart recorder; subsequent to the last reading the experiment was stopped.

5.2.5. Results

After each experiment of the factorial design for a given type of noise, the series of estimates of slope was used to calculate the more sophisticated Box-Jenkins regulator. A list of the parameters fitted to the dynamic-stochastic optimizer, and the reduction obtained in the sum of squared errors which was used as the basis of the fitting, is given for each experiment in Tables 5.2 - 5.4. Figures 5.5 - 5.10 show graphically the action of the first and second types of noise on the system as well as the combined effects of noise and control action for the two controllers and for different perturbation signals. In Tables 5.5 - 5.13 the penalties incurred for the three series are summarized, both for the simple and sophisticated optimizers. It was noted that for Series III, as shown in Tables 5.11 - 5.13, no improvement was obtained at all, in fact there were greater losses. From the comparably less random nature of the noise series these results were somewhat unexpected; it is thought that they could be due to there being too low a signal to noise power ratio for optimization to take place, although the simulation studies reported at the end of the chapter throw light on other possible reasons. In the other two cases there was some apparent improvement, which however required considerable statistical analysis for conclusive proof. This analysis of the results was broken down into four stages:

TABLE 5.2: Parameters fitted to the predictor controller for operating in the presence of Series I noise.

Run No.	Period sec.	Amplitude volts	$\Sigma\varepsilon^2$ 0th iteration	$\Sigma\varepsilon^2$ last iteration	% of 0th iteration	Parameters fitted					
						λ	g	k	γ_{-1}	γ_0	γ_1
ST77	180	1.0	1.12	1.09	97.5	0	0.971	0.316	- 0.05	0.178	- 0.01
ST79	180	0.5	1.41	1.37	97.2	0.014	1.02	0.204	0.024	- 0.024	0.001
ST89	120	0.75	1.24	1.04	84.0	0.036	0.993	0.002	0.215	- 0.307	0.002
ST52	60	1.0	0.49	0.24	49.0	0.101	0.763	0.071	0.046	0.205	0.102
ST54	60	0.5	0.21	0.13	62.0	0.003	0.658	0.135	- 0.024	0.186	0.092

TABLE 5.3: Parameters fitted to the predictor controller for operating in the presence of Series II noise

Run No.	Period sec.	Amplitude volts	$\Sigma\varepsilon^2$ 0th iteration	$\Sigma\varepsilon^2$ last iteration	% of 0th iteration	Parameters fitted					
						λ	g	k	γ_{-1}	γ_0	γ_1
ST81	180	1.0	1.75	1.40	80.0	0.89	0.78	0.004	0.049	- 0.130	- 0.048
ST83	180	0.5	0.894	0.473	53.0	0.093	1.33	0.123	0.727	- 0.728	- 0.071
ST91	120	0.75	0.451	0.121	26.8	0.007	0.655	0.161	0.063	0.606	- 0.101
ST58	60	1.0	0.235	0.098	41.7	0.056	0.447	0.083	0.237	0.384	0.079
ST56	60	0.5	0.196	0.077	39.3	0.150	0.539	0.142	- 0.060	0.215	0.044

TABLE 5.4: Parameters fitted to the predictor controller for operating in the presence of Series III noise

Run No.	Period sec.	Amplitude volts	$\Sigma\varepsilon^2$ 0th iteration	$\Sigma\varepsilon^2$ last iteration	% of 0th iteration	Parameters fitted					
						λ	g	k	γ_{-1}	γ_0	γ_1
ST101	180	1.0	1.54	0.934	60.5	0.017	0.237	0.064	0.156	- 0.720	0.001
ST105	180	0.5	0.712	0.587	82.5	0.034	0.906	0.027	0.158	- 0.274	0.002
ST109	120	0.75	0.673	0.579	86.0	0.009	0.957	0.003	0.431	- 0.186	- 0.013
ST69	60	1.0	0.201	0.086	42.8	0.002	0.502	0.106	0.401	0.207	0.005
ST71	60	0.5	0.135	0.096	71.0	0	0.461	0.089	0.201	- 0.193	- 0.010

TABLE 5.5: Losses incurred during the first halfhour through not operating at the optimum when system is disturbed by Series I

Period sec.	Amplitude °C	Controller I Run No.	Controller I Perf. criterion	Controller II Run No.	Controller II Perf. criterion
180	10.0	ST7	136.9	ST77	87.4
180	10.0			ST99	117.6
180	5.0	ST9	102.6	ST79	87.6
120	7.5	ST16	108.6		
120	7.5	ST19	120.4	ST89	62.0
120	7.5	ST50	66.2		
60	10.0	ST12	205.7	ST52	59.1
60	10.0	ST67	168.9		
60	5.0	ST14	138.9	ST54	181.3
60	5.0	ST28	165.5		

TABLE 5.6: Losses incurred during the first hour through not operating at optimum when system is disturbed by Series I

Period sec.	Amplitude °C	Controller I Run No.	Controller I Perf. criterion	Controller II Run No.	Controller II Perf. criterion
180	10.0	ST7	283.6	ST77	170.0
180	10.0			ST99	278.0
180	5.0	ST9	350.0	ST79	158.0
120	7.5	ST16	272.1		
120	7.5	ST19	248.1	ST89	149.0
120	7.5	ST50	132.1		
60	10.0	ST12	397.8	ST52	135.7
60	10.0	ST67	331.0		
60	5.0	ST14	398.0	ST54	351.3
60	5.0	ST28	355.5		

TABLE 5.7: Losses incurred during 1½ hours of run through not operating at optimum when system is disturbed by Series I.

Period secs	Amplitude °C	Cont-roller I Run No.	Cont-roller I Perf. Criterion	Cont-roller II Run No.	Cont-roller II Perf. Criterion
180	10.0	ST7	636.5	ST77	372.6
180	10.0			ST99	382.6
180	5.0	ST9	639.4	ST79	191.2
120	7.5	ST16	552.8		
120	7.5	ST19	463.4	ST89	253.5
120	7.5	ST50	337.0		
60	10.0	ST12	776.0	ST52	284.6
60	10.0	ST67	700.8		
60	5.0	ST14	777.5	ST54	813.0
60	5.0	ST28	791.3		

TABLE 5.8: Losses incurred in the first halfhour through not operating at optimum when system is disturbed by Series II

Period secs	Amplitude °C	Cont-roller I Run No.	Cont-roller I Perf. Criterion	Cont-roller II Run No.	Cont-roller II Perf. Criterion
180	10.0	ST30	96.0	ST81	23.0
180	5.0	ST32	93.5	ST83	66.8
120	7.5	ST20	23.7	ST91	46.4
120	7.5	ST23	46.8	ST97	53.0
120	7.5	ST48	65.8		
60	10.0	ST24	147.2	ST58	42.0
60	5.0	ST26	77.8	ST56	151.8

TABLE 5.9: Losses incurred during the first hour through not operating at optimum when system is disturbed by Series II.

Period secs	Amplitude °C	Controller I Run No.	Controller I Perf. Criterion	Controller II Run No.	Controller II Perf. Criterion
180	10.0	ST30	541.3	ST81	96.8
180	5.0	ST32	337.9	ST83	136.8
120	7.5	ST20	263.7	ST91	236.0
120	7.5	ST23	283.1	ST97	110.0
120	7.5	ST48	350.8		
60	10.0	ST24	522.0	ST58	287.4
60	5.0	ST26	396.8	ST56	593.4

TABLE 5.10: Losses incurred during 1½ hours through not operating at optimum when system is disturbed by Series II.

Period secs	Amplitude °C	Controller I Run No.	Controller I Perf. Criterion	Controller II Run No.	Controller II Perf. Criterion
180	10.0	ST30	617.6	ST81	145.7
180	5.0	ST32	472.0	ST83	180.7
120	7.5	ST20	317.7	ST91	363.5
120	7.5	ST23	358.2	ST97	134.6
120	7.5	ST48	486.8		
60	10.0	ST24	906.0	ST58	520.6
60	5.0	ST26	754.1	ST56	1097.9

TABLE 5.11: Losses incurred during the first halfhour through not operating at optimum when system is disturbed by Series III.

Period secs	Amplitude °C	Cont-roller I Run No.	Cont-roller I Perf. Criterion	Cont-Roller II Run No.	Cont-roller II Perf. Criterion
180	10.0	ST84	344.8	ST101	543.8
180	5.0	ST87	220.4	ST105	546.0
120	7.5	ST93	335.4	ST109	531.2
60	10.0	ST62	520.4	ST69	782.1
60	5.0	ST60	642.7	ST71	899.5

TABLE 5.12: Losses incurred during the first hour through not operating at the optimum when the system is disturbed by Series III.

Period secs	Amplitude °C	Cont-roller I Run No.	Cont-roller I Perf. Criterion	Cont-roller II Run No.	Cont-roller II Perf. Criterion
180	10.0	ST84	820.6	ST101	1498.6
180	5.0	ST87	668.0	ST105	1168.0
120	7.5	ST93	858.4	ST109	1298.0
60	10.0	ST62	1108.3	ST69	1317.0
60	5.0	ST60	1230.0	ST71	1506.1

TABLE 5.13: Losses incurred during the 1½ hours through not operating at the optimum when the system is disturbed by Series III

Period secs	Amplitude °C	Cont-roller I Run No.	Cont-roller I Perf. Criterion	Cont-roller II Run No.	Cont-roller II Perf. Criterion
180	10.0	ST84	1355.4	ST101	2302.2
180	5.0	ST87	1066.4	ST105	2594.1
120	7.5	ST93	1308.8	ST109	2678.0
60	10.0	ST62	2397.2	ST69	2703.3
60	5.0	ST60	2546.1	ST71	2916.1

DISTURBANCE
DISTURBANCE + CONTROL ACTION (SIMPLE)
DISTURBANCE + CONTROL ACTION (PREDICTOR)

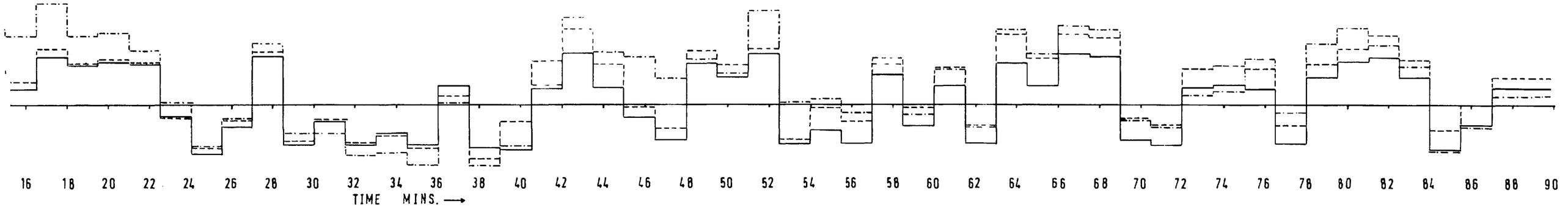

DISTURBANCES & DISTURBANCES + CONTROL ACTION: SERIES 1, 180 sec. & 1 volt PERTURBING SIGNAL

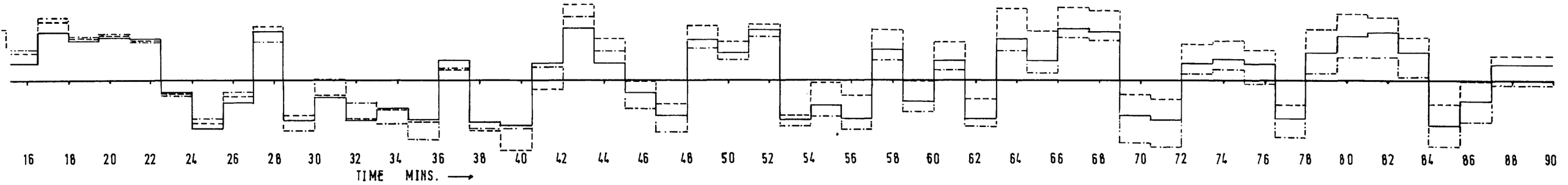

DISTURBANCES & DISTURBANCES + CONTROL ACTION: SERIES 1, 180 sec. & 1/2volts PERTURBING SIGNAL

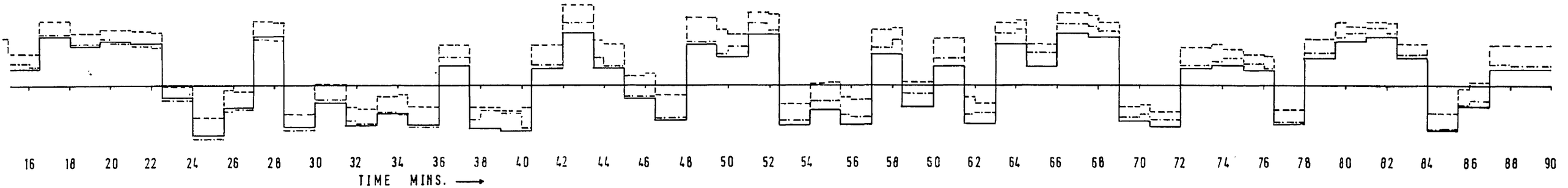

DISTURBANCES & DISTURBANCES + CONTROL ACTION: SERIES 1, 120 sec. & 3/4 volts PERTURBING SIGNAL

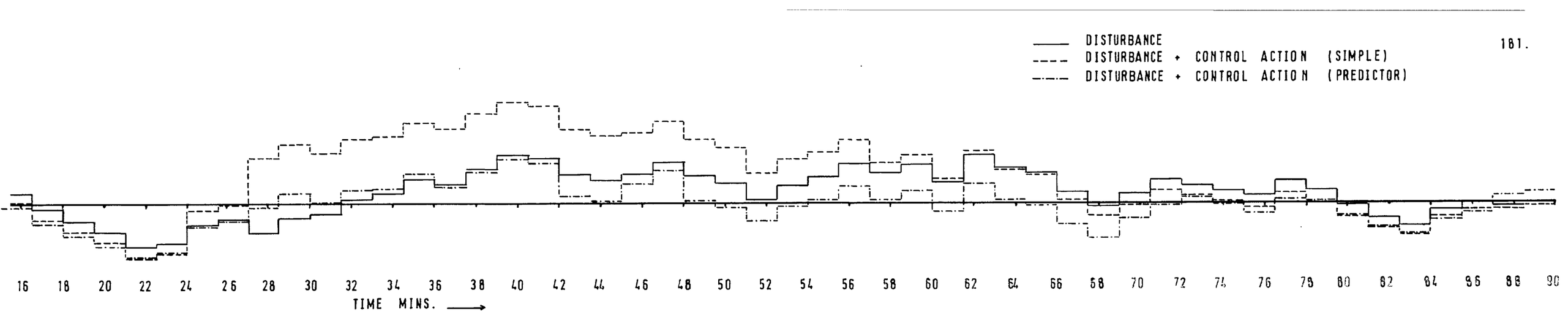

DISTURBANCES & DISTURBANCES + CONTROL ACTION: SERIES 2, 180 sec. & 1 volt PERTURBING SIGNAL

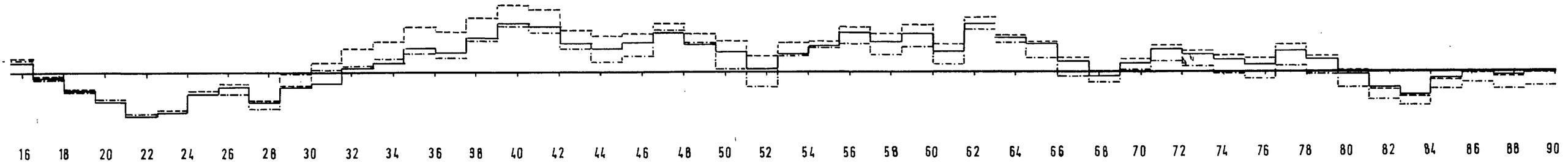

DISTURBANCES & DISTURBANCES + CONTROL ACTION: SERIES 2, 180 sec. & 1/2 volt PERTURBING SIGNAL

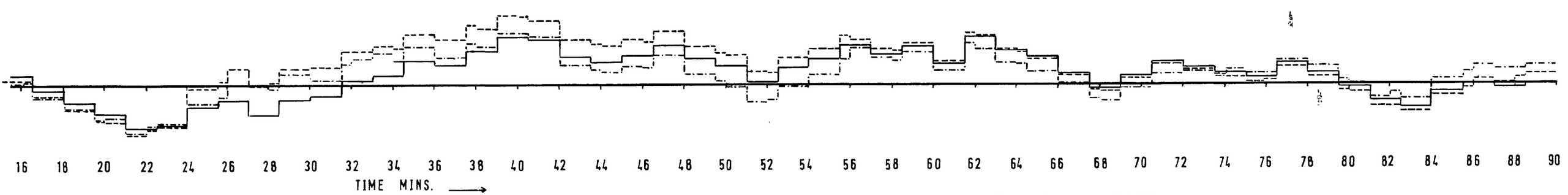

DISTURBANCES & DISTURBANCES + CONTROL ACTION: SERIES 2, 120 sec. & 3/4 volt PERTURBING SIGNAL

(i) it was shown that the errors incurred were not systematic,

(ii) the standard deviation of the experimental error was estimated,

(iii) the statistical t-test was used to show that the improvements were significant,

(iv) a quantitative estimate was made of the improvements obtained.

(i) Randomization of the experimental runs was not possible, to the extent that would have been desirable, for two reasons. Firstly, in all cases, experiments using the simple Draper and Li controller (henceforth referred to as Controller I) had to be run before the Box and Jenkins controller (Controller II) could be designed. Secondly, considerable time was required to set the motor driving the sine-wave generator to a particular speed, therefore it was very much more convenient to run experiments at a given frequency consecutively.

Examination of runs ST16, 19 and 50 suggested that there was a definite improvement of ST50 on the other two. However, ST20, 23 and 48 indicated that the system had got worse in about the same period of time. These two examples, which if taken individually would indicate that systematic trends had occurred in the system, jointly show that this was probably not the case. Also, during this series of experiments, no downward movement of the optimum value of the objective function that

could be associated with the catalyst decay reported in Chapter 4 was noted. Hence it was concluded that these effects were due solely to experimental error.

(ii) The experimental error present in the results was taken to be independent of both the series and the controller used. If this assumption was correct, then it was reasonable to use runs that had been repeated to calculate the overall standard deviation of the error. Hence the runs used were:

ST16, 19 and 50

ST20, 23 and 48

ST14 and 28

ST12 and 67

ST77 and 99

ST91 and 97

Because of the complications introduced by having the information broken down into groups of two or three runs, the method used in calculating the standard deviation is given below as a series of steps:

(a) the mean of each group was calculated,

(b) for each group the sum of squared deviations from the mean was calculated,

(c) these were summed over all groups to give the total sum of squared deviations,

(d) the number of degrees of freedom was calculated by subtracting the total number of groups used from the total number of runs,

(e) the unbiased variance of the errors was calculated by dividing the total sum of squared deviations by the number of degrees of freedom,

(f) square-rooting the variance gave the unbiased standard deviation of the errors.

The resulting calculated values for the standard deviations of the error in the Performance Criterion at times 30, 60 and 90 minutes after the start of each experiment are given below in Table 5.14.

TABLE 5.14: Unbiased estimates of the standard deviations of the error in the Performance Criterion.

Time interval in hours	Total sum of squared deviations from mean	No. of degrees of freedom	Unbiased variance $\hat{S}^2$	Unbiased standard deviation $\hat{S}$
½	3806	8	475.8	21.8
1	25521	8	3190.1	56.5
1½	56876	8	7109.5	84.4

(iii) Because of the large variance of the experimental error, no useful information could be obtained from comparing individual runs of the factorial experiments carried out. Thus the whole of the factorial experiment for a given type of noise was used in assessing the significance of improvements caused by Controller II. However, for both Series I and II, experiments at the period of 60 secs and 5°C amplitude showed apparent worsening of the situation with Controller II. It was thought that here again the effective signal to noise power

ratio was too small for satisfactory optimization and therefore analysis for each series was carried out with and without the inclusion of these runs.

The null hypothesis H_0, assumes that there was no improvement between Controller I and II. Therefore the effective mean difference in Performance Criterion between I and II should be zero. If, however, the difference was effectively greater than zero, the null hypothesis is disproved and there was some improvement. The hypothesis was tested using the Student t-statistic:

$$t = \frac{\overline{X} - 0}{\hat{S}_\Delta} \sqrt{N} \qquad (5.2.1)$$

where $\overline{X}$ = mean difference between I and II,

$\hat{S}_\Delta$ = standard deviation of difference,

N = number of points used.

The standard deviation of the difference was obtained from (5.2.2):

$$\hat{S}_\Delta^2 = 2\hat{S}^2 \qquad (5.2.2)$$

$$\hat{S}_\Delta = \sqrt{2}\ \hat{S} \qquad (5.2.3)$$

The results obtained are given below in Tables 5.15 and 5.16.

The influence of the fifth point in the factorial design shows up on comparing the results for the first half hour as given in Tables 5.15 and 5.16. It is noted that in the first case no significant improvement took place, while in the other it did. For other times of running, the Box and Jenkins controller does show improvement to the 95% level in the case of both series, and on occasions the significance even increases

TABLE 5.15: Test of significance carried out on results of the whole factorial design for operation with noise Series I and II.

Noise series	Time	Σ (differences)	Mean of differences	$\hat{S}_\Delta$	No. of pts considered	t
I	½h	184.5	36.9	30.9	5	2.68
I	1h	575.0	115.0	80.0	5	3.22
I	1½h	1351.2	270.2	119.7	5	5.10
II	½h	126.3	25.3	30.9	5	1.83
II	1h	810.0	162.0	80.0	5	4.53
II	1½h	942.5	188.5	119.7	5	3.52
$t_{0.975}(4) = 2.78$			$t_{0.995}(4) = 4.6$			

TABLE 5.16: Test of significance carried out on results of the whole factorial design minus the point at 60 sec, ½ volt perturbation for operation with noise Series I and II.

Noise series	Time	Σ (differences)	Mean of differences	$\hat{S}_\Delta$	No. of pts considered	t
I	½ h	213.9	53.5	30.9	4	3.46
I	1h	551.0	137.7	80.0	4	3.44
I	1½h	1358.2	339.5	119.7	4	5.67
II	½h	205.0	51.0	30.9	4	3.30
II	1h	1006.0	251.0	80.0	4	6.28
II	1½h	1286.0	321.0	119.7	4	5.36
$t_{0.975}(3) = 3.18$			$t_{0.995}(3) = 5.84$			

to the 99% level. Therefore, from the experiments run, it has been proved conclusively that improvement can be obtained by using a form of predictor controller when certain types of noise are disturbing the system.

(iv) A conservative estimate of the percentage improvement obtained by using the more sophisticated optimizer was now made. Again, because of the large experimental error, analysis was carried out on the whole factorial designs. The significant part of the average change between two sets of experiments was obtained by subtracting the 95% confidence intervals of the difference from the evaluated difference.

95% confidence interval of the change

$$= t_{0.975}\ (N - 1)\ \frac{\hat{s}_{\Delta}}{\sqrt{N}} \qquad (5.2.4)$$

Significant change = average change - 95% confidence interval of the change (5.2.5)

The percentage improvement on the average losses incurred through not operating at the optimum was now calculated by dividing the significant difference by the average losses incurred with Control I plus its 95% confidence interval.

Percentage average improvement

= {significant change}/{average losses + 95% confidence interval of losses} x 100% (5.2.6)

TABLE 5.17: Estimates of the quantitative improvements obtained from the whole factorial experiments by introducing predictor optimizers for operation in the presence of Series I and II types of disturbance.

Noise Series	Time hr.	Ave. Change	95% cf. lts. of Change	Signif. Change	Ave. Loss with Cont.I	95% cf. lts. of Loss	Max. Poss. Loss	Min.Sig. % improve-ment
I	½	36.9	38.4	-	135.4	27.0	162.4	-
I	1	115.0	99.4	15.6	317.4	70.2	387.6	4.0
I	1½	270.2	148.5	121.7	650.0	105.0	755.0	16.2
II	½	25.3	38.4	-	92.0	27.0	119.0	-
II	1	162.0	99.4	62.6	419.4	70.2	489.6	12.8
II	1½	188.5	148.5	40.0	627.5	105.0	732.0	5.5

TABLE 5.18: Estimates of the quantitative improvements obtained from four points of the factorial experiments by introducing predictor optimizers for operation in the presence of Series I and II types of disturbance.

Noise Series	Time hr.	Ave. Change	95% cf. lts. of Change	Signif. Change	Ave. Loss with Cont.I	95% cf. lts. of Loss	Max. Poss. Loss	Min.Sig. % improve-ment
I	½	53.5	49.1	-	131.4	31.5	162.9	-
I	1	137.7	127.2	10.5	303.8	90.0	393.8	2.7
I	1½	339.5	190.0	149.5	616.3	134.0	750.3	19.9
II	½	51.0	49.1	1.9	95.5	31.5	127.0	1.5
II	1	251.0	127.2	123.8	425.1	90.0	515.1	24.0
II	1½	321.0	190.0	131.0	595.8	134.0	729.8	18.0

Since this is the analysis of the worst case there is a 95% certainty that the average percentage improvements will not be smaller than those calculated. The results of this analysis are shown in Tables 5.17 and 5.18.

5.3. Investigations made with Digital Simulator

Although statistical analysis had clarified a lot, there still remained some doubt as to the validity of any conclusions that could be drawn from the experimental investigations; for instance, it was not immediately clear why the method had shown improvements in the case of the random series of disturbances (Series I), while none had been shown for the second order integrated series (Series III). The large experimental error encountered had made it impossible to perceive small changes taking place between individual runs, by direct comparison of these runs. Hence it was decided that in the digital simulation model, a system was available, which by its nature would behave in more or less the same manner as the plant had done, and not being subject to experimental error, any results it yielded would be completely reproducible. This not only allowed the experimental runs to be repeated, but also made it possible to extend the investigations and to obtain better quantitative estimates of the improvements that were possible.

5.3.1. Simulating experimental runs

In order to make the digital runs simulate the runs encountered as closely as possible, a number of precautions were taken: parameters that could be varied were given values used on the actual plant runs, also where practicable operations were performed in the same manner; for instance the sinusoidal perturbations were started and allowed to settle down before initiating optimization and noise inputting. As in the experimental runs the correlating integrator was sampled once a cycle, at which stage the control signal was updated; the value of the Performance Criterion was also noted every thirty minutes.

Again the estimates of slope obtained from runs employing the simple Draper and Li optimizer were used in fitting the more sophisticated predictor optimizer. At times during the practical programme it had been found that, at this the fitting stage, one or more of the dynamic parameters took up physically unrealistic values, e.g. assuming a negative dead time or time constant. The way the problem was by-passed was by introducing constraints which caused the objective function being minimized to become very large if any were broken; this was inefficient programming because it meant that although a certain amount of minimization could take place, it did not necessarily follow that the best minimum available was being found. For this reason it was

decided to use a method of constrained optimization developed by Murtagh and Sargent (M6), which combines an unconstrained method aimed at quadratic convergence with Rosen's (R2) method of gradient projection. The resulting changes in the value of the objective function due to the new method were marked, but they in turn gave rise to difficulties which are reported further on.

After fitting the new predictor optimizer to the system, the experiments were repeated as on the previous occasion. Besides re-running the three factorial experiments of the practical investigation, two further noise disturbances were studied. In the first instance the power of Series III was reduced by attenuating each value by a half, and in the second case the frequency of Series III was reduced by making a step change due to the disturbance once every 180 seconds rather than once every 90 seconds.

5.3.2. Results

Table 5.19 shows for each run carried out with Controller I the resulting parameters fitted to the Box and Jenkins optimizer after specified numbers of iterations. The constraints placed on the parameters were:

$$0 \leq \lambda \leq 1$$

$$0 \leq g$$

$$0 \leq k \leq 1$$

where λ = dead time, g = steady-stage gain of system,
k = parameter of first order transfer function.

TABLE 5.19

Parameters fitted to the predictor-controllers on the basis of the estimates of slope obtained with Controller I.

Noise Series	Run No.	Amplit of pert volts	Period of pert secs	No. of iteration	Sum of sq. of error	% of ss at 0th iteration	Parameters fitted					
							λ	g	k	γ_{-1}	γ_0	γ_1
I	SII.1	1.	180	0	1.81	100.	.0401	.9798	0.	.0195	.0199	-0.0079
I	SII.2	1.	180	1	1.73	95.5	.0954	.9479	0.	.0721	.0736	.1277
I	SII.3	1.	180	2	1.57	86.7	.2206	.8527	0.	-0.1885	.3309	.0476
I	SII.4	0.5	180	0	1.20	100.	.0503	.9748	0.	.0295	.0250	-0.0056
I	SII.5	0.5	180	1	1.14	95.	.1087	.9677	.0419	.0984	.0760	.0863
I	SII.6	0.5	180	2	1.02	85.	.2033	.9080	.0615	.0271	.2162	-0.0201
I	SII.7	0.75	120	0	.806	100.	0.	1.0104	.0216	-0.0198	-0.0108	.0072
I	SII.8	0.75	120	1	.792	98.4	0.	1.0285	.0305	-0.0313	-0.0167	-0.0073
I	SII.9	0.75	120	2	.678	84.	0.	1.2188	.1117	-0.0897	-0.0150	.0382
I	SII.10	1.	60	0	.0767	100.	.0212	.9975	.0160	.0014	.0027	.0441
I	SII.11	1.	60	1	.0757	98.7	.0354	.9836	0.	.0201	.0198	.0425
I	SII.12	1.	60	2	.0754	98.4	.0398	.9805	0.	.0328	.0265	.0421
I	SII.13	0.5	60	0	.0565	100.	.0207	.9992	.0185	.0017	.0015	.0930
I	SII.14	0.5	60	1	.0562	99.5	.0209	1.0036	.0265	.0039	-0.0016	.0918
I	SII.15	0.5	60	2	.0554	98.1	.0221	1.0248	.0611	.0182	-0.0114	.0842

TABLE 5.19
continued

Noise Series	Run No.	Amplit of pert. volts	Period of pert. sec.	No. of iteration	Sum of sq. of error	% of ss at 0th iteration	Parameters fitted					
							λ	g	k	γ_{-1}	γ_0	γ_1
II	SII.16	1.	180	0	1.71	100.	.033	.9833	0.	.0127	.0165	-0.0102
II	SII.17	1.	180	1	1.64	96.	.0599	.9776	.0096	.0490	.0223	-0.0603
II	SII.18	1.	180	2	1.46	83.	.1272	.9454	0.	.1394	.0539	-0.0369
II	SII.19	0.5	180	0	.647	100.	.0302	.9846	0.	.0099	.0150	-0.0101
II	SII.20	0.5	180	1	.635	98.1	.0282	.9433	0.	-0.0016	.0474	-0.0592
II	SII.21	0.5	180	2	.604	93.4	.0323	.7874	0.	-0.0261	.1796	-0.0238
II	SII.22	0.75	120	0	.416	100.	.0281	.9857	0.	.0080	.0141	-0.0054
II	SII.23	0.75	120	1	.297	71.4	.1706	.8388	0.	.1812	.1553	-0.0489
II	SII.24	0.75	120	2	.291	70.	.1808	.8144	0.	.1852	.1709	-0.0297
II	SII.25	1.	60	0	.0281	100.	.0211	.9892	0.	.0010	.0107	.0070
II	SII.26	1.	60	1	.0113	40.2	.0485	.7223	0.	.0226	.2692	.0975
II	SII.27	1.	60	2	.0111	39.5	.0488	.7152	0.	.0217	.2748	.1017
II	SII.28	0.5	60	0	.0084	100.	.0208	.9894	0.	.0007	.0105	.0114
II	SII.29	0.5	60	1	.0048	57.2	.0362	.7481	0.	.0102	.2463	.1702
II	SII.30	0.5	60	2	.0048	57.2	.0347	.7535	0.	.0065	.2396	.1671

TABLE 5.19
continued

Noise Series	Run No.	Amplit of pert. volts	Period of pert. secs.	No. of iteration	Sum of sq. of error	% of ss at 0th iteration	Parameters fitted					
							λ	g	k	γ_{-1}	γ_0	γ_1
III	SII.31	1.	180	0	3.12	100.	.0245	.9875	0.	.0045	.0123	.0066
III	SII.32	1.	180	1	2.94	94.3	.0542	.9483	0.	.0258	.0522	-0.0605
III	SII.33	1.	180	2	1.51	48.4	.0528	.7190	0.	.2082	.1645	.0068
III	SII.34	0.5	180	0	1.32	100.	.0234	.9881	0.	.0034	.0118	.0111
III	SII.35	0.5	180	1	1.22	92.4	.0559	.8930	0.	.0254	.1026	-0.0702
III	SII.36	0.5	180	2	1.02	77.3	0.	.7456	0.	-0.0080	.1819	-0.0745
III	SII.37	0.75	120	0	.622	100.	.0235	.9880	0.	.0034	.0119	.0087
III	SII.38	0.75	120	1	.519	83.4	.0833	.8658	0.	.0561	.1243	-0.0903
III	SII.39	0.75	120	2	.188	30.2	.2897	.5542	0.	.2498	.3699	-0.0421
III	SII.40	1.	60	0	.0600	100.	.0205	.9895	0.	.0005	.0105	.0367
III	SII.41	1.	60	1	.0067	11.2	.0275	.3673	0.	.0064	.5374	.1660
III	SII.42	1.	60	2	.0066	11.0	.0775	.3584	0.	.0049	.5415	.1675
III	SII.43	0.5	60	0	.0148	100.	.0205	.9895	0.	.0006	.0105	.0420
III	SII.44	0.5	60	1	.0026	17.6	.0480	.6744	0.	.0078	.2822	.3915

TABLE 5.19
continued

Noise Series	Run No.	Amplit of pert volts	Period of pert secs	No. of itera-tion	Sum of sq. of error	% of ss at 0th itera-tion	Parameters fitted					
							λ	g	k	γ_{-1}	γ_0	γ_1
IV	SII.45	1.	180	0	2.01	100.	.0280	.9858	0.	.0078	.0140	.0024
IV	SII.46	1.	180	1	1.91	95.	.0657	.9751	.0029	.0424	.0357	-0.0573
IV	SII.47	1.	180	2	1.08	53.8	.4570	.9290	.1327	.4161	.2334	.0352
IV	SII.48	0.5	180	0	.652	100.	.027	.9862	0.	.0069	.0135	.0073
IV	SII.49	0.5	180	1	.544	83.4	.104	.9056	0.	.0744	.1034	-0.0916
IV	SII.50	0.5	180	2	.202	31.0	.391	.7190	0.	.3013	.3738	-0.0073
IV	SII.51	0.75	120	0	.397	100.	.0234	.9881	0.	.0034	.0118	.0082
IV	SII.52	0.75	120	1	.324	81.5	.0695	.8737	0.	.0396	.1229	-0.0690
IV	SII.53	0.75	120	2	.0769	19.3	.2717	.4983	0.	.1518	.4640	-0.0125
IV	SII.54	1.	60	0	.335	100.	.0204	.9896	0.	.0004	.0104	.0377
IV	SII.55	1.	60	1	.0078	23.3	.0379	.7049	0.	-0.0024	.2610	.1492
IV	SII.56	1.	60	2	.0076	23.0	.0383	.6972	0.	-0.0026	.2666	.1512
IV	SII.57	0.5	60	0	.0088	100.	.0203	.9896	0.	.0003	.0103	.0467
IV	SII.58	0.5	60	1	.0017	19.3	.0309	.7659	0.	-0.0023	.2071	.3671

TABLE 5.19
continued

Noise Series	Run No.	Amplit of pert volts	Period of pert secs	No. of iteration	Sum of sq. of error	% of ss at 0th iteration	Parameters fitted					
							λ	g	k	γ_{-1}	γ_0	γ_1
V	SII.59	1.00	180	0	1.87	100.	.0282	.9857	0.	.0080	.0141	-0.0056
V	SII.60	1.00	180	1	1.16	61.5	.0474	.9499	0.	.0365	.0442	-0.1587
V	SII.61	1.00	180	2	1.05	56.2	0.	.8583	0.	.0542	.0847	-0.1231
V	SII.62	0.50	180	0	.360	100.	.0358	.9820	0.	.0154	.0179	-0.0169
V	SII.63	0.50	180	1	.210	58.4	.1453	.8579	0.	.1231	.1416	-0.1437
V	SII.64	0.50	180	2	.134	37.2	.0666	.6830	0.	.2957	.3200	-0.1265
V	SII.65	0.75	120	0	.341	100.	.0240	.9877	0.	.0040	.0121	-0.0039
V	SII.66	0.75	120	1	.227	66.5	.0492	.9028	0.	.0277	.0888	-0.1216
V	SII.67	0.75	120	2	.122	35.6	.0608	.5546	0.	.0486	.4336	.1418
V	SII.68	1.00	60	0	.040	100.	.0209	.9893	0.	.0009	.0106	.0008
V	SII.69	1.00	60	1	.007	17.5	.0261	.9088	0.	.0034	.0691	.2447
V	SII.70	1.00	60	2	.003	7.5	.0360	.7734	0.	.0096	.1790	.5614
V	SII.71	0.50	60	0	.009	100.	.0209	.9893	0.	.0010	.0107	-0.0023
V	SII.72	0.50	60	1	.005	55.5	0.	1.2320	0.	-0.0216	-0.2253	.1779
V	SII.73	0.50	60	2	.004	44.4	0.	1.7540	0.	-0.0669	-0.7226	.4221

Because of the need for starting the hill climbing routine used in fitting the new control parameters some distance away from the constraints, it was not possible to use the parameter value of the first controller as the starting point. Hence no evaluation was generally available of the sum of squared errors due to the simple optimizer, though it is assumed that the values given at the end of the zeroth iteration are a good approximation. Values of the sum of squared errors are also given in the table for each controller fitted, together with a term specifying them as a percentage of the sum of squared error at the starting point. It is noted from this last factor that the proportional reduction obtained in the sum of squared errors at specific iterations increases with decreasing period of perturbation and with decreasing randomness of the disturbance. It is thought that the first is true because greater amounts of information are available, while the second factor follows because the disturbance being modelled is smoother.

The values of the Performance Criterion obtained during the simulations are listed in Table 5.20; they are broken down into groups which depend on the noise series used, the frequency of perturbation and the amplitude of perturbation. The run numbers define whether Controller I or II was used; also given for each type of noise are the results obtained from simulations in which the system was disturbed, but no

Table 5.20:-

Values of the Performance Criterion obtained for different runs

Noise Series	Run No.	Performance Criterion			Improvement			% Improvement		
		½h	1h	1½h	½h	1h	1½h	½h	1h	1½h
I	No Control	163.3	453.7	605.7						
I	SI.1	215.7	424.4	615.5						
I	SII.1									
I	SII.2	249.2	452.9	657.0						
I	SII.3	281.2	659.4	860.7						
I	SI.2	193.9	386.8	566.6						
I	SII.4									
I	SII.5	216.6	393.7	586.4						
I	SII.6	216.1	481.8	679.3						
I	SI.3	168.4	378.7	538.						
I	SII.7									
I	SII.8	168.	394.3	547.9	0.4			0.2		
I	SII.9	167.5	378.7	564.2	0.9			0.5		
I	SI.4	165.1	389.1	541.						
I	SII.10									
I	SII.11	166.1	344.4	555.7		44.7			11.5	
I	SII.12	166.1	343.9	555.7		45.2			11.6	
I	SI.5	164.2	409.	556.4						
I	SII.13									
I	SII.14	165.4	338.	578.7		71.			17.4	
I	SII.15									

Table 5.20:-

Continued ..... /

Noise Series	Run No.	Performance Criterion			Improvement			% Improvement		
		½h	1h	1½h	½h	1h	1½h	½h	1h	1½h
II	No Control	237.7	343.6	426.2						
II	SI.6	199.3	466.2	577.9						
II	SII.16	198.1	468.2	577.9	0.8			0.4		
II	SII.17	196.9	396.7	524.2	2.4	69.5	53.7	1.2	14.9	9.3
II	SII.18	195.4	478.6	590.6	3.9			2.0		
II	SI.7	206.2	396.5	496.6						
II	SII.19									
II	SII.20	205.0	361.0	465.2	1.2	35.5	31.4	0.6	9.0	6.3
II	SII.21	197.1	432.1	537.6	9.1			4.4		
II	SI.8	208.1	389.7	481.8						
II	SII.22									
II	SII.23	193.6	366.3	489.6	14.5	23.4		7.5	6.0	
II	SII.24									
II	SI.9	216.	353.3	437.0						
II	SII.25	214.6	361.1	446.4	1.4			0.7		
II	SII.26	197.6	517.3	717.2	18.4			8.5		
II	SII.27	197.1	526.2	733.1	18.9			8.8		
II	SI.10	225.1	346.5	428.2						
II	SII.28	224.1	352.4	433.8	1.0			0.4		
II	SII.29	211.8	484.3	708.8	13.3			6.0		
II	SII.30									

Table 5.20:-

Continued ..... /

Noise Series	Run No.	Performance Criterion			Improvement			% Improvement		
		½h	1h	1½h	½h	1h	1½h	½h	1h	1½h
III	No Control	329.3	791.6	1257.5						
III	SI.11	352.0	939.4	1609.6						
III	SII.31									
III	SII.32	350.	881.1	1462.6	2.0	58.3	147.	0.6	6.2	9.1
III	SII.33	420.4	1311.3	2269.4						
III	SI.12	336.8	867.2	1490.8						
III	SII.34									
III	SII.35	334.8	831.6	1383.	2.0	35.6	107.8	0.6	4.1	7.2
III	SII.36	335.9	836.1	1391.8	0.9	31.1	99.	0.3	3.6	6.6
III	SI.13	338.7	825.9	1405.9						
III	SII.37									
III	SII.38	334.	752.6	1197.5	4.7	73.3	208.4	1.4	8.9	14.8
III	SII.39	341.1	981.3	1584.1						
III	SI.14	336.4	798.2	1336.9						
III	SII.40	341.4	838.7	1479.0						
III	SII.41	369.6	1153.1	2110.8						
III	SII.42									
III	SI.15	332.6	787.2	1293.9						
III	SII.43	335.1	804.9	1365.4						
III	SII.44	357.0	1112.7	2070.4						

Table 5.20:-

Continued ..... /

Noise Series	Run No.	Performance Criterion			Improvement			% Improvement		
		½h	1h	1½h	½h	1h	1½h	½h	1h	1½h
IV	No Control	118.7	459.5	606.6						
IV	SI.16	151.3	455.2	726.3						
IV	SII.45									
IV	SII.46	150.1	393.1	622.2	1.2	62.1	104.1	0.8	13.6	14.4
IV	SII.47	276.	1140.7	2048.9						
IV	SI.17	132.	436.2	671.4						
IV	SII.48									
IV	SII.49	132.9	392.1	619.8		44.1	51.6		10.1	7.7
IV	SII.50	202.5	1018.4	1565.3						
IV	SI.18	132.7	404.9	623.5						
IV	SII.51									
IV	SII.52	131.7	338.5	557.7	1.0	66.4	65.8	0.8	16.4	10.5
IV	SII.53	191.7	351.7	822.2						
IV	SI.19	123.9	408.5	595.4						
IV	SII.54									
IV	SII.55	145.7	557.2	1354.2						
IV	SII.56									
IV	SI.20	121.2	431.3	599.4						
IV	SII.57									
IV	SII.58	143.2	618.1	1510.						

Table 5.20:-

/Continued ..... /

Noise Series	Run No.	Performance Criterion			Improvement			% Improvement		
		½h	1h	1½h	½h	1h	1½h	½h	1h	1½h
V	No Control	224.1	722.2	1532.7						
V	SI.21	193.3	770.7	1136.1						
V	SII.59									
V	SII.60	196.3	579.3	758.8		191.4	377.3		24.8	32.2
V	SII.61	192.7	636.3	805.9	0.6	134.4	330.2	0.3	17.4	29.1
V	SI.22	205.6	741.2	1319.8						
V	SII.62									
V	SII.63	190.9	739.1	1156.	14.7	2.1	163.8	7.2	0.3	12.4
V	SII.64	184.8	666.9	846.2	20.8	74.3	473.6	10.1	10.	35.9
V	SI23	209.5	755.9	1393.0						
V	SII.65									
V	SII.66	207.7	654.5	1072.9	1.8	110.3	320.1	0.9	14.6	23.0
V	SII.67	172.0	730.2	1218.4	37.5	25.6	174.6	17.9	3.4	12.5
V	SI.24	215.9	737.6	1381.8						
V	SII.68									
V	SII.69	206.6	823.5	1533.7	9.3			4.1		
V	SII.70									
V	SI.25	219.6	728.8	1435.0						
V	SII71									
V	SII.72	219.8	775.6	1466.0						
V	SII.73									

control action taken. In cases where new controllers were fitted but the runs were not performed blanks appear in the table. Where Controller II has shown an improvement over I, the actual and percentage improvements are shown.

In the case of the first four series, it is noted that the simple optimizer which uses perturbations of 180 secs and 1 volt gave worse results than if no control had been used; however, it is also seen that improvement occurred with increasing frequency and decreasing amplitude. In the case of Series II and III the optimal perturbing signal is never reached, although for Series I and IV it does appear to lie within the factorial design. There are three possible reasons for incurring greater losses than when operating with no control: should the power of the perturbing signal be large compared to the noise, then the extra losses could be due to movement introduced by this signal; alternatively the disturbance could be moving too fast for the control action to be effective, or because of the non-parabolic shape of the objective function too high a control action on the steep side may lead to a continual trailing of the controller on the other side. The effect of this latter factor is amply illustrated in the first part of Figure 5.8. In the case of Series V disturbances enter at a slower rate which results in the simple optimizer giving a better performance than if the system were operated

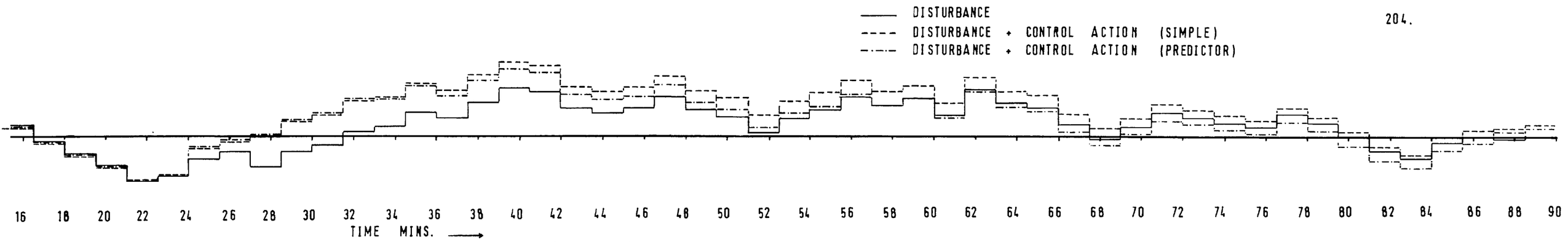

DISTURBANCES & DISTURBANCES + CONTROL ACTION: SERIES 2, 180 sec. & 1 volt PERTURBING SIGNAL

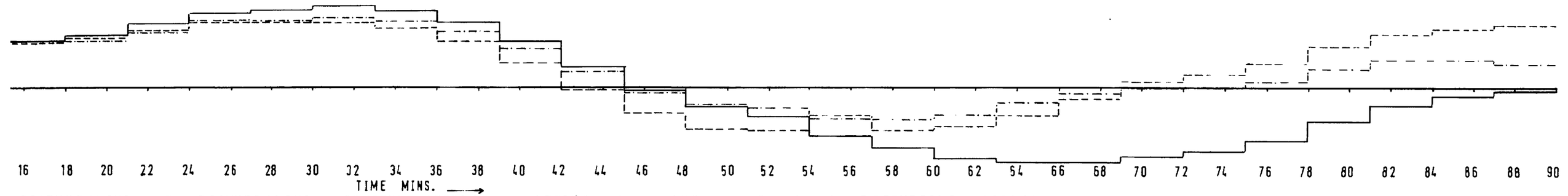

DISTURBANCES & DISTURBANCES + CONTROL ACTION SERIES 5, 180 sec. & 1 volt PERTURBING SIGNAL

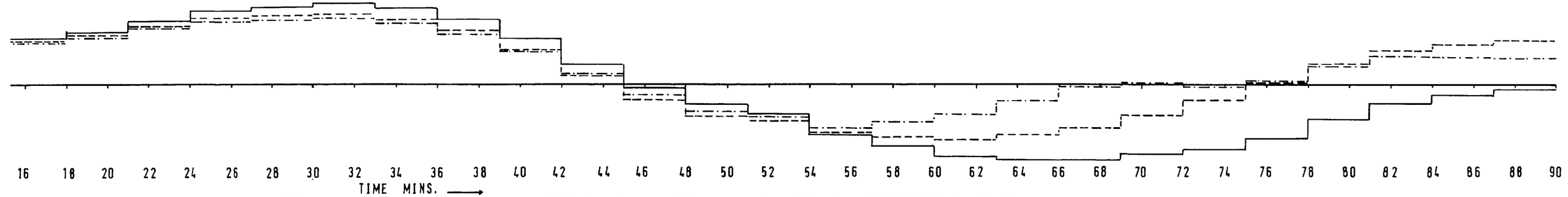

E DISTURBANCES & DISTURBANCES + CONTROL ACTION: SERIES 5, 180 sec. & 1/2 volt PERTURBING SIGNAL

with no control.

The application of the predictor controller did not always give improved performance; frequently the first iteration in the fitting of the parameters yielded a better controller while the second gave a worse one. The reasons for this are not straightforward: it could be due to errors in the series arising from the stepping nature of the disturbances and the control action. It follows that because of this occurrence, the possibility of successful predictor optimizers existing for cases where none have been fitted cannot be discounted.

In order to search for suitable predictor-optimizers in cases where none had been found, a slightly altered fitting routine was used. Previously the Murtagh hill-climber had moved in a straight line towards the point where measurement had shown the optimum to be situated; this movement continued until such a time as either a constraint or a minimum was reached, then the gradient was re-estimated and information about the state of the minimization printed out. The modified routine, however, only moved a fixed distance proportional to the gradient before this was re-estimated and information printed out. This new routine, by reducing the interval at which new controllers were produced, was used quite successfully on data which had not previously yielded an improved predictor-optimizer.

Table 5.21 shows values of the Performance Criterion obtained after 90 minutes of operation with a number of successfully updated controllers. It is seen that whenever the original minimizing routine has failed to produce an improved optimizer the stepping routine has been tried. In certain cases for Series II and III a third controller has been fitted on the basis of data produced by Controller II, while for Series V as much as a fourth controller has been fitted. Table 5.22 gives for each element of the factorial experiments the best controller that has been found together with the percentage improvement each controller gave over the basic Draper and Li optimizer.

Series I and II do not show the same success as would have been expected from the experimental work, for the first series improvements were only noted during the first hour of the 60 sec perturbation runs; the gains made then were subsequently turned into losses during the last half hour. The second series does show slight improvement for the shorter period perturbation but again, losses were made during the last half hour. For the longer period perturbations it is found that improvements were made when operating with Series II - V; in fact it will be noticed from 5.22 that almost 70% improvement was obtained in one of the experiments with Series V.

On the whole, the first four series studied indicate

TABLE 5.21

Best values of performance criterion obtained after 1½ hours of operation

SYSTEM			Controller I	Controller II		Controller III		Controller IV	
Noise	Period sec.	Amp. volts	Draper	Min.	Step	Min.	Step	Min.	Step
I	180	1.00	615.5	657.0	698.2				
I	180	0.50	566.6	586.4	621.6				
I	120	0.75	538.0	547.9	549.9				
I	60	1.00	541.0	555.7	565.1				
I	60	0.50	556.4	578.7	559.2				
II	180	1.00	577.9	524.2		529.6	529.6		
II	180	0.50	496.6	465.2		498.2	509.5		
II	120	0.75	481.8	489.6	465.6	501.7	475.4		
II	60	1.00	437.0	446.4	430.4	489.5	426.5		
II	60	0.50	428.2	433.8	426.6				
III	180	1.00	1609.6	1462.6		1968.0	1454.0		
III	180	0.50	1490.8	1383.0		1711.0	1242.6		
III	120	0.75	1405.9	1197.5		1078.0			
III	60	1.00	1336.9	1479.0	1510.2				
III	60	0.50	1239.9	1365.4	1312.5				
IV	180	1.00	726.3	622.2					
IV	180	0.50	671.4	619.8					
IV	120	0.75	623.5	557.7					
IV	60	1.00	595.4	1354.2	671.5				
IV	60	0.50	599.4	1510.0	608.6				

TABLE 5.21

continued

SYSTEM			Controller I	Controller II		Controller III		Controller IV	
Noise	Period sec.	Amp. volts	Draper	Min.	Step	Min.	Step.	Min.	Step.
V	180	1.00	1136.1	758.8		617.6		637.0	394.6
V	180	0.50	1319.8	846.2		520.4		604.8	402.8
V	120	0.75	1293.0	1072.9		682.6		661.5	
V	60	1.00	1381.8	1533.7	1165.6				
V	60	0.50	1435.0	1466.0	1312.6				

Table 5.22:-

Shows controller that gave best results for each set of conditions together with the percentage improvement obtained over the Draperski controller

System			Best Controller						
Noise	prd sec.	Amp volts	λ	g	k	γ_{-1}	γ_0	γ_1	% Improvement
I	180	1.00	0.	1.	0.	0.	1.	0.	0.0
I	180	0.50	0.	1.	0.	0.	1.	0.	0.0
I	120	0.75	0.	1.	0.	0.	1.	0.	0.0
I	60	1.00	0.	1.	0.	0.	1.	0.	0.0
I	60	0.50	0.	1.	0.	0.	1.	0.	0.0
II	180	1.00	0.0599	0.9776	0.0096	0.0490	0.0223	-0.0603	9.3
II	180	0.50	0.0282	0.9433	0.	-0.0016	0.0474	-0.0592	6.3
II	120	0.75	0.0336	0.9448	0.	0.0336	0.0552	-0.0234	3.4
II	60	1.00	0.	0.3451	0.	-0.1402	0.0359	-0.0177	2.4
II	60	0.50	0.0028	0.9647	0.	0.0020	0.0344	-0.0070	0.4
III	180	1.00	0.0773	0.8313	0.	0.0546	0.0925	-0.0737	9.7
III	180	0.50	0.0391	0.3738	0.	-0.0741	0.2904	-0.1455	16.7
III	120	0.75	0.1980	0.3185	0.	0.1860	0.5155	-0.2325	23.3
III	60	1.00	0.	1.	0.	0.	1.	0.	0.0
III	60	0.50	0.	1.	0.	0.	1.	0.	0.0
IV	180	1.00	0.0657	0.9751	0.0029	0.0424	0.0357	-0.0573	14.3
IV	180	0.50	0.1037	0.9056	0.	0.0744	0.1034	-0.0916	7.7
IV	120	0.75	0.0695	0.8737	0.	0.0396	0.1229	-0.0690	10.6
IV	60	1.00	0.	1.	0.	0.	1.	0.	0.0
IV	60	0.50	0.	1.	0.	0.	1.	0.	0.0

Table 5.22:-

Continued ...../

System			Best controller						
Noise	prd sec	Amp volts	λ	g	k	γ_{-1}	γ_0	γ_1	% Improvement
V	180	1.00	0.1775	0.0861	0.	0.2109	0.3523	-0.1954	65.3
V	180	0.50	0.2299	0.0635	0.	0.2327	0.2368	-0.1852	69.5
V	120	0.75	0.	0.6226	0.	-0.0826	0.2341	-0.1931	48.8
V	60	1.00	0.	0.4016	0.	0.1257	0.2646	0.0162	16.4
V	60	0.50	0.2040	0.6839	0.	0.0279	0.2785	-0.0125	8.5

the benefit of using a form of predictor regulator rather than the simple adaptive optimizer, but the results also suggest that in many cases it is better not to use any control at all. Series V consists of a set of disturbances which move widely but much more slowly than the other four, and with this it is found that improvements made with the simple optimizer could be increased still further with the predictor-optimizer.

5.4. Comparison of Experimental and Simulation Results

When Controller I was used to correct for disturbances of the first three series, it was found that the values of the Performance Criterion were of the same order, whether obtained experimentally or by simulation. This would confirm, within the limits of the experimental error, the correctness of using the digital simulation model for verifying and extending the experimental work.

Although it was shown experimentally that improvement could be obtained by introducing a predictor-controller when the system was subject to either random or first order integrated disturbances, it was not confirmed by the simulations. However, a statistical analysis has shown that the former is correct, and a glance at Figures 5.8 - 5.10 illustrates, that in these cases at least, improvements had taken place over the first hour which were probably increased or maintained for the remainder of each run. Figure 5.11 shows

the simulation results for Series II with a 1 volt, 180 sec perturbing signal; this being equivalent to the runs generating Figure 5.8, the two may be compared directly. It is noted immediately that there is a large change in the trajectory of Controller I (figure 5.8) after 27 minutes, although it cannot be confirmed this is probably due to the large combined change of the noise and control action taking place in the previous cycle. It is also noted that in all runs with Series II (Figures 5.8 - 5.11), movement to the negative side of the optimum started taking place after about 16 minutes, but little or no countering control action occurred until 8 minutes later when the trend of the noise changed direction. Both of these phenomena could be due to the way the Draper and Li optimizer is influenced by step changes (Section 2.6). In addition trajectories for Controller II in Figures 5.8 and 5.11 suggest that the experimentally obtained controller had probably made smaller losses than the simulation one, a fact which again emphasises the difficulty of fitting the best control parameter. Because Series I is random, it is reasonable to assume that no optimizer control action could make an improvement. However it was found that in some cases the simple Controller I can do better than no control, therefore for this particular series of disturbances further improvement should have been possible with a predictor optimizer, also the simulation

studies showed success in correcting for Series III where the experimental ones had not. In conclusion it is suggested that these failures are probably due to the weakness of the parameter fitting method, although another possible explanation of the differences between the experimental and simulation results is that in the simulations the noise steps were always entering at the same part of the perturbation cycle whereas in the other case this could not be guaranteed.

5.5. Conclusions

Because of poor reproducibility, the experimental programme did not yield as much information as had originally been hoped for; however, in the light of the results obtained, a clearer picture of the predictor-optimizer's performance would only have been obtained with considerably more work. Nevertheless, it was shown that the method of predictor-optimization was successful, and over the whole factorial design, gave, for both Series I and II, an average improvement of about 10%. Unfortunately no improvement was obtained with the highest frequency perturbation signals or in the case of Series III. The former was due to other disturbances drowning the highly attenuated signal, while the latter, in the light of the simulation studies, was probably because of the fitting technique.

The simulation studies of the optimization method were carried out using a digital dynamic model of the plant and peripheral equipment. It was felt that within the limits of experimental error the simulation runs had reproduced the performance of the system well enough for information obtained to be considered indicative of the system's behaviour. The method employed in fitting the predictor-optimizer was found to have a weakness in that minimization of the objective function obtained generally led to the best controller settings being passed, hence frequently worse performance was obtained when using the controller settings at the minimum.

The simulation results were not consistent with the experimental ones in the case of Series I, although in fact they were more reasonable. Failure of the three longer period experiments to show improvement was because random noise, which was changing at a faster rate, was being dealt with, while success of the two faster period ones was due to the absence of system noise masking the attenuated output signal. All other signals were better controlled for with the predictor-optimizer. Finally this method of extremum seeking was shown to be very much better when dealing with noise which varied at half the rate of the original noise; it was found here that improvements of up to 70% were made over the original Draper and Li optimizer.

CHAPTER 6

Conclusions and Suggestions for Further Work

6.1. Introduction

The chapter summarizes the main conclusions reached in the present study. The subject matter is dealt with in the same order as in the preceding chapters, but the last section gives suggestions for further work.

6.2. Conclusions

6.2.1. Feasibility of predictor-optimization

The theoretical backgrounds of the Draper and Li extremum seeking controller, and the Box and Jenkins predictor controller, were given together with a simplified method of modelling the system's dynamics. It was reported that Box and Jenkins had proposed the union of their predicting method with Draper and Li's adaptive optimization method, so that moving extrema could be followed. Although this was shown to be feasible, warning was given regarding the difficulties that could be encountered. The discrete manner in which estimates of the slope were obtained was shown, by means of simulation, to be the main cause of trouble in studying the dynamics of extremum seekers. Even though the system's dynamics might be linear, the example showed that introduction of the optimalizing loop caused the total system to

become so non-linear that the change in the estimate of slope could give a wholly wrong indication of the direction in which the mean operating point had moved. The second danger pointed out was from having a non-quadratic objective function; it was illustrated with an example how the best mean operating point was some distance from the optimum, on the shallow side of the hill. Finally, an algorithm was given for finding this point in the case of a real system being operated in the presence of noise.

6.2.2. Steady-State Model of Reactor

The plant was operated at different conditions of temperature and steam flow to obtain steady-state data describing the performance of the reactor. Subsequent fitting of a model to this data confirmed Price's findings that a four-parameter model gave an adequate picture of the system. The Arrhenious parameter and activation energy obtained to describe the rate constant agreed well with results obtained by Price (P6) and Kisiel (K4), but the parameters describing the thermodynamic equilibrium constant showed much better agreement with parameters calculated theoretically by Mars (M2) from free energy data, than with those yielded by Price and Kisiel's data.

After fitting the optimal parameter values to the model, linear and non-linear confidence limits at the 95% level were evaluated. Because of the large disagreement

between the two regions it was concluded that the model was highly non-linear; also, on the basis of this and Beale's (B6) work, it was realized that the confidence limits evaluated gave no more than an indication of the true confidence region, although it was safe to assume that there is a greater than 95% certainty that the true model lies within the ellipsoid of the linear confidence limits.

Comparison of the error variance for the model and the experimental error variance showed that although the former was about three times as large as the latter, the model had represented the date adequately. Further investigation indicated that the main remaining source of error was the sensitivity setting on the Infra Red Analyser; if corrections were made for this then the error variance of the model could be reduced to the same magnitude as the experimental error variance.

During the experimental programme reported here there was no indication of changes occurring in the catalyst activity, although after a further programme deterioration was noted. Because of this it was decided to perform another set of steady-state experiments to remodel the reactor. The resulting values of the parameters fitted showed little change in the thermodynamic equilibrium constant, although a surprising drop had taken place in the values of both the rate constant parameters. Reasons for the differences were

at first sought on the macro-scale by examining for changes in the paricle size due to sintering, but as this was discounted smaller changes in the surface were considered by comparing micrographs of the catalyst before and after use; again no real difference was noted. At the same time electron diffraction pattern analysis carried out confirmed the presence of iron and chromium oxides but revealed no other compound which could possibly have acted as a poison. However meausrements carried out on the spent catalyst showed that the mean surface area was 50% lower than would normally be expected. Hence it was thought that the loss in activity and accompanying "compensating effects" was probably due to this.

6.2.3. Dynamic modelling of system

Price (P6) had obtained a dynamic model of the system by means of frequency response techniques; although this had proved adequate, the method of fitting the parameters had led to very large uncertainties in the values of the dead times estimated, also the method was considered to take up a lot of experimental time which would not always be available in industrial situations. Hence it was decided to model the dynamics using a pseudo-random binary signal to excite the system.

Implementation of the method was carried out by generating the PRBS on an eight-stage shift register mounted

on a hybrid computer, and the outputs were recorded on paper tape by a data logging system. Generation of the system's impulse response fucntions and the fitting of parameters to models of given structure was carried out off-line on a digital computer. Again as in the case of steady-state modelling of the reactor, both linear and non-linear confidence limits were calculated, and from the way they compare it is seen that the degree of non-linearity in the system's dynamics was considerably smaller.

Comparison of the results obtained with the two methods showed that greater credibility could probably be given to dead times evaluated by using PRBS's, although it was felt that the time constants fitted were not as reliable. However, it was thought that exciting the system at a slower rate with a shorter PRBS might improve the estimates of the latter.

Finally, a comparison was made of the relative amounts of experimental and computational time required by each method, and it was concluded that whereas the PRBS method needed about a tenth of the experimental time required by the other, about ten times more computing was necessary. Hence in deciding between one and the other the total experimental and computing costs have to be considered.

6.2.4. Experimental implementation of the predictor-optimizer

The method of predictor-optimization was tried out experimentally on the temperature side of the pilot plant system. While maintaining constant steam and dry gas flow rates, different types of disturbances were introduced via the temperature controller, to effectively move the objective function's optimum relative to the currently known operating temperature without changing the value of this optimum. Correction for the action of these disturbances was attempted by using the simple adaptive optimization technique on the temperature side. The data obtained during these runs was then used to design the more sophisticated predictor-optimizer. The original experiments were then repeated to compare the relative performance of the controllers. The influence of the amplitude and period of the perturbing signal was also investigated by means of two-dimensional, five point factorial experiments.

Unfortunately, because of the large amounts of experimental error present in the work, it was not possible to gain as much information from the experimental programme as had at first been hoped. However, it was shown that the predictor-optimizer gave a significant improvement when dealing with what were assumed to be random and first order integrated series. It was also possible to estimate that an average improvement of about 10% had taken place over the whole

factorial design. Although it was not possible to assess quantitatively the effects of period and amplitude, it was nevertheless found that, at higher frequencies of perturbation, the large attenuation of the signal through the system together with the internally generated noise, led to a negligible correction being produced. Hence it was decided that the longer period signals were better. Complete failure of the predictor-optimizer occurred when dealing with a second order integrated noise series; this was thought to be due to failure of the routine fitting the predictor-optimizer rather than to any excessive power of the disturbances.

6.2.5. Simulation studies of the predictor-optimizer

A digital simulation model of the plant and peripheral equipment which had been written on the basis of information collected during the steady-state and dynamic modelling of the system, was used to repeat and extend the experimental investigations. Although the results of the simulation work did not entirely agree with the experimental ones, it was useful in that it showed up an inherent weakness in the fitting routine; namely, that after setting up the objective function for fitting parameters to the predictor-optimizer, too much movement towards the minimum resulted in the best optimizer being missed. It was also shown that improvement of up to 70% could be obtained if the rate of noise input

were slowed down by a factor of two.

6.3. Suggestions for Further Work

Since the pilot plant is readily available, it would be interesting to try out, and compare with results already obtained, the use of a continuous sensitivity method to estimate the parameters of the plant's dynamic model. This uses no special excitation signal other than disturbances occurring naturally in the plant and operates via an on-line analogue dynamic model of predetermined structure.

The most obvious problem that arises out of the present work is the development of a more realistic model of the adaptive system's dynamics. Such work at this stage would appear to necessitate accurate knowledge of the system's actual mean operating point, which if available would of course tend to eliminate the problem of following the moving hill.

However, in the absence of further clarification of the dynamics it would nevertheless seem logical to study the use of the Box and Jenkins predictor-optimizer in following the optimum of a more complicated objective function, for instance one requiring measurements from different points in the plant. Kisiel (K4) and Price (P6) have already shown that compensation has to be made for the differing dynamics of the paths from the measuring points. Using the analogue set up which is available at present, it is possible to

compensate for linear transfer functions, but unfortunately dead times can only at best be reproduced by Padé delays, and these have the disadvantage of being frequency limited. One possible way of circumventing the latter problem is the introduction of a small digital computer into the system so that its memory can be used in generating the necessary dead times. There still remain of course the difficulties encountered due to the dynamics, but once again the limits of the predicting method could be ascertained.

Apart from the study of Wiener and Mazani (W2, W3) very little has been done towards the development of a method for analysing and modelling multivariate stochastic processes. When working in the time domain they suggest using a method which involves matrix inversion and is therefore unsuitable unless the size of the matrix is small; this means a low dimensionality series requiring little history and tolerating high prediction errors. However, it may be possible to develop this for following the moving optimum of a multidimensional objective function.

Another interesting study would be the use of an analogue model of the system in a feedforward capacity. Again the effect of disturbances on the system could be investigated, although initially it would be more convenient to use low frequency noise in order to reduce the effect of plant dynamics, as further information is obtained so the frequency

could be increased and compensation for the dynamics introduced. A further refinement would be the introduction of the sensitivity method to update parameters in the analogue model.

APPENDIX 2.1.

Derivation of the difference equation for representing a second order transfer function of the type shown in equation 2.4.7.

$$\text{Transfer function} = \frac{1}{(T_1 p + 1)(T_2 p + 1)} \qquad \text{(A2.1.1)}$$

$$\text{Response to step change} = \frac{1}{p} \cdot \frac{1}{(T_1 p + 1)(T_2 p + 1)} \qquad \text{(A2.1.2)}$$

Breaking (A2.1.2) down into partial fractions

$$= \frac{1}{p} - \frac{1}{T_1 - T_2}\left(\frac{T_1}{p + 1/T_1} - \frac{T_2}{p + 1/T_2}\right) \qquad \text{(A2.1.3)}$$

Finding the inverse

$$= 1 - \frac{1}{T_1 - T_2}\left(T_1 e^{-t/T_1} - T_2 e^{-t/T_2}\right) \qquad \text{(A2.1.4)}$$

from which the generalized weighting term is obtained:

$$w_i = \frac{1}{T_1 - T_2}\left(T_1 e^{-(i-1)T/T_1}(1 - e^{-T/T_1}) - T_2 e^{-(i-1)T/T_2}(1 - e^{-T/T_2})\right)$$

where T is the sampling interval. (A2.1.5)

By definition the output from the system at time nT is

$$y_n = \sum_{i=1}^{\infty} w_i x_{n-i} \qquad \text{(A2.1.6)}$$

Using (A2.1.5) and (A2.1.6) we can obtain

$$y_{n+1} = w_1 x_n + y_n\left(e^{-T/T_1} + e^{-T/T_2}\right) - y_{n-1}\left(e^{-T/T_1} e^{-T/T_2}\right) - \frac{1}{T_1 - T_2}\left(T_1(1 - e^{-T/T_1})e^{-T/T_2} - T_2(1 - e^{-T/T_2})e^{-T/T_1}\right)x_{n-1} \qquad \text{(A2.1.7)}$$

Putting $\beta_j = (1 - e^{-T/T_j})$, (A2.1.7) is found to convert to

$$y_{n+1} = y_n\left((1 - \beta_1) + (1 - \beta_2)\right) - y_{n-1}\left((1 - \beta_1)(1 - \beta_2)\right) + \frac{1}{T_1 - T_2}\left\{(T_1\beta_1 - T_2\beta_2)x_n - \left(T_1\beta_1(1 - \beta_2) - T_2\beta_2(1 - \beta_1)\right)x_{n-1}\right\}$$

which in turn converts to (A2.1.8)

$$\left(\beta_1 + (1 - \beta_1)\Delta\right)\left(\beta_2 + (1 - \beta_2)\Delta\right)y_{n+1} = \frac{1}{T_1 - T_2}\left\{(T_1\beta_1 - T_2\beta_2)x_n - \left(T_1\beta_1(1 - \beta_2) - T_2\beta_2(1 - \beta_1)\right)x_{n-1}\right\} \quad \text{(A2.1.9)}$$

Finally

$$(1 + k_1\Delta)(1 + k_2\Delta)y_{n+1} = \frac{1}{T_1 - T_2}\left\{\left(\frac{T_1}{\beta_2} - \frac{T_2}{\beta_1}\right)x_n - (T_1k_2 - T_2k_1)x_{n-1}\right\} \quad \text{(A2.1.10)}$$

where $k_j = \dfrac{(1 - \beta_j)}{\beta_j}$

APPENDIX 2.2.

The output signal from the correlator is derived analytically for the system illustrated in Figure 2.2 in which a first order transfer function is followed by a quadratic objective function and the optimizer. The input signal to the system is made up of a sinusoid and D.C. signal which have achieved steady-state and a step change which has occurred recently enough for its transients to influence the output.

1st order transfer function = $\dfrac{1}{T_1p + 1}$

Input signal = $x + a\sin\omega t + bH(t - \alpha)$

where x = mean operating point

a = amplitude of sinusoid

ω = angular velocity of sinusoid

b = magnitude of step change

$H(t-\alpha)$ = Heaviside function, step of + 1 occurring at time $t = \alpha$

Because the transfer function is linear each component of the signal may be considered separately.

∴ output from transfer function

1st component = x (A2.2.1)

2nd component = $a\left\{e^{-t/T_1} + \frac{1}{T_1\omega}\sin\omega t - \cos\omega t\right\}\frac{\omega T_1}{1 + \omega^2 T_1^2}$ (A2.2.2)

However because the sinusoid has been established for a long time the transient term is ignored.

∴ 2nd component = $\frac{a}{\sqrt{1 + \omega^2 T_1^2}}\sin(\omega t - \phi)$ (A2.2.3)

where $\phi = \sin^{-1}\left(\frac{\omega T_1}{\sqrt{1 + \omega^2 T_1^2}}\right)$

3rd component = $bH(t - \alpha)\left\{1 - e^{-(t-\alpha)/T_1}\right\}$ (A2.2.4)

Complete signal = $x + \frac{a}{\sqrt{1 + \omega^2 T_1^2}}\sin(\omega t-\phi) + bH(t-\alpha)$

$\times \left\{1 - e^{-(t-\alpha)/T_1}\right\}$ (A2.2.5)

The quadratic function is taken to have a maximum and is described by βy^2, where y is the operating point.

. . output from non-linear element

$$= \beta\Big\{x^2 + \frac{a^2}{1+\omega^2T_1^2}\sin^2(\omega t-\phi) + \frac{2xa}{\sqrt{1+\omega^2T_1^2}}\sin(\omega t-\phi)$$
$$+ b^2H(t-\alpha)\Big(1 - 2e^{-(t-\alpha)/T_1} + e^{-2(t-\alpha)/T_1}\Big)$$
$$+ 2xbH(t-\alpha)\Big(1 - e^{-(t-\alpha)/T_1}\Big)$$
$$+ \frac{2ab}{\sqrt{1+\omega^2T_1^2}}H(t-\alpha)\Big(1 - e^{-(t-\alpha)/T_1}\Big)\sin(\omega t-\phi)\Big\} \qquad \text{(A2.2.6)}$$

The transfer function of the high pass filter

$$= \frac{T_F p}{T_F p + 1} \qquad \text{(A2.2.7)}$$

Considering each component separately

$$\text{1st component} = \beta x^2 e^{-t/T_F} = 0 \qquad \text{(A2.2.8)}$$

$$\text{2nd component} = \frac{\beta a}{1+\omega^2T_1^2}\frac{1}{2}\Big\{e^{-t/T_F} -$$
$$- \frac{1}{1+4\omega^2T_F^2}\Big((\cos2\phi - 2\omega T_F\sin2\phi)e^{-t/T_F}$$
$$- 2\omega T_F\sin(2\omega t-2\phi)$$
$$+ 4\omega^2T_F^2\cos(2\omega t-2\phi)\Big)\Big\}$$

$$= \beta\frac{a^2}{2}\frac{1}{1+\omega^2T_1^2}\frac{1}{1+4\omega^2T_F^2}\Big\{2\omega T_F\sin(2\omega t-2\phi)$$
$$- 4\omega^2T_F^2\cos(2\omega t-2\phi)\Big\} \qquad \text{(A2.2.9)}$$

$$\text{3rd component} = \frac{2xa\beta}{\sqrt{1+\omega^2T_1^2}}\frac{1}{1+\omega^2T_F^2}\Big\{-(\omega T_F\cos\phi + \sin\phi)e^{-t/T_F}$$
$$+ \omega T_F\cos(\omega t-\phi) - \omega^2T_F^2\sin(\omega t-\phi)\Big\}$$

=

$$= \frac{2x\alpha\beta}{\sqrt{1 + \omega^{2}T_1^{2}}} \frac{1}{1 + \omega^{2}T_F^{2}} \left\{\omega T_F \cos(\omega t - \phi) + \omega^{2}T_F^{2}\sin(\omega t - \phi)\right\} \quad \text{(A2.2.10)}$$

In the above three equations, the simplifications were possible because the signals had long been established, and so the transients could be ignored.

$$\text{4th component} = \beta b^{2} H(t - \alpha)\left\{e^{-(t-\alpha)/T_F} - \frac{2}{T_F - T_1}\left(T_F e^{-(t-\alpha)/T_1} - T_1 e^{-(t-\alpha)/T_F}\right) + \frac{1}{T_F - \frac{T_1}{2}}\left(T_F e^{-2(t-\alpha)/T_1} - \frac{T_1}{2} e^{-(t-\alpha)/T_F}\right)\right\} \quad \text{(A2.2.11)}$$

$$\text{5th component} = 2bxH(t - \alpha)\left\{e^{-(t-\alpha)/T_F} - \frac{1}{T_F - T_1}\left(T_F e^{-(t-\alpha)/T_1} - T_1 e^{-(t-\alpha)/T_F}\right)\right\} \quad \text{(A2.2.12)}$$

$$\text{6th component} = \frac{2ab}{\sqrt{1 + \omega^{2}T_1^{2}}} H(t-\alpha)\left\{e^{-(t-\alpha)/T_F}\right.$$

$$\times \left[\left\{\frac{1}{1 + \omega^{2}T_F^{2}} + \frac{1 - T_F/T_1}{(T_F/T_1 - 1)^{2} + \omega^{2}T_F^{2}}\right\}\sin(\omega\alpha - \phi) - \left\{\frac{\omega T_F}{1 + \omega^{2}T_F^{2}} + \frac{\omega T_F}{(T_F/T_1 - 1)^{2} + \omega^{2}T_F^{2}}\right\}\cos(\omega\alpha - \phi)\right]$$

$$+ \frac{\omega T_F}{1 + \omega^{2}T_F^{2}}\cos(\omega t - \phi) + \frac{\omega^{2}T_F^{2}}{1 + \omega^{2}T_F^{2}}\sin(\omega t - \phi)$$

$$- e^{-(t-\alpha)/T_1}\left\{\frac{\omega T_F}{(T_F/T_1 - 1)^{2} + \omega^{2}T_F^{2}}\cos(\omega t - \phi) + \frac{T_F^{2}/T_1^{2} - T_F/T_1 + \omega^{2}T_F^{2}}{(T_F/T_1 - 1)^{2} + \omega^{2}T_F^{2}}\sin(\omega t - \phi)\right\}\right\} \quad \text{(A2.2.13)}$$

Each of these components now has to be multiplied by the correlating signal $\sin(\omega t - \phi)$ and integrated from 0 to 2π, or α to 2π if α is greater than zero. Addition of the outputs from the integration then gives the estimates of gradient being sought.

APPENDIX 4.1

Correlation Analysis

So as to assess the dependence of the steady-state model's error on the parameters being measured a correlation analysis was carried out on both Price's (P6) data and the data contained in Chapter 4.

Some examples are given below:

Price's data

Normalized variance-covariance matrices before correcting for sensitivity:

% CO v error	steam flow v error	temp v error
$\begin{pmatrix} 1.0 & 0.852 \\ 0.852 & 1.0 \end{pmatrix}$	$\begin{pmatrix} 1.0 & 0.750 \\ 0.750 & 1.0 \end{pmatrix}$	$\begin{pmatrix} 1.0 & -0.264 \\ -0.264 & 1.0 \end{pmatrix}$

after correcting for sensitivty:

% CO v error	steam flow v error	temp v error
$\begin{pmatrix} 1.0 & 0.0003 \\ 0.0003 & 1.0 \end{pmatrix}$	$\begin{pmatrix} 1.0 & -0.388 \\ -0.388 & 1.0 \end{pmatrix}$	$\begin{pmatrix} 1.0 & 0.169 \\ 0.169 & 1.0 \end{pmatrix}$

1st section of 1st data

Normalized variance-covariance matrix before correcting for sensitivity:

% CO v error

$$\begin{pmatrix} 1.0 & 0.724 \\ 0.724 & 1.0 \end{pmatrix}$$

after correcting for sensitivity:

% CO v error

$$\begin{pmatrix} 1.0 & 0.024 \\ 0.024 & 1.0 \end{pmatrix}$$

REFERENCES

A1. Alpeter, R.J., Deem., W.B. and Frey, A.L.
IFAC (London) 1966.
Stability and optimal gain in extremum seeking adaptive control of a gas furnace.

A2. Alpeter, R.J., Deem, W.B. and Frey, A.L.
JACC, June 1966.
An application of sampled data adaptive optimization.

B1. Box, G.E.P. and Jenkins G.M.
Book to be published.
Models for prediction and control.

B2. Box, G.E.P. and Jenkins, G.M.
J.Roy.Stat.Soc., Series B, 24, 297 (1962).
Some statistical aspects of adaptive optimization and control.

B3. Box, G.E.P. and Jenkins, G.M.
34th Session, I.S.I., Ottawa, Canada 1963.
Further contributions to adaptive quality control: simultaneous estimation of dynamics: non-zero costs.

B4. Box, G.E.P., Alpeter, R.J. and Kotnour, K.D.
Trans.Inst.Soc. America 5, 255 (1966).
A discrete predictor controller applied to sinusoidal perturbation adaptive optimization.

B5. Beale, E.M.L.
J.Roy.Stat.Soc., Series B, 22, 41 (1960).
Confidence regions in non-linear estimation.

B6. Briggs, P.A.N., Hammond, P.H., Hughes, M.T.G., Plumb, G.O.
Advances in Automatic Control, I.M.E. Symp. (Nottingham) April 1965.
Correlation analysis of process dynamics using pseudo-random binary test perturbations.

D1. Draper, C.S. and Li, Y.T.
A.S.M.E. Special Publication, 1951.
Principles of optimizing control systems and applications to the internal combustion engine.

D2. Douce, J.L. and Bond, A.D.
Proc. I.E.E. 110, 619 (1963).
Development and performance of a self optimizing system.

D3. Deem, W.B.
Ph.D. Thesis, University of Wisconsin, 1965.
A systems engineering study of a two variable extremum adaptive controller of a gas furnace.

D4. Davies, O.L.
Oliver & Boyd, 1954.
The design and analysis of industrial experiments.

D5. Dowden, D.A.
Personal communication.

E1. Eckman, D.P.
J. Wiley & Sons, 1965.
Automatic process control.

E2. Electronic Associates Ltd.
Advanced techniques manual. 1966.

F1. Fel'dbaum, A.A.
Automatic & Remote Control 20, 1024 (1959).
The steady-state processes in the simplest discrete extremal system with random noise present.

F2. Fel'dbaum, A.A.
Automatic & Remote Control 21, 111 (1960).
Statistical theory of gradient systems of automatic optimization for objects with quadratic characteristics.

G1. Gorelick, N.G.
Automatic & Remote Control 27, 1023 (1966).
Statistical theory of gradient systems of automatic optimization with one and two trial steps, and their comparative analysis.

G2. Grishko, N.V.
Automatic & Remote Control 20, 497 (1959).
A peak holding regulator that follows the peak.

G3. Grishko, N.V.
Automatic & Remote Control 22, 904 (1961).
The determination of optimal characteristics for an extremal system with random disturbances.

G4. Goodman, T.P. and Reswick, J.B.
Trans.A.S.M.E. 78, 259 (1965).
Determination of system characteristics from normal operating records.

G5. Godfrey, K.R. and Briggs, P.A.N.
Personal communication.

H1. Hammond, P.H. and Duckenfield, M.J.
Automatica 1, 147 (1963).
Automatic optimization by continuous perturbation of parameters.

H2. Hwang, K.C.
Ph.D. Thesis, California Institute of Technology, 1965.
A mathematical study of the transient behaviour of a fixed-bed catalytic reactor.

H3. Hougen, J.O.
C.E.P. Monographs, Series 4, 60 (1964).
Experience and experiments with process dynamics.

H4. Huffman, D.A.
Proc. 3rd London Symposium on Information Theory.
Academic Press, 77 (1956).

J1. Jenkins, G.M.
Biometrika 41, 405 (1954).
Tests of hypotheses in the linear autoregressive model.

J2. Jenkins, G.M.
Personal communication.

J3. Jackson, A.
Personal communication.

K1. Kutuzov, V.A. and Tarasenko, V.P.
Automatic & Remote Control 26, 265 (1965).
Effects of noise on the operation of extremal step systems with variable parameters.

K2. Kalman, R.E. and Bucy, R.S.
J.Basic Eng., 15 March 1961.
New results in linear filtering and prediction theory.

K3. Kisiel, A.J. and Rippin, D.W.T.
IFAC (Teddington) Symposium, 1965.
Adaptive optimization of a water gas shift reactor.

K4. Kisiel, A.J.
Ph.D. Thesis, University of London, 1965.
The adaptive optimization of a water gas shift reactor.

K5. Kemball, C.
Proc.Roy.Soc. A217, 376 (1953).

L1. Lance, G.W.
London, Iliffe, 1960.
Numerical methods for high speed computers.

M1. Meisen, A.
Internal report, California Institute of Technology, 1966.
Discussion of a computer programme describing the transient behaviour of a fixed-bed catalytic reactor.

M2. Mars, P.
Chem.Eng.Sci. 14, 375 (1961).
Factors governing the behaviour of the adiabatic water gas shift reactor.

M3. Moe, J.M.
Chem.Eng.Prog. 58, 33 (1962).
Design of water gas shift reactors.

M4. Marquardt, D.W.
IBM share programme.
Least squares estimation of non-linear parameters.

M5. Mandel, J.
J. Wiley & Sons, 1964.
Statistical analysis of experimental data.

P1. Paulauskas, T.T.
Automatic & Remote Control 23, 31 (1963).
The investigation of a gradient system of automatic optimization with random interference at the input and output of the object.

P2. Perel'man, I.I.
Automatic & Remote Control 26, 1041 (1965).
Investigation of steady-state conditions in simple extremal step systems in the presence of noise and drift of the controlled system's characteristic.

P3. Perel'man, I.I.
Automatic & Remote Control 22, 1315 (1961).
The statistical investigation of an extrapolating extremal control system for an object with a parabolic characteristic.

P4. Pervozvanskii, A.A.
Automatic & Remote Control 21, 673 (1960).
Continuous extremum control systems in the presence of noise.

P5. Price, R.J. and Rippin, D.W.T.
2nd UKAC Control Convention (Bristol), April 1967.
Simultaneous two variable on-line optimization of a water gas shift reactor.

P6. Price, R.J.
Ph.D. Thesis, University of London, 1966.
One and two variable on-line optimization of a water gas shift reactor.

P7. Powell, M.J.D.
Computer Journal 7, 303 (1965).
A method for minimizing a sum of squares of non-linear functions without calculating derivatives.

P8. Peterson, W.W.
MIT Press and J. Wiley, 1961.
Error correcting codes.

R1. Roberts, J.D.
Advances in Automatic Control. IME (Nottingham) April 1965.
On the design of optimal extremal regulators.

S1. Stakhovskii, R.I.
Automatic & Remote Control 19, 729 (1958).
Twin-channel automatic optimalizer.

S2. Schuster, A.
Terr.Mag. 3, 13 (1898).
On the investigation of hidden periodicities.

S3. Schwartz, C.E. and Smith, J.M.
Ind.Eng.Chem. 45, 1209 (1953).
Flow distribution in packed beds.

S4. Schindler, R.N. and Aris, R.
A.I.Che.E. 22, 319 (1967).
Studies in optimization. Questing control of a stirred tank reactor.

S5. Schindler, R.N. and Aris, R.
A.I.Ch.E. 22, 337 (1967).
Questing control of a two phase reactor.

S6. Schindler, R.N. and Aris, R.
A.I.Ch.E. 22, 345 (1967).
Questing control with economic criterion.

S7. Scheffé, H.
J. Wiley, 1959.
The Analysis of Variance.

T1. Tovstukha, T.I.
Automatic & Remote Control 21, 398 (1960).
The effect of random noise on the steady-state operation of a step-type extremal system for an object with a parabolic characteristic.

V1. Van Nice, R.I. and Mathias, R.A.
Adaptive Control Systems. ed. Caruthers, F.P. and Levenstein, H., Pergammon, 1963.
Extremum adaptation in the presence of noise and drift.

W1. Wise, H.E., Price, R.J. and Rippin, D.W.T.
5th Congress of the International Association for Analogue Computation (Lausanne), August 1967.
A comparison of the use of pseudo-random binary sequences and frequency response methods for the determination of the dynamics of a pilot scale water gas shift reactor.

M6. Murtagh, B.A. and Sargent, R.W.H.
I.M.A. and B.C.S. Joint Conference on Optimization (Keele), March 1968.
Constrained minimization method with quadratic convergence.

R2. Rosen, J.B.
J.Soc.Ind.Appl.Math. 8, 181 (1960).
The gradient projection method for non-linear programming.
Linear contraints.